6-2017

Novel Spectroscopic Tools to Differentiate Drug-DNA Binding Interactions

Fadwa Dhafer Hamad
Western Michigan University

NOVEL SPECTROSCOPIC TOOLS TO DIFFERENTIATE DRUG-DNA BINDING INTERACTIONS

by

Fadwa Dhafer Hamad

A thesis submitted to the Graduate College
in partial fulfillment of the requirements
for the degree of Master of Science
Chemistry
Western Michigan University
June 2017

Thesis Committee:

Ramakrishna Guda, Ph.D., Chair
Sherine Obare, Ph.D.
Ekkehard Sinn, Ph.D.

NOVEL SPECTROSCOPIC TOOLS TO DIFFERENTIATE DRUG-DNA BINDING INTERACTIONS

Fadwa Dhafer Hamad, M.S.

Western Michigan University, 2017

DNA-drug interactions play a major role in therapeutics, diagnostics, forensics and imaging. Drugs bind to DNA in several ways based on the mode of interaction and they alter protein-DNA interactions or breaks/cleaves DNA that can lead to the cure of the disease. The major goal of the research carried out in this thesis is to develop novel optical spectroscopic tools that can differentiate Drug-DNA binding interactions mode whether its intercalation or minor-groove binding. To achieve this goal, we developed two-photon absorption (2PA) cross-section based technique to differentiate between Drug-DNA binding modes. The investigations were carried out on two drug molecules, DAPI and Thiazole Orange (ThO) binding to Salmon Sperm-DNA and Calf Thymus-DNA. DAPI binds to the DNA via minor-groove while ThO intercalates with DNA. Relative 2PA cross-section studies have shown about 3-fold enhancement for DAPI whereas ThO has shown no enhancement. These results confirmed our hypothesis. To further establish this method, studies were carried out using two more drug molecules, Netropsin and Doxorubicin with Salmon Sperm-DNA. Netropsin is a non-fluorescent drug that required a marker to read its binding interaction with DNA. Two types of markers have been used, Hoechst-33258 was used as minor-groove marker and Thioflavine T as intercalator. Doxorubicin drug is fluorescent and the binding results via the 2PA cross-sections have shown a slight decrease in 2PA-fluorescence, suggesting the intercalation binding mode with DNA.

DEDICATION

This dissertation is lovingly dedicated to my mother and my father, for their support, encouragement, and constant love that has sustained me throughout my life. To my family - my husband and my kids - for their support and love.

ACKNOWLEDGEMENTS

Primarily, I would like to express my sincere gratitude to my advisor Dr. Ramakrishna Guda for his endless support, guidance, patience, and advice in the course of this project. I admire and would love to acquire his intrinsic qualities of patience, objective judgment and decision making. Without his constant guidance, motivation, enthusiasm, and immense knowledge this work would not have been possible. In addition, I would like to express my deepest gratitude to Dr. Sherin Obare, for her great support by providing the TA position for me, and her endless support. Also a big appreciation for the other committee member for their availability in my committee meetings and also for their encouragements, and insightful comments

I also convey my gratitude to the dedicated faculty and staff at Western Michigan University. Dr. Michael Barcelona, Dr. Andre Venter, Dr. Ekkhard Sinn, Dr. Gary Blackmer, Dr. William G. Rantz and Staff members: Pam McCartney, Robin Lenkart, Tami A Yonkers. In my daily work I have been blessed with a friendly and cheerful group of fellow students. I am grateful for the members of Dr. Guda's research group (Dr. Abu Bakar Abu Hagar, and Dr. Mohammad Hatshan), who have been invaluable for practical help, discussions, and constructive criticism.

Last, but not least, I would like to dedicate this dissertation to my parents for all their love and encouragement, to my brothers and sister, to my husband for his unbelievable support, and to my amazing kids Reem, Rand, and Haider. In conclusion, I recognize that my study would not

have been possible without the financial support from the Department of Chemistry for teaching assistantships and recognition awards.

Fadwa Dhafer Hamad

TABLE OF CONTENTS

Table of Contents—Continued

Table of Contents—Continued

Table of Contents—Continued

Table of Contents—Continued

LIST OF TABLES

LIST OF FIGURES

List of Figures—Continued

List of Figures—Continued

List of Figures—Continued

CHAPTER 1

INTRODUCTION

Millions of people worldwide are affected by deadly diseases such as cancers of various kinds that include ovarian, prostate, breast etc. Although there are several therapeutics that target these cancers, aggressive forms remain problematic to treat. For example, there are myriad hormone-based therapies against breast cancer, but the hormone insensitive breast cancer such as triple negative breast cancer remains difficult to treat. [(1)] Among different treatment options for cancer treatment, chemotherapy is widely used. Most of the drugs that are used for chemotherapy work by binding with DNA and altering protein-DNA interactions leading to apoptosis. One of the important interactions is the drug-DNA binding which has been the focus of several research investigations. Fluorescent binding molecules have been widely used in cellular biology with potential applications in forensic, diagnostic, bio-analysis and drug research to develop better drugs. Drugs and fluorophores that display enhanced fluorescence upon binding to DNA have been utilized in fluorescence microscopy, quantifying nucleic acids in gel electrophoresis, flow cytometry as well as pathogen detection.

The binding of an external drug molecule with DNA results in significant changes in their properties, which has an important impact on physiological functions. The mechanism of binding and the mode that the drug bind to DNA is considered one of the keys behind targeting DNA with therapeutic drugs and fluorescence probes.[(2)] The main goal of this thesis is to develop novel optical spectroscopic tools to study Drug- DNA interaction for the drugs that fluoresce and follow the binding modes for the Drugs that do not fluoresce. Since most of the research presented in this

thesis is based on DNA- drug interactions, a detailed description about the importance of DNA and different binding modes with drugs is provided here.

1.1 Overview of DNA

Deoxyribonucleic acid (DNA) stores the genetic information in the form of Watson–Crick base pairs, or the organization of total sum of genetic information (or genome) of an organism in the form of double-stranded DNA. The DNA consists of two long polymers of nucleotides, with backbones made phosphate groups joined by ester bonds. These two strands run in opposite directions to each other and are therefore anti-parallel.[3] Genes are the smallest unit of inherited information. They can also be defined as a linear segment of DNA that serves as a code or template to make specific proteins. The code is read by copying stretches of DNA into the related nucleic acid RNA in a process called transcription. [4] The molecule forms a double helix in which two strands of DNA spiral about one another forming something that looks like an immensely long ladder twisted into a helix, or coil (Figure 1.1).[5]

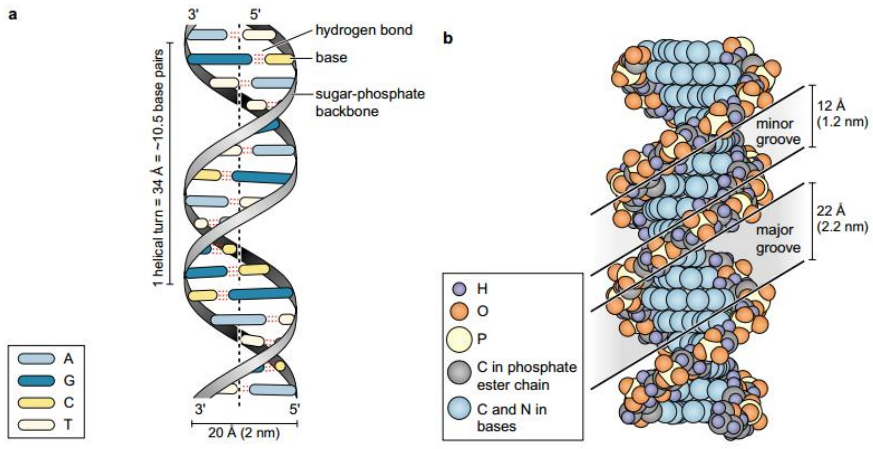

Figure. 1.1 The structure of the DNA double helix. [5]

1.2 DNA-Structure and Specificity

DNA is the source of biological information in the cell. This information is encoded in the base sequence of the sense strand of the nuclear DNA duplex. The noncoding or antisense strand of double-helical DNA has a polarity opposite to that of the sense strand with a complementary sequence of nucleotides depending on Watson–Crick (W–C) rules base pairing Adenine (A), Cytosine (C), Guanine (G) and Thymine (T)). Typically, (A) prefers to pair up with (T), while (C) with (G). The two W–C base pairs (Figure 1.2) are by far the most numerous base pairs in DNA and have a high structural isomorphism. The purine component of the W–C base pairs can also be part of either the sense or antisense strand of the DNA duplex without disrupting the overall structure of the double helix. DNA that consists of W–C base pairs can therefore form a regular duplex structure with the same overall conformation throughout the duplex, independently of the particular sequence of bases. And the complementarity of the antiparallel strands forming a double helix is crucial in DNA replication since the complementary strand is synthesised by adding the Watson–Crick complementary bases of the parent strand. This ability of DNA is an important prerequisite for its role as the carrier of biological information. [3]

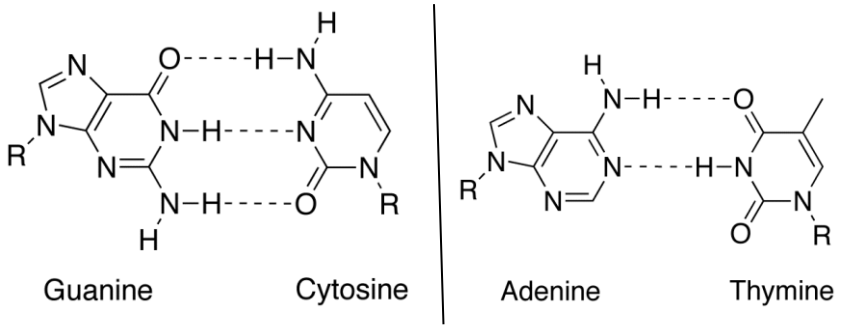

Figure.1.2 Watson- Crick base pair [3]

The fundamental unit of the DNA polymer is the nucleotide monomer. It consists of three covalently linked chemical motifs: an aromatic nucleobase, a deoxyribose sugar, and a phosphate group (Fig 1.3). In dsDNA, nucleobases on opposite anti-parallel backbone strands interact with one another to form 'Watson-Crick' hydrogen bonding base pairs. Adenine forms two stable hydrogen bonds with thymine, and guanine forms three stable hydrogen bonds with cytosine. The base-pairing hydrogen bonds provide the specificity for strand-strand hybridization, while the hydrophobic base stacking provides the energetic driving force. [8]

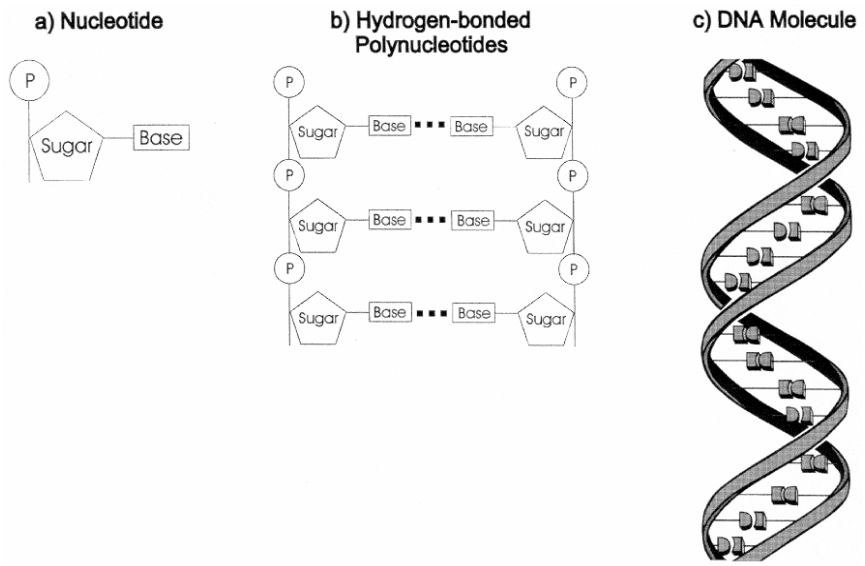

Figure 1.3. (A) Nucleotides are composed of a sugar, a phosphate group, and a nitrogen-containing base. B) Nucleotides form long polynucleotides that can hydrogen bond with one another. C) Hydrogen-bonded polynucleotides coil and twist into DNA molecules. [7]

1.3 Thermal Stability of DNA

The specific base pairing of complementary base nucleotides and the nonspecific stacking interactions of these bases both play major roles in the structure stabilization of a nucleic acid

duplex. The hydrogen bonding and stacking interactions have low energies, allowing a convenient opening and closing of the double helix. For this reason, when a solution of a nucleic acid molecule in the duplex state undergoes an increase in temperature, the duplex melts and disruption of both hydrogen bonds and base pair stacks takes place. The strands are no longer held together and the double helix unfolds to its constituent complementary strands, which are considered two random coils. This transition (helix-to-coil) can be followed experimentally by different techniques like ultraviolet (UV), circular dichroism (CD) and NMR spectroscopies and viscosity. The change in absorbance, or hypochromic shift, of a nucleic acid solution at 260 nm increases as much as 40% as the bases unfold. This hypochromic shift arises because the stacked aromatic bases in DNA interact *via* their π electron clouds, which are away from the solvent in the duplex state. The increase in temperature provides the energy to disrupt base pairing, yielding a higher exposure of the bases to the solvent, which, in turn, increases the probability of π electron transitions. This increase in absorbance follows exactly the process of strand separation, resulting in an absorbance versus temperature curve of the sigmoidal shape.[6,9]

The isometry of W–C (A•T) and (G•C) base pairings allow for the formation of a regular DNA double helix without the need for specific nucleotide sequences. The large number of possible sequences forming DNA double helices allows for the storage of genetic information (the basic function of DNA). Furthermore, the thermal stability of a particular DNA molecule and its overall energetics can be obtained from melting curves, which follow the transition of a DNA double helix into its component single strands with increasing temperature. [6, 9]

1.4 DNA and chemical modifications

Chemical modification describes the modification, addition or removal, through chemical reaction, of any of a variety of macromolecules, including proteins and nucleic acids. It refers to

the use of chemical reagents in vitro rather than to post-translational modification of biological molecules during biosynthesis in vivo. For DNA, the binding of proteins with DNA plays a vital role in the regulation and control of gene expression, replication, and recombination. Furthermore, enzymes that recognize and modify specific oligonucleotide sequences are critical components of biological DNA manipulation and repair systems, like the regulation process for the expression of therapeutic proteins. The other side of DNA modification takes place by important biological functions, which is DNA hybridization that is used widely in biotechnology. So, the study of protein-DNA interactions and DNA hybridization is an important area of molecular biology, aided in part by recent advances in NMR and X-ray structural determination methods.[10] The ability to detect and repair replication errors in DNA is essential to the maintenance of genome integrity which is considered one of the important modifications of DNA. For example in Escherichia coli, this function is served by the methyl-directed MutHLS mismatch repair pathway (a strand-specific pathway) that involves at least 10 different proteins.[11, 12]

1.5 DNA Forms

1.5.1 Single-Stranded DNA

DNA exists primarily as a duplex to stabilize and protect our genome. However, as a result of many cellular processes, such as replication and transcription, single-stranded DNA (ssDNA) is exposed. The ssDNA consists of side nitrous bases attached to a sugar-phosphate polymeric backbone. The repetitive unit (link) of the backbone includes six skeletal bonds. In an individual chain link, one of the four bases: T, C, G, A is attached to the sugar ring's Cl atom. The backbone has no symmetry with respect to the movement along it and, thus, the backbone's structure defines

the chain direction. One end of the chain is known as the 5' end, and the other is known as the 3' end (Fig. 1.4). [13]

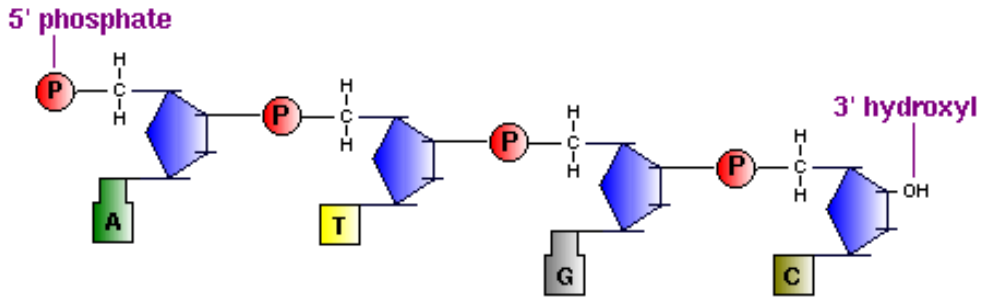

Figure1.4. Schematic diagram of single-stranded DNA's chemical structure. [14]

The ssDNA needs to be stabilized and protected because the genomic DNA must be unwound in order to be replicated or repaired. The ssDNA also needs to get the protection from the chemical attack as well as open to the possibility of forming secondary structures. The binding of the single-stranded DNA (ssDNA)-binding proteins (SSB) will prevent any of these events from occurring. They bind to ssDNA with high affinity and it's denominated as SSB in bacteria, and replication protein A (RPA) in eukaryotes. They play a vital organizational role in the central genome maintenance of the cell, providing docking platforms for a wide range of enzymes to gain access to genomic substrate. Furthermore, the binding of a single ssDNA-binding protein causes the ssDNA to be more accessible for the next protein to bind.[15]

1.5.2 Double-Stranded DNA

Three major forms of DNA are double stranded and connected by interactions between complementary base pairs. These are terms: A-form, B-form, and Z-form DNA. They are also named Duplex-DNA where each type of nucleobase on one strand bonds with just one type of

nucleobase on the other strand. [16] Why does a DNA molecule consist of two strands? This is one of the most important questions that should be asked to understand the DNA biology. Because the primary function of DNA is to store and transmit genetic information, DNA must have two properties. It must be unwound and chemically stable in order to reduce the possibility of damage and leaving it vulnerable to nuclease and chemical attack, in addition to the possibility of forming secondary structures. The second property is the DNA must also be capable of copying the information it contains.

The two-stranded structure of DNA gives it both of these properties and the nucleotide sequence contains the information found in DNA required for repair and replication. The X-ray crystallography suggested a helical periodicity were combined by Watson and Crick in 1953. In the proposed model for a double helical structure for DNA, the two strands of DNA (each in a right-hand helix) wound around the same axis. The two strands are held together by H-bonding between the bases (in anti-conformation) as shown in the fig. 1.5.[17]

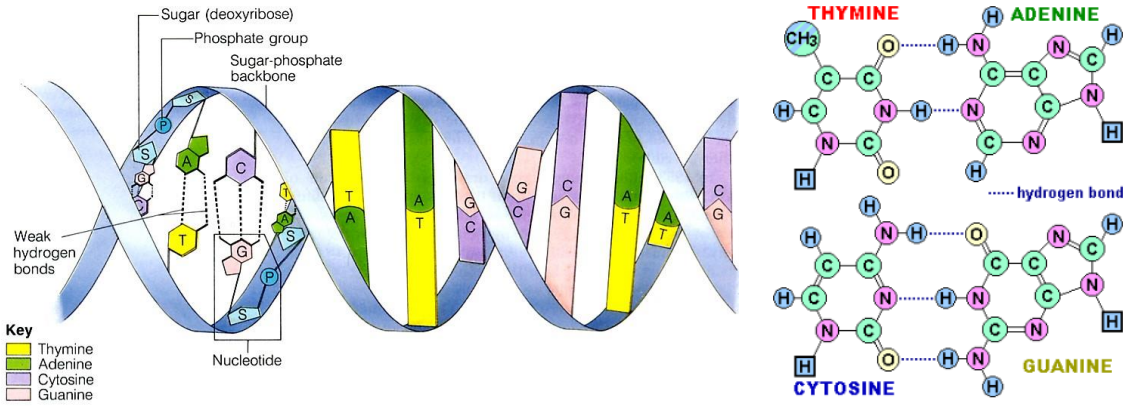

Figure.1.5. Double helical structure for DNA and the Hydrogen bondingbetween nucleotid [17].

The B-form, which is the most celebrated member of the DNA structure family, is the closest to the original Watson–Crick model. It is observed under conditions of high relative humidity and is characterized by a near-perfect `ten' units per turn and the base pairs being located nearly astride the helix axis and normal to it. [18, 19] The term A-DNA was first used to describe the X-ray pattern recorded for fibers of the sodium salt of calf thymus DNA under conditions of low humidity and was subsequently used to describe the structure which gives rise to this pattern. It is a right-handed double helix with 11 residues per turn. The base pairs are considerably displaced from the helix axis as well as being inclined to it. The main differences between the A form and B form of DNA is due to the difference in the conformation of the deoxyribose sugar ring in each form.[20, 21] C-form DNA was first observed for the lithium salt of calf thymus DNA and has about 9.3 residues per turn of helix. Both the C form and A form can be obtained depending on the salt content of the medium. The C- form is also double-stranded helices with right-handed twists, but with slightly different structural parameters. The Z-DNA is a left-handed double helical structure with a 4.4 nm turn length and 12 base pairs per turn. Under conditions of low humidity and in the presence of certain salts, some parts of the DNA molecule rich in purine-pyrimidine sequences (stretches of alternating G and C sequences) are in a special way prone to conversion into the Z form. All the forms (A, B, C and Z) are stable within a range of ionic or humidity conditions and the way one can observe them depending on the primary structure of the polynucleotide chain. [22] The structures for A-, B-, C- and Z-DNA are shown in Figure 1.6. A-DNA , B-DNA and C-DNA are right-handed uniform double-helical structures, while Z-DNA is a left-handed double helix with a dinucleotide repeat and the backbone follows a zigzag path.[23]

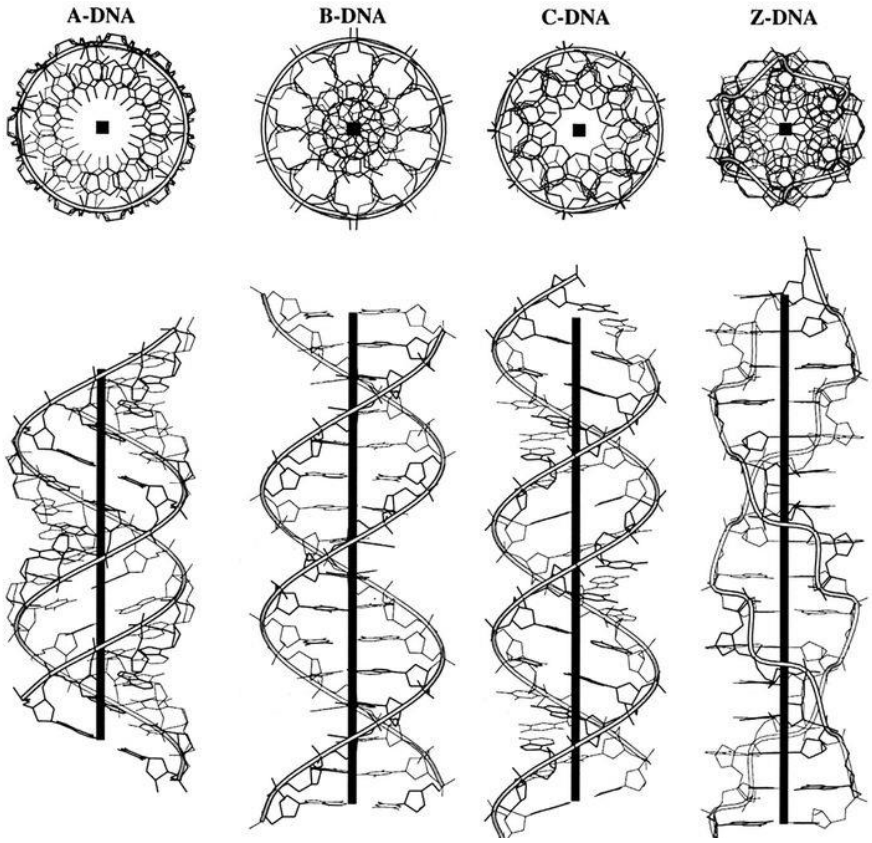

Figure.1.6. The different forms of DNA. [20]

1.5.3 Quad DNA

G-Quad DNA describes a family of four-stranded quadruplex DNA structures with Hoogsteen-type hydrogen bonding between the four guanines in each of the stacked G-tetrads. They can be formed with a parallel arrangement of four strands, as observed for poly (G) and some G- rich oligonucleotides, and also by folded-back chains of oligonucleotides, as observed for some naturally occurring telomeric DNA sequences, which have runs of Gs with A/T interruptions.[24, 25, 26] In the past few years, considerable efforts were focused on designing and synthesizing compounds that can target G-quad-DNA efficiently. This new impetus originates in a growing

body of evidence that bolsters G-quad structures as crucial elements to control cancer cell proliferation. [27]

G-quad-DNA results from the hydrophobic staking of several quartets, each quartet being a planar association of four guanines held together by eight hydrogen bonds. A cation like (Na or K) is located between two quartets forming cation-dipole interactions with eight guanines. This reduces the electronic repulsion of the 8 central oxygen atoms, thus enhancing hydrogen bond strength and stabilizing quartet stacking. G-quartets may now have applications in areas varied from super molecular chemistry to medicinal chemistry. It considers an excellent module for nanotechnology and guanine rich sequences to form higher order structures as synapsable-DNA.[28]

1.6 DNA and Technology

The scientists are using DNA technology for a wide variety of purposes and products. One of the examples of DNA technology is cloning, which is the process of making multiple, identical copies of a gene. Cloning also gives us pest-resistant plants, vaccines, heart attack treatments and even entirely new organisms. DNA technology has a major impact on the pharmaceutical industry, agriculture, disease therapy and even crime scene investigations. The application of DNA in Forensics is a significant advancement in science in last two decades. DNA typing has become increasingly automated and miniaturized. Also, with the coming of short tandem tepeat (STR) technology, even the minutest sample of degraded DNA can yield a profile, providing valuable case information. In addition, DNA vaccines, compared to traditional antigen vaccines have several practical and immunological advantages that make them very attractive for the aquaculture industry. [29, 30]

Furthermore, DNA chip technology that utilizes microscopic arrays (microarrays) of molecules immobilized on solid surfaces for biochemical analysis is one of the new examples of DNA technology. Microarrays can be used for expression analysis, polymorphism detection, DNA re0sequencing, and genotyping on a genomic scale. Also the interactions of flavonoids with DNA, tRNA, and metal ions are of major biochemical and biological importance to demonstrate the potential antioxidant activity of polyphenolic compounds. [31]

1.7 DNA–Drug Interactions

The interaction of DNA with drugs is among the important aspects of biological studies in drug discovery and pharmaceutical development. The binding interactions of external molecules with DNA often result in significant changes in their properties and gene expression, which influences cell proliferation and has important impact on physiological functions. Thus, understanding the mechanisms of drug–DNA binding is crucial for predicting the parameters that required for therapeutic drugs.[32] DNA as carrier of genetic information is a major target for drug interaction because of the ability to interfere with transcription (gene expression and protein synthesis) and replication which is a major step in cell growth and division. The latter is central for tumorigenesis and pathogenesis. Over the last three decades, massive advances and efforts have been focused on ligand-DNA interactions. The study of ligand-DNA interactions is important for a complete understanding of replication and transcription processes, which are attractive targets for the rational design of anticancer and antibiotic drugs. Most chemotherapeutic anticancer drugs currently used are coming from or derived from DNA-binding ligands which interact with the DNA duplex by three general binding modes: DNA intercalation, groove binding and covalent binding (will be explained in the next section).[32]

1.7.1 DNA-Drug Interaction Modes

There are several types of interactions associated with which ligands bind to DNA. These include intercalation, non-covalent groove binding, covalent binding/cross-linking, DNA cleaving, nucleoside-analog incorporation. Consequences of these binding interactions involve changes to both the DNA and drug molecules to accommodate the new complex formation. In many cases, changes to the structure of the DNA duplex result in altered thermodynamic stability and are manifested as changes in the functional properties of the DNA. In specific word, DNA may undergo conformational changes to B-form, A-form, Z-form, quadruplexes, triplexes and other structures as a result of the binding process to different compounds [32, 33]

The interaction of drugs with DNA occurs principally through control of transcription factors and polymerases, through RNA binding to DNA double helix to form nucleic acid triple helical structures or RNA hybridization (sequence specific binding) to exposed DNA single strand regions forming DNA-RNA hybrids that may interfere with transcriptional activity. But the most dominant DNA-interactive ligands categories include those by small aromatic ligand molecules that bind to DNA double helical structures. The type of chemical interactions between small molecules and DNA is an important tool for the prediction of potential physiological and/or therapeutic consequences of such interactions. The DNA interactions with small aromatic molecules can be classified as covalent and non-covalent, where non covalent interactions can be further classified as intercalation and groove binding. [34]

1.7.2 Intercalation Binding Mode

The interaction of DNA with small molecule through intercalation (non-covalent) takes place when a planar aromatic ring systems inserted between base pairs and is generally independent of base pair sequence. Planar organic molecules containing several aromatic condensed rings often bind DNA in an intercalative mode to provide the required stacking forces for locating the ligands between the stack of the base pair of DNA. Intercalation requires changes in the sugar-phosphate torsional angles to accommodate the aromatic compound which is accompanied by other changes in the helical parameters such as unwinding, bending, etc. The stability of intercalation complexes is governed by van der Waals, electrostatic and hydrophobic forces. Molecules that bind to double-stranded DNA (ds-DNA) by interactive mode have been significantly used as drugs. [34, 35]

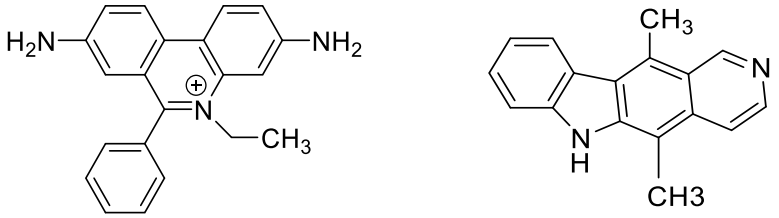

Ethidium Ellipticine

Figure. 1.7 Chemical structures of some intercalators.[36]

Since the structure of DNA by Watson and Crick was proposed, several established therapeutic modalities have been worked on for targeting DNA. Intercalators (Fig. 1.7) which can bind to DNA and inhibit the activity of many enzymes that utilize DNA as a substrate is one of the proposed model. The drugs that intercalate to DNA are used as anti-cancer drugs and this is mainly because of the development of reductively-activated drugs as hypoxia-selective agents and as 'carriers' for the delivery of other reactive functionality. [37] Furthermore, the most widely and successfully used anticancer agents are the non-specific DNA damaging chemicals which include

topo isomerases inhibitors (TOPO) I and II, and alkylating agents. In addition it has been shown that the intercalating agent causes an increase in DNA length, like some antitumor antibiotic drugs (daunomycin, doxorubicin, echinomycin, etc.).[34, 35]

1.7.3 Minor-Groove Binding Mode

Minor groove-binding (interaction of drugs with grooves of DNA) involves greater binding affinity and higher sequence specificity than that of intercalation. DNA minor-groove binding is demonstrated for neutral, mono-charged and multi-charged ligands. The dominant forces for small molecule minor-groove binding interactions are van der Waals, electrostatic, hydrogen and hydrophobic bonding. Sequence specificity for the resulting complex is attributed to hydrogen-bonds between the small molecule and base pairs. Due to the dimensional difference in grooves are widely dissimilar, thus different shaped molecules are required to target them. The binding of these molecules cause close contacts with the walls of the groove, and many hydrogen bonding and electrostatic interactions with the bases and the phosphate backbone. As an example, the DNA can bind with polyamides composed of N-methylimidazole, N-methylpyrrole, and N-methyl-3-hydroxypyrrole which are crescent-shaped molecules that bind to the minor groove of DNA as antiparallel dimers. Side-by-side pairings of aromatic residues stack five-membered heterocycles against each other and the walls of the minor groove, positioning the polyamide backbone and aromatic 3-substituents for intimate contacts with the edges of nucleotide bases on the adjacent DNA strand. [38]

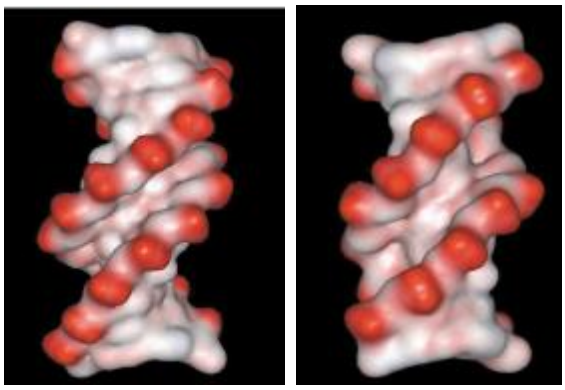

Figure 1.8. (A) Minor-groove binding in to A/T rich region of DNA, B) minor-groove binding in to G/C rich region of DNA. [38]

Compounds that bind in the minor-groove are of current research interest for their therapeutic potential against diseases starting from cancer to a variety of infectious diseases, and also for biotechnology applications. Minor-groove binders also have a number of other properties, such as inhibition, as well as activation of transcription that have provided fundamental new information on gene expression, with a chance for development of completely new and highly specific methods of disease treatment.[39] Minor-groove binders frequently show strong A/T selectivity. This is because A/T-rich grooves have higher electrostatic potential than in the G/C-filled ones which lead to A/T selectivity for the dicationic small molecules, dimensions of the minor-groove at A/T sites are narrower and deeper than G/C locations. (Figure 1.8) Also, the topology at A/T sites allows for easier filling and greater van der Waals contacts by small molecules, while the amino group of G in G/C locations stick out into the groove, thus prohibiting van der Waals contacts comparatively to those achievable at the A/T sites. [34] Minor-groove binders typically have a number of common structural features; a curved shape or the ability to adopt such a shape, groups with positive charges, H-bond donating ability and a relatively flat

conformation (Fig. 1.9). The minor groove in A/T sequences can more easily take on the narrow width that is required for tight binding of the heterocyclic-amidine system of the dictions than the groove in G/C or mixed base pair sequences. The extra H-bond of the G/C base pairs typically leads to a wider minor groove and presents a steric block to deep penetration of compounds into the groove. [38, 40]

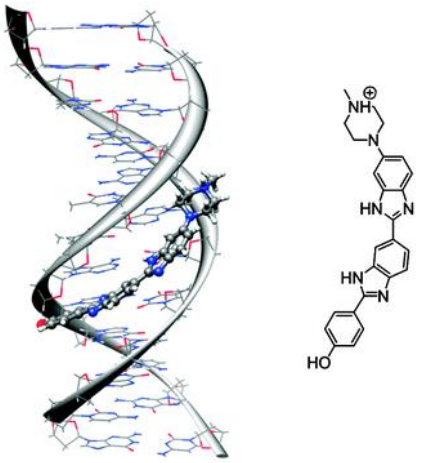

Figure1.9. Chemical structure of the complex between DNA and Hoechst 33258.[50]

1.7.4 Major-Groove Binding Mode

Major-groove binding arises from the hydrogen bonding of molecule or protein to the DNA. The major-grooves are the site for binding of many DNA interacting proteins. Proteins usually bind to DNA by major-groove after recognition and reading the sequence information. However, non-peptidyl compounds bind with the minor-groove allowing simultaneous major groove recognition by proteins. Thus it is important to have a major-groove binding molecule that could block access to proteins that recognize the same groove.[41] Duplexes made up of polypurine–polypyrimidine sequences can be read by oligomer that bind in the major-groove, and form hydrogen bond with bases of the purine strand.[42] They have a beneficial effects that arise

from their binding to DNA nucleobases, by preferentially to the two N7 atoms belonging to two adjacent G nucleobases or, to a lesser extent A/G sequences.[41]

1.7.5 Covalent–Cross Linking Binding Mode

Another important subclass of DNA-binding drugs exert their activities in a metal-dependent fashion, based on the coordination or recognition of a specific metal ion. Platinum complexes are famous examples about this sub-class and specifically, Cisplatin is a well-known anti-cancer drug that works depend on covalent cross-linking mechanism. The formation of the bonds between atoms present in the DNA that prevents DNA from being separated for synthesis or transcription, this mechanism causes mispairing of the nucleotides leading to mutations. [43] The discovery of cisplatin lead in a new period of DNA-interactive anticancer agents based upon coordination chemistry. [44]

1.8 DNA-Protein Interaction and Applications

DNA binding proteins controls several important biological processes, like transcription, recombination, restriction, and replication. Measuring the effects of mutations on binding of DNA and amino acid residues considered a major step in these interactions. DNA-binding proteins also used for gene activation and it is a fundamental regulatory mechanism consisting of the chromatin modifying and transcription complexes to initiate the RNA synthesis.The principle behind the protein-DNA interaction is the DNA can interact with protein through two ways: either specifically or non-specifically. In the case of non-specific interactions, the sequence of nucleotides does not matter, as far as the binding interactions are concerned. Example of non-specifically DNA-protein binding is the interaction between Histone (protein) and DNA (Histone-DNA interaction), and they occur between functional groups on the protein and the sugar-

phosphate backbone of DNA. Specific DNA - protein interactions depend on the sequence of bases in the DNA and the orientation of the bases that can vary with twisting and writhing. These DNA protein interactions are strong, and are mediated by hydrogen bonding, ionic interactions, and other forces (van der Waals, hydrophobic). [45, 46] One of the most widely studied examples of DNA-binding proteins is the transcription factor. The interactions between transcription factors and their DNA binding sites are of particular interest, since these interactions control critical steps. Recently, the protein binding microarray technology permits rapid, high-throughput characterization of in vitro DNA binding specificities for DNA binding proteins by assaying their binding to double-stranded DNA microarrays.

DNA–protein interactions can be determined by several in-vitro experimental techniques. Some of the well-known in-vitro techniques are foot printing assay, southwestern assay, electrophoretic mobility shift assay, yeast one-hybrid assay, phage display and proximity ligation assay. The foot printing assay one of the common methods, and the principle behind that is based on protection of protein-bound DNA from degradation. The technique is used to decipher the specific sequence to which a DNA-binding protein or other molecule binds. The method employs chemical or enzymatic digestion of a naked, and protein bound-DNA oligomers. Both reactions are then compared by gel electrophoresis. [46] As these binding modes has potential in different forms, it is important to monitor how the drugs bind to the DNA to predict the therapeutic potential of the drug. There are several spectroscopic techniques available in literature that are aimed at monitoring these interactions. But, they cannot different DNA binding modes easily. One of the main goals of the present study is to find novel optical techniques that can monitor and differentiate drug-DNA interactions. As the drugs are focal point of research presented in the thesis, a detailed description is provided here.

1.9. Overview of the Investigated Drugs

1.9.1 DAPI

DNA binding drugs have potential applications as anti-cancer and anti-viral agents. Aromatic diamidines have different DNA-binding modes with an emphasis on DNA groove specificity for the groove-binding and intercalation modes. While most DNA-interacting agents selectively bind to DNA by either groove-binding or intercalation, some compounds can exhibit both binding modes. The binding mode with the most favorable free energy for complex formation depends on the DNA sequence and structural features of the bound ligand. DAPI (4, 6-diamidino-2-phenylindole) (Fig. 1.10), one of aromatic diamidines has become one of the most widely used DNA probe owing to its large increase in fluorescence quantum yield upon binding to double-stranded DNA. [47, 48]

DAPI is a blue fluorescent drug that fluoresces brightly upon selectively binding to the double stranded DNA. Two modes of interactions have been proposed between DAPI and DNA, one is the minor-groove binding mode that prefer A/T-rich region as interaction sites, whereas the other one is the intercalative binding mode with G/C or mixed A/T and G/C DNA sequences. However, the minor-groove binding to A/T regions is 2 orders of magnitude stronger than the intercalative binding mode. [49] The fluorescence of DAPI (ex = 358 nm, em = 461 nm) increases approximately 30 times when 20-fold base-pair excess of DNA is added. Its selectivity for DNA and high cell permeability allows efficient staining of nuclei with little background from the cytoplasm. DAPI is a classic nuclear counterstain for immunofluorescence microscopy, as well as an important component of high-content screening methods requiring cell-based quantitation of

DNA content. The fluorescence quantum yield of DAPI is strongly enhanced by AT base pair sequences, and it is widely used as a specific fluorescence marker for chromosomal DNA. [50]

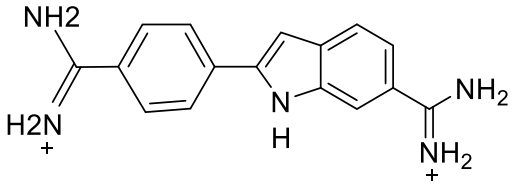

Figure 1.10. Chemical structure of (DAPI) drug (4, 6 diamidio-2-phenylindole). [51]

DAPI binds preferably to A/T-regions in the minor groove of DNA, and its high-affinity binding mode has been characterized in detail by crystallography. DAPI is not chiral and does not display circular dichroism signal (CD) when free in solution. However, upon binding to DNA, it acquires strong induced CD signal owing to interactions with the chiral substrate. For ligands bound to DNA, the induced CD measurements are very sensitive to the binding geometry. Therefore several different binding modes can be recognized for DAPI. For example, at low binding ratio the CD spectrum for the DAPI-DNA binding mode starts to change due to allosteric change of the DNA structure induced by DAPI ligand. [47, 51] DAPI is able to show different biological effects including antibiotic, antitypanosomal, and antiviral activity. [47] DAPI has proven to be a very efficient nucleic acid stain in studies of the organization of chromatin in eukaryotes. [50, 51] DAPI also allows easy identification of mitotic figures and can be used to supplement cytochemical studies involving cell division in the nervous system. [52]

1.9.2 Thiozole Orange

There are variety of organic fluorescent dyes that were used as drugs. They can be incorporated at specific positions within the oligonucleotide sequence or DNA that are considered

important tools for many techniques like genetic analysis, DNA microarrays, or single base mismatch analysis. Many of the organic dyes have negligible fluorescence in solution, and obtain intense fluorescence when bound to nucleic acids. The increase in fluorescence is due to a rise in rigidity when the rotation around the bond between the aromatic systems is restricted which closes a channel for non-radioactive decay.[53] Thiazole orange (TO) is one of the asymmetric cyanines dyes that consists of two aromatic ring systems connected by a bond that is a part of conjugated system.(Fig 1.11)

TO provides high fluorescence upon intercalation with DNA and the fluorescence quantum yield has been reported to increase about 18,900 upon binding to DNA. The binding is presumably intercalative as shown by linear dichroism and NMR measurements.[53, 54] The use of intercalating dyes not only report the binding site of recognition helix, but also anchor the peptide at a certain specific site of DNA has been significantly enhanced the binding affinity. The other advantage of intercalating dyes is their relatively long absorption maxima, which reduces problems of background absorption from biological material. [55] TO or its analogues could be used to produce dimeric dyes which would be excellent candidates for compounds that would form stable, highly fluorescent complexes with dsDNA. Furthermore, laser excitation at 488 nm and simultaneous confocal detection at 500-565 nm (dsDNA-TO emission) or dimeric Thiazole-orange (TO TO) allowes detection, quantitation, and accurate sizing of restriction fragments ranging from 600 to 24,000 basepairs at pico-gram sensitivity per band.[56]

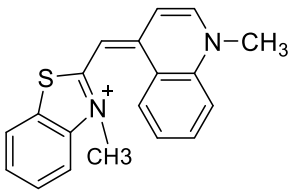

Figure 1.11. Chemical structure of TO.[56]

1.9.3 Hoechst Derivatives

The Hoechst derivative stains are part of a family of blue fluorescent stains for labeling DNA in fluorescence microscopy and can also be used as drugs. Because these fluorescent stains label DNA, they are also commonly used to visualize nuclei and mitochondria. Two of these closely related dyes are: Hoechst 33258 (Figure 1.12) and Hoechst 33342. Both dyes are excited by ultraviolet light at around 350 nm, and both emit blue/cyan fluorescence light around an emission maximum at 461 nm. Unbound dye has its maximum fluorescence emission in the 510–540 nm range. The dye Hoechst 33258 [bis (benzimidazo1e)] derivative becomes brightly fluorescent when bound to A/T rich sequences of double-stranded DNA.

It produces a bright microscope image of chromosomal DNA with high contrast due to minimal interference from dye bound to other cell components. It is helpful for visualization of newly synthesized DNA, since the fluorescence of Hoechst 33258 is quenched by 5-bromodeoxyuridine (BrdU) which has been incorporated into chromosomes. Quenching of 33258 Hoechst fluorescence by BrdU can be canceled by appropriate alterations in solvent conditions. That lead to revealing changes in dye fluorescence of microscopic specimens specifically due to BrdU incorporation. In addition, Hoechst 33258 can interact with G/C rich sequences in a different way than via the phosphate charge. The corresponding fluorescence increase of the dye is much less intense than with A/T sequences. [57, 58]

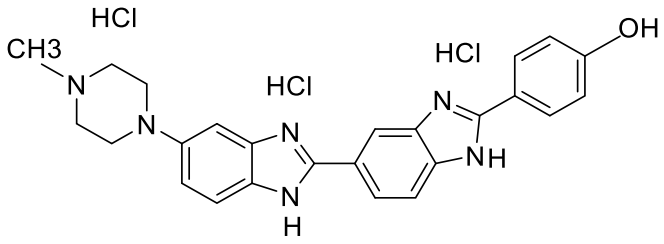

Figure1. 12. Molecular structure of Hoechst 33258.[59]

The interaction of Hoechst 33258 with DNA has been studied by different spectroscopic techniques to elucidate the binding mechanism. There is a considerable shift between the excitation and emission spectra that makes Hoechst dyes useful in experiments that use multiple fluorophores. The binding of Hoechst with DNA is accompanied with a decrease in extinction coefficient and shift in the adsorption spectra to a higher wavelength, without increase in viscosity when Hoechst bind to DNA. These findings suggest that Hoechst does not bind to DNA by intercalation or by ionic interaction with the phosphate groups, but rather by an attachment to the outside of the double DNA helix by interacting with the base pairs (minor groove). This type of binding allows greater sensitivity to the base composition than when binding occurs with intercalating agents. Hoechst dyes are soluble in water and in organic solvents such as dimethyl formamide or dimethyl sulfoxide. Aqueous solutions are stable at 2–6 °C for at least six months when protected from light. For long-term storage the solutions are instead frozen at ≤-20 °C. [59, 60]

The current high level of interest in these drugs is not only because of their potential to range of diseases, but is also due to their ability to act as DNA sequence recognition agents and modifiers of protein–DNA function. The Hoechst stains may be used on live or fixed cells, and are often used as a substitute for another nucleic acid stain, DAPI. This is because, both DAPI and Hoechst bind to minor groove site of DNA and they have close value of association constant (Ka). The key difference between them is that the additional ethyl group of Hoechst renders it more lipophilic, and thus more able to cross intact cell membranes. Furthermore, Hoechst 33258 is longer than DAPI (because it contacts 5 base-pairs) whereas DAPI contacts only three base-pairs.

These dyes can also be used to detect the contents of a sample DNA by plotting a standard emission-to-content curve.[61]

1.9.4 Netropsin

Netropsin (Figure 1.13) and its close relative distamycin are antiviral and antitumor antibiotics. They have received extensive study as an example of base-specific binding drug, although they are too toxic for clinical use. Netropsin is an oligopeptide antibiotic that is considered a highly basic, small molecule produced by Streptomyces netropsis. It exhibits a wide spectrum of toxicities including antibacterial, unti-fungal, -viral activities and the inhibition of DNA or RNA tumor viruses in mammalian cells. Netropsin is non-intercalative DNA-binding drug molecules. NMR experiments show that Netropsin binds within the minor groove of the intact double helix, using hydrogen bonds between Netropsin amide NH and exposed adenine N-3 and thymine 0-2 at the minor-groove. [62, 63]

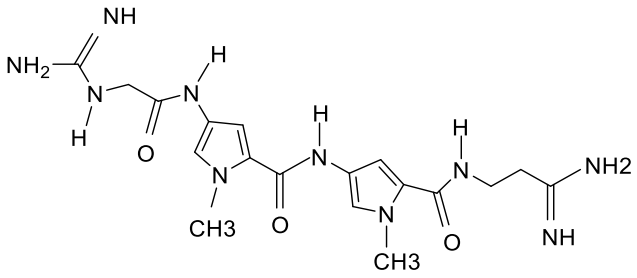

Figure 1.13. Molecular structure of Netropsin. [62]

Netropsin can interact with DNA as an anticancer drug and form a complex that has been elucidated by X-ray analysis. The result appears that the antitumor antibiotic drug binds within the minor-groove by displacing the water molecules of the spine of hydration. Netropsin amide NH

provide hydrogen bonds to bridge DNA adenine N-3 and thymine O-2 atoms occurring on adjacent base pairs and opposite helix strands, exactly as with the spine of hydration. The tightness of the groove, forces the Netropsin molecule to sit symmetrically in the center, with its two pyrrole rings so that each ring is parallel to the walls of its respective region of the groove. Drug binding didn't cause any unwinding or elongation for the double helix, but it does force open the minor groove by 0.5-2.0 A, (didn't disrupt the Watson-Crick base pairs but does perturb resonances of the protons located on the base pair edges that face the minor groove). It bends back the helix axis by 8 degrees across the region of attachment. The Netropsin molecule has an intrinsic twist that favors insertion into the minor groove of DNA, and it is given a small additional twist upon binding.

The base specificity that makes Netropsin bind preferentially to runs of four or more A X T base pairs is provided not by hydrogen bonding but by close van der Waals contacts between adenine C-2 hydrogens and CH groups on the pyrrole rings of the drug molecule. Furthermore, because of the principal difference between A /T and G/ C base pairs in the minor groove region is the presence of the N-2 amine groups on guanine, It has been suggested (since many years ago) that the lack of binding of Netropsin to G/C base pairs might arise from steric hindrance by this NH_2 group. Netropsin binds only to double helical DNA and it does not bind to most DNA-RNA hybrids or most single strands. [(62)]

The binding of Netropsin to DNA is very strong and exists partially even in media of high ionic strength. This binding has been intensively studied and it can be utilized for different applications. For example, it has been reported that the binding of Netropsin is used for the isolation of (A/T)-rich satellite components of DNA from Drosophila melanogaster. [(65)] Also, the complexity of calf thymus DNA can be used as an advantage to study the factors influencing changes in DNA density produced by addition of Netropsin. [(64)] Netropsine as a minor-groove

binders also have a number of other properties, such as inhibition, as well as activation of transcription that have provided fundamental new information on gene expression with the potential for development of completely new and highly specific methods of disease treatment.[65] Fig. 1.14 shows the binding of Netropsin as an anticancer drug binds to minor groove of DNA at (A/T) center by. It widens the groove slightly and bends the helix axis back by 8 degree, without neither unwinding or elongating the double halix.[66]

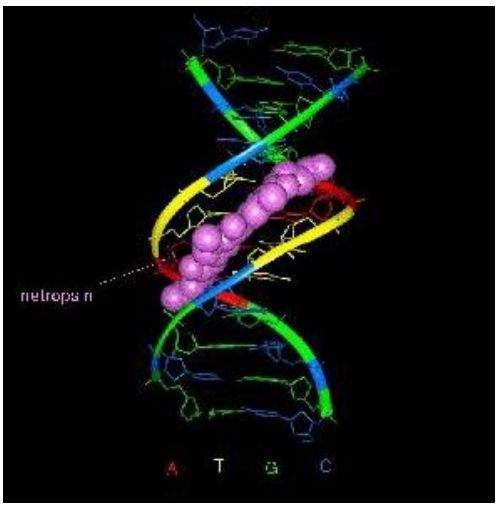

Figure 1.14. Minor-groove binding of Netropsin with ds- DNA.[66]

1.9.5 Doxorubicin

Doxorubicin (Dox) is one of the best-known members of the anthracycline family of antibiotics. It was first introduced in the 1960s and is widely used as an anticancer drug for many tumors as it is considered one of the most effective anticancer drugs developed [67]. It is sold under the trade names Adriamycin**,** which is commonly used as cancer chemotherapy. Dox derived by chemical semi synthesis from a bacterial species. It is an anthracycline antitumor antibiotic, closely related to the natural product Daunomycin, and like all anthracyclines, it works by intercalating DNA. Dox has the ability to penetrate tissues highly effectively, and its ability to

remain inside nucleated cell is due to its lipophilic characteristics and DNA intercalating binding properties.[68] Additionally, doxorubicin inhibits topoisomerase II (that relaxes supercoils in DNA for transcription) which results in an increased and stabilized cleavable enzyme-DNA linked complex during DNA replication. As a result, it will subsequently prevent the ligation of the nucleotide strand after double-strand breakage.[69,70] Dox also forms oxygen free radicals resulting in cytotoxicity secondary to lipid peroxidation of cell membrane lipids.

The formation of oxygen free radicals also contributes to the toxicity of the anthracycline antibiotics, namely the cardiac and cutaneous vascular effects. [70] The fluorescence characteristics of Dox and Daunomycin (another anthracycline anti-tumor drugs) are often used to monitor their localization within lipid bilayers, liposomal delivery systems, and their interaction with DNA and other macromolecules by monitoring the fluorescence intensity at the emission λ_{max}.[71] The planar aromatic chromophore portion of the molecule intercalates between two base pairs of the DNA. While the six-membered daunosamine sugar sits in the minor-groove and interacts with flanking base pairs immediately adjacent to the intercalation site, as evidenced by several crystal structures. By intercalation, doxorubicin can also induce histone eviction from transcriptionally active chromatin, which result in DNA damage response. Also epigenome and transcriptome are deregulated in doxorubicin-exposed cells. [67, 70]

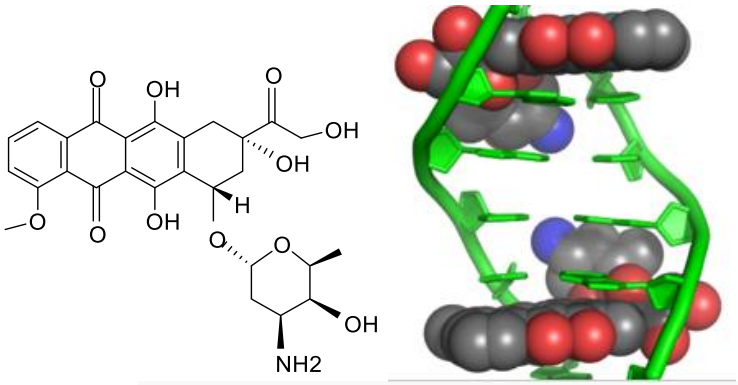

Figure 1.15. Diagram of two Dox molecules intercalating with DNA.

Dox is also a powerful iron-chelator. The iron-doxorubicin complex can bind DNA and cell membranes producing free radicals that immediately cleave DNA and cell membranes. [70] Like most drugs, Dox enters the cell via passive diffusion, generally accumulating to intracellular concentrations that exceed the extracellular compartments by 10- to 500-fold. Dox seems to accumulate mostly in the liver, and that is most likely due to the organ's role in metabolism.[68] It is commonly used in the treatment of a wide range of cancers, including hematological malignancies blood cancers, (like leukemia and lymphoma), many types of carcinoma (solid tumors) and soft tissue sarcoma. It is often used in combination chemotherapy as a component of various chemotherapy regimens. The drug is administered intravenously as a hydrochloride salt, and it is photosensitive thus, containers are often covered by an aluminum bag and/or brown wax paper to prevent light from affecting it. Dox considered as primary therapy for Hodgkin's lymphoma disease, as well as cancers of the bladder, breast, stomach, lung, , multiple myeloma, and others. Doxorubicin is also known to be fluorescent, and its fluorescence is quenched by binding to DNA, and shielded by micelle encapsulation. It is also known to self-quench at high concentrations. [70, 71]

1.9.6 Thioflavin T

Dye used to visualise stacked β sheets in vitro and in vivo, specifically its Fluorescent cell-permeable amyloid binding benzothiazole salt. Binding induces a shift in excitation maximum (from 385 nm to 450 nm) and emission maximum (from 445 nm to 482 nm). Highly soluble in water and limited ability to cross the blood-brain barrier BBB. [73]

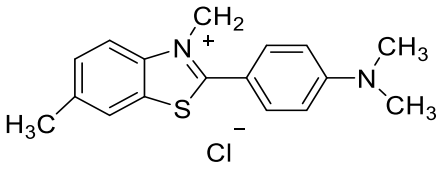

Figure 1.16. Molecular structure of Thioflavin T (Th T)

Thioflavin T stain considers a common method for amyloid fibrils detection, which is based on the characteristic changes in Thioflavin T (ThT) fluorescence intensity upon binding of this dye to amyloid fibrils. ThT interaction with amyloid fibrils was highly specific, since the addition of the dye to solutions of proteins in folded, unfolded, or partially folded monomeric forms was not accompanied by changes in the emission intensity. Therefore, due to these unique properties, ThT represents a useful and convenient tool for the fast and reliable diagnostics of the presence of amyloid fibrils in disease-affected tissues and organs.[74] The quantum yield and fluorescence lifetime of Thioflavin T (ThT) basically depends on temperature and glycerol content in the dissolving mixture (water-glycerol). Fluorescent properties of ThT are typical for the specific class of fluorophores known as molecular rotors. It has been found that the low ThT fluorescence intensity in the solvents with low viscosity is caused by the non-radiative deactivation of the excited state, associated with the torsional motion of the ThT benzthiazole and aminobenzene rings relative to each other. Which results in the transition of ThT molecule to non-fluorescent twisted internal charge transfer (TICT) state. Torsional movements of the ThT fragments take place in the same temporal interval as solvent relaxation, which leads to non-exponential fluorescence decay of the dye in viscous solvents. This photo-physical model successfully explains the fluorescent properties of ThT in solvents with different viscosities. [74]

ThT, considers one of the two classic markers for the detection of amyloid fibrils (the main cause of Alzheimer's disease, Parkinson's diseases, and late-onset diabetes), which are Thioflavin T (ThT) and Congo Red (CR). These diseases characterized by deposition of Aβ fibrils in brain. The use of organic dyes (ThT, CR) leads to advance diagnosis of AD diseases, and the others, especially in elderly people. Thioflavine T specifically binds Aβ fibrils and that is the reason behind using it to stain amyloid in biological samples. The binding of ThT shows enhanced fluorescence upon binding with amyloid tissue sections with excitation and emission maxima at about 450 and 480 nm, respectively. That is why it considers a standard dye for amyloid detection. In addition, it is a charged molecule and hydrophilic, so it does not pass the blood–brain barrier. [72]

1.10 Existing Techniques to Monitor Drug-DNA Interaction

There are several techniques that are available in literature to monitor drug-DNA interactions that include the classical competition dialysis assay or UV-Vis spectrophotometry to capillary electrophoresis-mass spectrometry or the powerful tandem HPLC-MS or the renewed gel mobility electrophoresis assay. Some of the common techniques include UV-Visible absorption, fluorescence spectroscopy, vibrational spectroscopy, viscometry, X-ray diffraction, NMR, circular dichroism, chromatography and capillary electrophoresis. UV-Vis absorption spectroscopy can be utilized to detect the DNA-drug interaction by measuring the changes in the absorption properties of the DNA or the drug. Infrared spectroscopy is also employed for the studying drug-DNA interaction as it can distinguish different forms of DNA also via the changes in the vibrational frequencies of base pairs upon drug binding. Fluorescence of the drug was also used to monitor the drug binding to DNA. Viscometry is a common technique for following the binding of the

drugs that are intercalators. Most of these techniques are powerful, but they cannot differentiate the mode of interaction being intercalator or minor-groove binder or covalent cross linking. Such a technique would be useful not only for monitoring the binding but also gives insights into the action the drug. The main goal of the research conducted in this thesis is to develop novel spectroscopic tools that can differentiate different drug-DNA binding modes. The research approach is to use two-photon absorption (2PA) spectroscopy to monitor drug-DNA binding which can differentiate various modes. What is 2PA and how it can be able to monitor and drug-DNA interaction modes is explained below.

1.11 Research Approach

The approach used in the thesis is to use 2PA spectroscopy to follow drug-DNA binding. Simultaneous absorption of two-photons to reach an excited state is called 2PA. It depends on the square of the light intensity and uses the near infrared radiation. It has inherent advantages compared to conventional one-photon spectroscopy. The ability of the molecule or drug to absorb two-photons is determined by 2PA cross-sections. Then, how the 2PA cross-sections can differentiate drug-DNA binding mode? In a recent study, Rebane and co-workers have shown that the 2PA spectroscopy can be quite sensitive to local electric fields in proteins with their work on fluorescent proteins. Previous work from the group has also shown that 2PA cross-sections in micelles are quite sensitive to the electrostatic fields of micelles. DNA possesses inherent electric field due to its phosphate backbone and drug-DNA interactions can be monitored with such a technique. So, our research approach was to use 2PA spectroscopy based technique to differentiate drug-DNA binding modes.

The local electric fields can have noticeable influence on 2PA cross sections via the following relationship:

$$\delta = \frac{2(2\pi)^4 f_L^4}{15(nhc)^2}(1 + 2cos^2\theta)|\mathrm{M_{ge}}|^2|\Delta\mu_{\mathrm{ge}}|^2 g(2v)$$

where δ is two-state two-photon absorption cross section, M_{ge} is the transition dipole moment vector existing between the ground (g) and excited (e) states, θ is the angle between vector M_{ge} and $\Delta\mu_{ge}$, $\Delta\mu_{ge}$ is the difference between the permanent dipole moments existing in the ground and excited states, *g(2v)* is normalized line shape function, *c* is the speed of light, *n* is the refractive index, *h* is the Planck's constant, and $f_L = \frac{(n^2+2)}{3}$ is a local field factor.

It has also been shown that the local electric fields result to change in dipole moment by increasing the induced dipole moment via:

$$\Delta\mu_{ge} = \Delta\mu_{ge}^0 + 0.5\Delta\mu_{ge}^{ind} = \Delta\mu_{ge}^0 \pm 0.5\left(\overline{\Delta\alpha}\right).\bar{E} = \Delta\mu_{ge}^0 \pm 0.5(\Delta\alpha)Ecos\theta$$

where $\Delta\alpha = \alpha_e - \alpha_g$ is the change in polarizability between the excited state and ground state, θ is the angle between the transition dipole moment of the molecule and electric field vector, $\Delta\mu^0_{ge}$ is the change in the permanent dipole moment in the zero-field situation, and *E* is local electric field vector.

From the expressions expressed above, 2PA cross-section is directly proportional to the square in of the change in permanent dipole moment and change in dipole moment. As a result, δ is sensitive to the electric field, and, thus, changing the chromophore's electrostatic environment and the orientation changes the δ. In the case of drugs binding to DNA, alignment of drug

polarizability vector with electric field is possible and it can lead to enhancement or changes in 2PA cross-sections that can give an idea about the binding mode of the drug with the DNA.

1.12. Outline of the Thesis

This thesis is focused on the study of Drug-DNA interactions, which is one of the major points of concern in the biomedical applications and pathogen detection. The thesis as a whole is comprised of four chapters. The first chapter is introduction to the thesis. Areas like the DNA-Drug interaction and DNA-protein interaction are covered here. In addition, the implications of DNA-Drug interaction on diseases are also covered. A brief introduction about the methodology behind the development of novel techniques used in the thesis is provided here. Furthermore, the use of two-photon absorption fluorescence spectroscopy to monitor DNA-Drug interaction for the drugs that fluoresce and differentiate between the binding modes for them was the first approach, while following the DNA-drug interaction for the drugs that are not fluorescent was the second approach.

The second Chapter covered various experimental techniques that are used for the investigations that included one-photon fluorescence techniques, 2PA cross-sections, time-resolved spectroscopic techniques, and circular dichroism.

The third Chapter of the thesis is on the differentiation of intercalation and minor-groove binding DNA interactions with DAPI and ThO drugs as examples. DAPI was chosen as it is a well-known minor-groove binder while ThO was known for its intercalation. The interaction of these drugs with salmon sperm and calf-thymus DNA was studied with one and two-photon fluorescence technique and the results suggested this technique can differentiate them efficiently.

Chapter Four of the thesis is focused on the use of 2PA fluorescence technique to monitor the binding interactions of the drugs that are not fluorescent by using two kinds of reporters that are minor-groove binders or intercalators. This study has focused on determining the binding interactions of Netropsin and Doxorubicin with DNA.

1.13 References

1. Wang, C.; Carter-Cooper, B.; Du, Y.; Zhou, J.; Saeed, M. A.; Liu, J.; Guo, M.; Roembke, B.; Mikek, C.; Lewis, E. A.; Lapidus, R. G.; Sintim, H. O. *Eur. J. Med. Chem.* **2016**, *118*, 266–275.
2. Doan, P. H.; Pitter, D. R. G.; Kocher, A.; Wilson, J. N.; Goodson, T. *J. Am. Chem. Soc.* **2015**, *137* (29), 9198–9201.
3. Marky, L. A.; Lee, H.-T.; Garcia, A. *Encycl. Life Sci.* **2010**, 1–9.
4. Lodish H, Berk A, Zipursky SL, et al. *Molecular Cell Biology*, 4th edition; W. H. Freeman: New York, **2000**.
5. Martin.E; Wolfram.S. *Principal of Nucleic Acid Structure,* **1984.**
6. Marky, L. A.; Lee, H.-T.; Garcia, A. *Encycl. Life Sci.* **2010**, 1–9.
7. Lewis, J.; Raff, M.; Roberts, K. *Am. J. Vet. Res.* **2014**, *75*, 613.
8. Moeinzadeh, S.; Jabbari, E. *Handbook of Nanomaterials Properties*; Vol 2; springer; **2014**, 285-297.
9. Breslauer, K. J.; Frank, R.; Blöcker, H.; Marky, L. A. *Proc. Natl. Acad. Sci. U. S. A.* **1986**, *83* (11), 3746–3750.
10. Brockman, J. M.; Frutos, A. G.; Corn, R. M. J. Am. Chem. Soc. **1999**, 121 (35), 8044–8051.
11. Au, K. G.; Cabrera, M.; Miller, J. H.; Modrich, P. *Proc. Natl. Acad. Sci. U. S. A.* **1988**, *85* (23), 9163–9166.
12. Lewis, J.; Raff, M.; Roberts, K. *Am. J. Vet. Res.* **2014**, *75*, 613.
13. Bochkareva, E.; Belegu, V.; Korolev, S.; Bochkarev, A. *EMBO J.* **2001**, *20* (3), 612–618.

14. Vologodski , A. Topology And Physics Of Circular DNA; CRC Press: Boca Raton, **1992**, pp 1-6.

15. Stroud, A.; Liddell, S.; Allers, T. *Front. Microbiol.* **2012**, *3* (JUN), 1–14.

16. Raven P., Johnson G., Jonathan K., Losos S., Singer R., Mason, *Biology*, 8rd ed; McGraw-Hill: Boston, 2008; p 49.

17. Langridge, R., Marvin, D. A., Seeds, W. E., Wilson, H. R., Hooper, C. W., *J. Mol. Biol*, **2**, Wilkins, M. H. F. & Hamilton, 1960; 38–64.

18. Harmouchi, M.; Albiser, G.; Premilat, S. *Eur. Biophys. J.* **1990**, *19* (2), 87–92.

19. Franklin, R. E.; Gosling, R. G. *Acta Crystallogr.* **1953**, *6* (8), 673–677.

20. Fuller, W., Wilkins, M. H. F., *Mol. Biol*. **12**, Wilson, H. R. & Hamilton: L. D., **1965**; 60-80.

21. Grimm, H.; Rupprecht, A. *Eur. Biophys. J.* **1989**, *17* (4), 173–186.

22. Seeman, N. C. *Annu. Rev. Biochem.* **2010**, *79* (April), 65–87.

23. Mohanty, D.; Bansal, M. *Nucleic Acids Res.* **1993**, *21* (8), 1767–1774.

24. Stern, J. C.; Anderson, B. J.; Owens, T. J.; Schildbach, J. F. *J. Biol. Chem.* **2004**, *279* (28), 29155–29159.

25. Biffi, G.; Tannahill, D.; McCafferty, J.; Balasubramanian, S. Nat. Chem. **2013**, 5 (3), 182–186.

26. Monchaud, D.; Allain, C.; Bertrand, H.; Smargiasso, N.; Rosu, F.; Gabelica, V.; De Cian, A.; Mergny, J. L.; Teulade-Fichou, M. P. *Biochimie* **2008**, *90* (8), 1207–1223.

27. S. Neidle, S. Balasubramanian. *Quadruplex Nucleic Acid*; RSC Publishing:Cambridge, **2006**; 301.

28. Heppell, J.; Davis, H. L. Adv. *Drug Deliv. Rev*. **2000**, 43 (1), 29–43.

29. Rudin, N.; Inman, K. *An Introduction To Forensic DNA Analysis*; CRC Press: Boca Raton, Fla., **2001**.

30. Al-Otaibi, J. S.; Teesdale Spittle, P.; El Gogary, T. M. *J. Mol. Struct.* **2016**, *1127*, 751–760.

31. Chang, Y.-M.; Chen, C. K.-M.; Hou, M.-H. *Int. J. Mol. Sci*. **2012**, 13 (3), 3394–3413.

32. Erdem, A.; Ozsoz, *M. Electroanalysis* **2002**, 14 (14), 965–974.

33. Adhikari, A.; Mahar, K. S. **2016**, 8 (6).

34. Denny WA. DNA-intercalating ligands as anti-cancer drugs: prospects for future design. *Anti-Cancer Drug Design* 1989; 4:241-63.

35. Gago, F. Methods **1998**, 14 (3), 277–292.

36. Wakelin, L. P. G.; Bu, X.; Eleftheriou, A.; Parmar, A.; Hayek, C.; Stewart, B. W. *J. Med. Chem.* **2003**, *46* (26), 5790–5802.

37. Neidle S. DNA minor-groove recognition by small molecules. *Natural Product Reports* .**2001**; 18:291-309.

38. Rye, H. S.; Yue, S.; Wemmer, D. E.; Quesada, M. A.; Haugland, R. P.; Mathies, R. A.; Glazer, A. N. *Nucleic Acids Research*. **1992**, pp 2803–2812.

39. Bailly, C.; Waring, M. J. *Nucleic Acids Res.* **1998**, *26* (19), 4309–4314.

40. Schleif R. DNA binding by proteins. *Science* **1988**; 241:1182-7.

41. Jain, A. K.; Bhattacharya, S. *Bioconjug. Chem.* **2010**, *21* (8), 1389–1403.

42. Gabelica, V. **2014**, 297.

43. Hurley, L. H. *Nat. Rev. Cancer* **2002**, *2* (3), 188–200.

44. Pabo, C.; Sauer, R. T. **1992**.

45. Dey, B.; Thukral, S.; Krishnan, S.; Chakrobarty, M.; Gupta, S.; Manghani, C.; Rani, V. *Mol. Cell. Biochem.* **2012**, *365* (1–2), 279–299.

46. Jansen, K.; Nordbn, B.; Kubista, M. Society **1993**, No. 28, 10527–10530.

47. Kapuściński, J.; Szer, W. *Nucleic Acids Res.* **1979**, *6* (11), 3519–3534.

48. Manzini, G.; Barcellona, M. L.; Avitabile, M.; Quadrifoglio, F. *Nucleic Acids Res.* **1983**, *11* (24), 8861–8876.

49. R.P. Haugland, in: M.T.Z. Spence (Ed.), *Handbook of Fluorescence Probes and Research Chemicals, Molecular Probes*, Eugene: OR, **1996**, p. 153.

50. Jansen, K.; Nordbn, B.; Kubista, *M. Society* **1993**, No. 28, 10527–10530.

51. Tanious, F. a; Veal, J. M.; Buczak, H.; Ratmeyer, L. S.; Wilson, W. D. *Biochemistry* **1992**, *31* (12), 3103–3112.

52. Nygren, J.; Svanvik, N.; Kubista, *M. Biopolymers* **1998**, 46 (1), 39–51.

53. Köhler, O.; Jarikote, D. V.; Seitz, O. *ChemBioChem* **2005**, 69–77.

54. Thompson, *M. Biomacromolecules* **2007**, 8 (11), 3628–3633.

55. Rye, H. S.; Yue, S.; Wemmer, D. E.; Quesada, M. a; Haugland, R. P.; Mathies, R. a; Giazer, A. N. Nucleic Acids Res. **1992**, 20 (11), 2803–2812.

56. Kiser, J. R.; Monk, R. W.; Smalls, R. L.; Petty, J. T. *Biochemistry* **2005**, *44* (51), 16988–16997.

57. Bailly, C.; Colson, P.; Hénichart, J. P.; Houssier, C. *Nucleic Acids Res.* **1993**, *21* (16), 3705–3709.

58. Comings, D.E., Mechanisms of chromosome handing, VIII. Hoechst 33258-DNA interaction. *Chromosoma*, **1975**, 229-143.

59. Latt, S.; Gail, S. *J. Histochem. Cytochem.* **1976**, *24* (1), 24–33.

60. Breusegem, S. Y.; Clegg, R. M.; Loontiens, F. G. *J. Mol. Biol.* **2002**, *315*, 1049–1061.

61. Kopka, M. L.; Yoon, C.; Goodsell, D.; Pjura, P.; Dickerson, R. E. *Proc. Natl. Acad. Sci. U. S. A.* **1985**, *82* (5), 1376–1380.

62. Zasedatelev, A. S.; Gursky, G. V. *Mol. Biol. Rep.* **1974**, *1*, 337–342.

63. Peacock, W.J., Brutlag, D., Goldring, E., Appels, R., Hinton, C.W. and Lindsley, D.L. Cold Spring Harbor Symp: *Quant. Biol*. **1973**, 405-416.

64. Lewis, E. A.; Munde, M.; Wang, S.; Rettig, M.; Le, V.; Machha, V.; Wilson, W. D. **2011**, *39* (22), 9649–9658.

65. N. Turro, J. Barton and D. Tomalia, *Acc. Chem. Res*., **1991**, 24, 332-340.

66. Pang, B.; Qiao, X.; Janssen, L.; Velds, A.; Groothuis, T.; Kerkhoven, R.; Nieuwland, M.; Ovaa, H.; Rottenberg, S.; van Tellingen, O.; Janssen, J.; Huijgens, P.; Zwart, W.; Neefjes, J. *Nat. Commun.* **2013**, *4* (May), 1908.

67. Tacar, O.; Sriamornsak, P.; Dass, C. R. *J. Pharm. Pharmacol.* **2013**, *65* (2), 157–170.

68. Frederick C.A., Williams L.D., Ughetto G., *Biochemistry*. **1990**, 29 (10), 2538– 49.

69. Hande, K. R. *Biochim. Biophys. Acta - Gene Struct. Expr.* **1998**, *1400* (1–3), 173–184.

70. Karukstis, K. K.; Thompson, E. H. Z.; Whiles, J. A.; Rosenfeld, R. J. *Biophys. Chem.* **1998**, *73* (3), 249–263.

71. Groenning, M. *J. Chem. Biol.* **2010**, *3* (1), 1–18.

72. Darghal, N.; Garnier-Suillerot, A.; Salerno, M. *Biochem. Biophys. Res. Commun.* **2006**, *343* (2), 623–629.

73. Stsiapura, V. I.; Maskevich, A. A.; Kuzmitsky, V. A.; Uversky, V. N.; Kuznetsova, I. M.; Turoverov, K. K. *J. Phys. Chem. B* **2008**, *112* (49), 15893–15902.

CHAPTER 2

EXPERIMENTAL TECHNIQUES

This Chapter describes the experimental techniques that are used to carry out the measurements discussed in the thesis. In this work, optical absorption, steady-state, time-resolved fluorescence and circular dichroism measurements are used in addition to two-photon absorption measurements. The main goal of this thesis is to develop two-photon absorption (2PA) tools to monitor Drug-DNA interaction for the drugs that are fluorescent and to differentiate between the binding modes. Most of the experimental techniques used in the thesis are related to absorption and emission of radiation and often uses high-intensity laser pulses to perform measurements. Therefore an introduction about laser is provided here.

2.1 Lasers

Laser is an acronym, and this word stands for "Light Amplification by Stimulated Emission of Radiation." Lasers are constructed portions of spectral waves which result in a highly intense light source. The unique properties of laser radiation make them suitable for studying several optical phenomena.[1]

2.1.1 Components of Laser

Laser consists of three parts, pumping mechanism, gain medium and a resonant optical cavity called the optical resonator. The optical cavity is composed of two highly reflective mirrors that make the light bounce back and forth between them to amplify the stimulated emission of

radiation which is generated in the gain medium. The gain medium is the system or material that can generate stimulated emission of certain wavelengths when population inversion is created. The pump source is used to excite the particles in the gain medium to achieve population inversion, a state at which the population in the higher energy state is greater than the lower energy state. Figure. 2.1 depicts the basic components of any laser. [2]

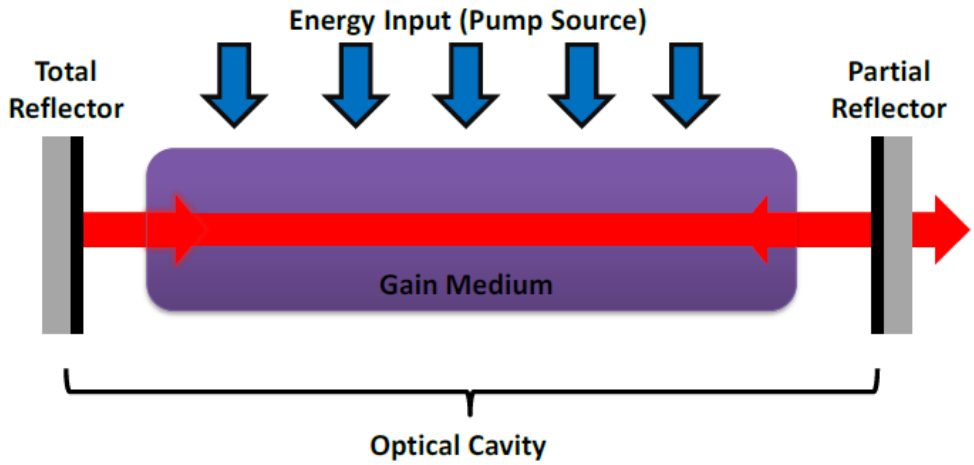

Figure. 2.1. Schematic diagram of the basic components of a laser.

2.1.2 Properties of Laser Light

The laser light has certain unique properties that make it useful for probing linear and nonlinear phenomena. The first one is the monochromaticity, which refers to the emission that comes out having same wavelength. It has narrow bandwidth. Its monochromaticity depends on the gain mechanism that is used and the nature of the source. The other one is coherence. Laser is coherent when all the emitted photons vibrate in phase agreement both in space and time. It is also a measure of precision of the waveform. The highly coherent laser beam can be more precisely focused.

The other property is the directionality, which means that all the photons travel in uni direction. Directionality of the laser correlates with the emission of an extremely narrow beam of light that spreads slowly. Within the laser apparatus, efficient collimation of photons into a narrow path results in a divergence factor of approximately 1 mm for every meter travelled. Directionality allows the laser beam to be focused on a very small sized spot. The last property of laser light is the brightness, which is when the light beam emitted is extremely intense and well centered. The brightness or intensity of the laser is one of the important properties and can be enhanced by using techniques like pulsing and Q-switching when extremely high peak power can be delivered in nanosecond pulses.[3] In this thesis, laser is used as the source for measuring 2-photon fluorescence and 2PA cross-sections. The description of techniques used in thesis are given below.

2.2 Optical Absorption

Optical absorption is the process of light attenuation through a material medium and the absorbance is calculated from the change in the intensities of the radiation. The drug-DNA interaction can be detected by UV-Vis absorption spectroscopy by measuring the changes in the absorption properties of the drug or the DNA molecules upon binding. The UV-Vis absorption spectrum of DNA exhibits a broad band (200-350 nm) in the UV region with a maximum at 260 nm. This maximum results from the chromophoric groups in purine and pyrimidine moieties responsible for the electronic transitions.[4-6]

The absorbance (A) can be represented by the following equation:

$$A = log\left[\frac{I_0}{I}\right] = \varepsilon_\lambda Cl$$

In the above equation, c is the species concentration. The intensities of the incident and the transmitted light are represented by I and I_o respectively. l is the path length of the cuvette, and ε is the molar extinction coefficient of the substance. The optical absorption measurements carried out in the thesis were performed on a Shimadzu UV-160a absorption spectrophotometer.

2.3 One-Photon Fluorescence Measurements

Absorption of the radiation takes the molecule to its excited state and it relaxes back to the ground state via fluorescence if the relaxation is radiative.[7, 8] Fluorescence measurements can be described by excitation and emission wavelengths, quantum yield, decay time and polarization. Fluorescence excitation and emission spectra provide information on the energies of the transitions. However, it's not the case that the whole number of excited molecules emit fluorescence radiation, since there are several other processes which compete with fluorescence emission. This can be characterized by the fluorescence quantum yield (the ratio of the number of quanta emitted to the number of quanta absorbed) and decay time (which is the time after that the number of excited molecules is reduced to 1/e).[9] Fluorescence measurement is a powerful tool for the investigation of biological materials. It can be utilized to analyze how changes in the biological environment influence fluorescence properties including quantum yield or emission profiles, an example of the use of fluorescence measurements is the imaging of Drug-DNA interaction.

In this system the fluorescence intensity is enhanced when the drug binds to DNA. The binding interaction increases the rigidity of the system so we can observe the activity in the biological environment as it's indicated by the change in fluorescence intensity. In addition, a shifts in the fluorescence and absorption spectra can be observed as a result for the activity of a biological system under study.[13] Fluorescence measurements presented in the thesis are carried

out in Edinburgh F900 spectrofluorimeter and Hitachi F2500 fluorimeter. For the case of Edinburgh F900, Xe-450W lamp was used as the excitation source and cooled R-928P PMT was used as the detector. The excitation and emission slit widths were changed so that the intensity does not saturate the detector.

2.4 Two-Photon Fluorescence

The increasing availability of intense laser sources with picosecond and femtosecond pulse widths have resulted in a wide use of two-photon absorption cross-section for fluorescence imaging microscopy. 2PA spectroscopy proven to be an excellent technique for noninvasive imaging, in addition to its advantage of a better penetration and relative harmlessness of longer wavelengths. It reduces photo bleaching by limiting it to the focal plane of the microscope. This reduction is especially important for imaging in thick samples, such as brain slices or pancreatic islets. [11, 12] Two-photon absorption (TPA) is a nonlinear optical process in which two photons of equal or different frequencies are simultaneously absorbed by a material.[16] 2PA cross-sections can be measured using different techniques such as open-aperture z-scan. Many researchers have used z-scan to determine the 2PA cross-sections. However, this technique can be incorrect as it might have overlapping contributions from excited state absorption. To overcome this issue, the researchers have used fluorescence-based techniques. Absolute 2PA cross-sections can be measured with the knowledge of the power of incident radiation and the power of emitted radiation. However, absolute 2PA cross-sections are difficult to measure as it is difficult to determine the exact amount of emitted radiation. For these reasons, in this thesis we have used relative two-photon excited fluorescence (TPEF) technique to determine the 2PA cross-sections. In this technique a standard 2PA, collection efficiency and instrument parameters are determined to be

used in the detection of the 2PA cross-section for the sample. Most importently for this method to be successful, the chromophores under investigation must be highly fluorescent and possess good fluorescence quantum efficiency.

Because of this reasons, the TPEF technique is limited to studying only fluorescent molecules since fluorescence quantum yield is one of an intrinsic property of a molecule. TPEF considers the simplest method that can be employed to determine the 2PA cross-section of the biological molecules and drugs. It provides different advantages, such as superior sensitivity to changes in transition dipole moments of the excited fluorophore Furthermore, it has greater spatial focusing with depth penetration relative to one-photon excitation, reduced probability of auto-fluorescence (scattering) and photo damage. [13, 14] Figure 2.2 shows the schematic diagram of TPEF setup that was used to determine the 2PA cross-sections of the investigated drugs in this thesis.

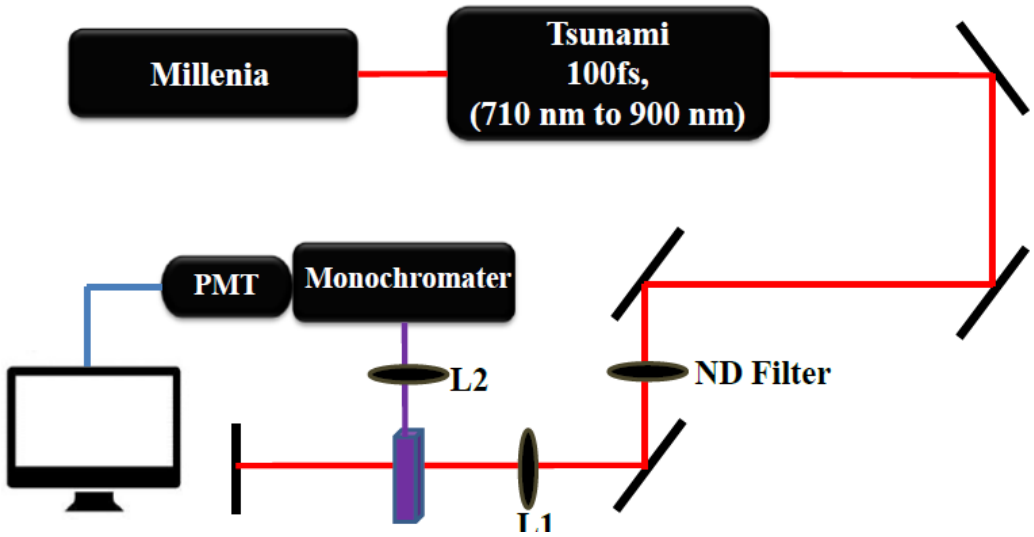

Figure 2.2. Schematic diagram of the setup used to determine the 2PA cross-sections. Millennia is the solid state pump laser. ND represents the neural density filter. L1 and L2 are focussing lenses. PMT represents the photomultiplier tube.

All the two-photon fluorescence experiments described in this thesis used broadband Ti: Sapphire laser (Tsunami, Spectra Physics, 100 fs, 700 to 900 nm) as the excitation source whose main wavelength was 800 nm and had tunable range of 800 ± 10 nm.[15] A rotating neutral density filter of varied light transparency (ND, neutral density filter) was used to control the power of incident radiation to carry out power-dependence measurements. Laser light is focused onto the sample cuvette which contains a solution of the drug under investigation (located in the Edinburgh F900 fluorimeter) by a lens (L1 and L2 lenses), and the fluorescence was collected perpendicular to the excitation source. The fluorescence obtained after two-photon excitation is again focused onto the slit of the monochromator and detected with cooled Hamamatsu R928P PMT. For the measurements, a concentration of 100 μM of Coumarin 485 standard in methanol was used.[15] All the investigated drugs under study produced a slope of 2 in the power-dependent flourescence measurements (Figure 2.3) suggesting the fluorescence arising out of two-photon excitaiton.

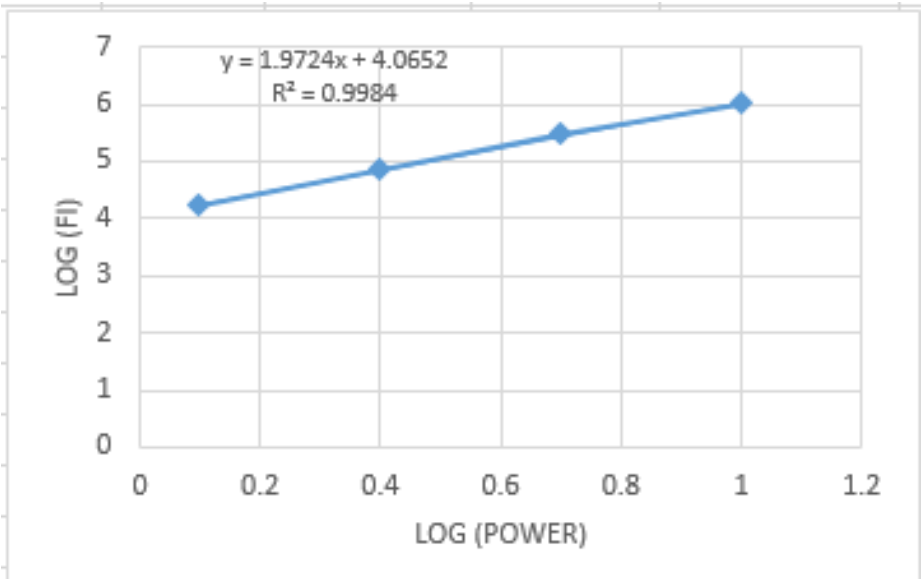

Figure 2.3. A plot representing the power dependence of fluorescence that showing a slope of 2.0 indicating the 2PA event.

The dye concentration was kept constant during the quantum yeild determination and through out the 2PA cross-section measuerments inorder to avoid ambiguity or overlap with the drug spectrum in the final rsult. The TPEF has a main benefit which is relatively easy to perform when its compared to conventional flourescence methods. In addition to its easiest performance without difficulties, it is also does not include any interferences from both excited state absorption and thermal lensing.

2.5 Time-Resolved Fluorescence Measurements

The fluorescence lifetime is the time required by a population of excited fluorophores to decrease exponentially to N/e via the loss of energy through fluorescence and other non-radiative processes. It works to elucidate the variation of fluorescence intensity as a fuction of time after the excited state has been created. It monitors the changes in the excited state and the mechanisims through which the excited state relaxeses into the ground state. The lifetime of photophycal processes vary significantly from tens of femtoseconds for internal conversion, to nanoseconds for fluorescence, and microseconds or seconds for phosphorescence.[17] The emission of fluorophore can be highly effected by its environment (like viscosity, pH, polarity, solvation, size and shape of molecules) or even by the presence of other interacting molecules. Thus, the fluorescence life time is a successful tool to detect biological interaction, specifically Drug-DNA interaction. It's also considered very useful if there are several emitting species present with overlapping emission spectra, because fluorescence lifetimes are measured at wavelength increments for the same data collection time. The resultant measurements can be represented by intensity-time axis to provide spectra at different times after excitation.[18] The variation of the fluorescence lifetime method

allows its application to diverse areas of study, including materials science, aeronautics, agriculture, forensics, biology, and medicine. [17] There are several techniques for measuring the fluorescence lifetime and in this thesis, we have used single photon counting technique.

2.5.1 Time-Correlated Single Photon Counting

Time-correlated single photon counting (TCSPC) is a well established method to deterime fluorescent lifetimes or the average time that a molecule spends in the excited state before returning to the ground state for flourescent organic chromophore.[19-21] The technique consist of the excitation part of the sample by pulses from a laser source, and the detection system that monitors the difference in time between the excitation pulse and the first photon from the sample arrives the detector. Since it is essential that the system accurately detects one photon for a large number of excitation pulses while neglecting other pulses, an extremely low count rate must be established inorder for the system to operate in single photon counting mode.[20,21] The outcome of this setting, is the distribution of a photon probability against time. This distribution follows a statistical Poisson distribution and software contained in the computer is used to retrieve the lifetime of the sample after deconvoluting the decay trace with instrument response function (IRF). The IRF is measured by replacing the sample with a scatter and changing the monitoring emission wavelength same as that of the excitation wavelength. The IRF has pulse width of 1 ns due to the time taken for electronics (PMTs) to register the photon event. With TCSPC, one can obtain time resolution of 230 ps after deconvoluting with IRF as shown in the schematic diagram of TCSPC (Figure 2.4).

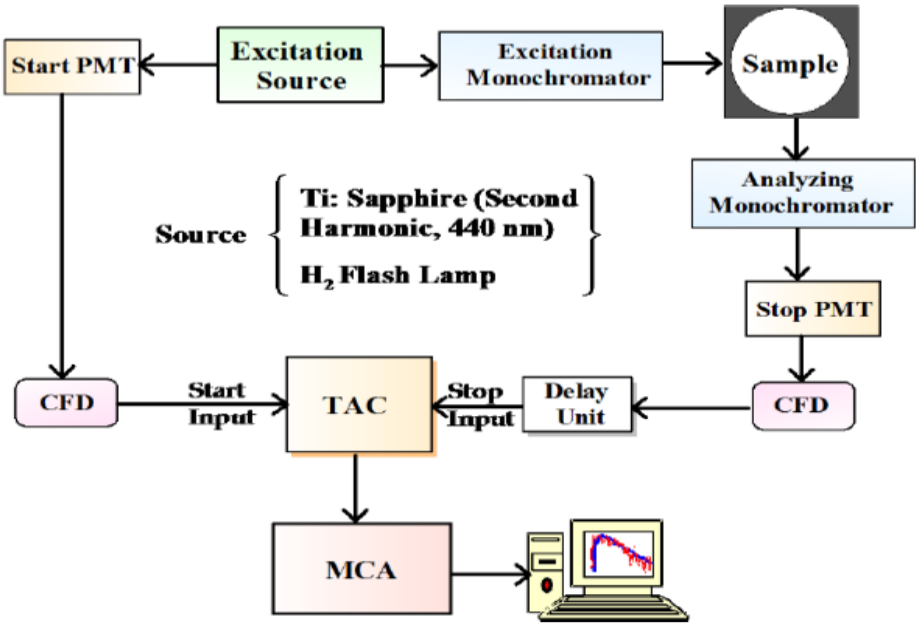

Figure 2.4. Schematic diagram of the TCSPC technique.

An excitation pulse (optical pulse) either from the flash lamp or a laser diode is split into two parts. One part is used to excite the sample kept in the sample chamber and the other part is used to generate a start pulse in the start PMT or photodiode. The optical signal at the start PMT generates an electrical START pulse, which is then routed through a constant fraction discriminator (CFD) to START the input of time to amplitude converter (TAC) to initialize the charging operation. The part of the optical pulse, which excites the sample effectively, gives rise to emission of photons. These photons are then detected by STOP PMT (at the right angle to the direction of excitation) to generate an electrical STOP pulse.

The STOP pulse is also routed to the TAC after passing through another CFD and a variable delay line. On receiving the STOP signal, the TAC stops its charging operation and generates an electrical output, with an amplitude proportional to the time difference Δt between the start and the stop pulses reaching the TAC. The TAC output pulse is then fed to the input of a multi-channel

analyzer (MCA) through an analogue to digital converter (ADC). The ADC generates a numerical value corresponding to the TAC output pulse and thus selects an appropriate channel of the MCA and the count is added to the channel. The above cycle (from excitation to data storage) is repeated a large number of times and as a result, a histogram of the counts versus the channel number of MCA is generated. It represents the true emission decay, when the collection rate of emission photons by the STOP pulse is very low, as illustrated by the statistical treatment. The emission decay observed has to be de-convoluted with the instrument response to get the actual lifetime. [22]A Cut -off filters were placed strategically before the focusing lens in order to remove any scattered exciting light that would enter the monochromator from the sample cell.

2.6 Circular Dichroism

Circular dichroism (CD) spectroscopy is an optical technique that measures the difference in the absorption of left and right circularly polarized light (the absorption that result from the interactions of chiral molecules with circularly polarized light). This technique has been widely employed in the studies of biological structures like nucleic acids, in addition to its advantages in monitoring protein- DNA interaction as well as Drug-DNA interaction. [25] The absorption of right- and left-handed circularly polarized light by chiral molecules differs. The difference in absorption is due to the differences in extinction coefficients for the two polarized rays.

CD is primarily used in the analysis of structure or conformation of macromolecules, structural features, kinetic and thermodynamic properties of molecules, and the effect of secondary structure changes upon changing conditions such as temperature and pH. CD is measured in or near the absorption bands of the molecule of interest, therefore it is measured over a wide range of wavelengths. The UV region is often used in the structural studies of DNA and proteins while the

UV/VIS region is used for the studies of charge transfer of protein-metal complexes. When the molecule contains chiral chromophores, the CPL (circular polarized light) is absorbed to a greater extent than the other light making the CD signal to be non-zero. This signal is usually positive or negative and that depend on whether LCPL (left CPL) is absorbed to a greater extent or the RCPL (RCPL). If the LCPL is absorbed to a greater extent than the right, in this case the signal will be positive, but if the LCPL is absorbed to a lesser extent than the RCPL then the signal will be negative. Most biological molecules are chiral, as illustrated by the 19 out of the 20 common amino acids being chiral and also they are forming proteins that are also chiral. Other biological molecules that are chiral are DNA and RNA.Circular dichroism is therefore an important spectroscopic technique for the study of biological molecules. The CD spectrum of a biomolecule is not a summation of the individual spectra of residues for the proteins or bases of the nucleic acids, but rather it's the three dimensional structure of the macromolecule itself. Each structure has a unique (signature) CD spectrum that can be used to identify the structural elements and study the changes in the structure of chiral macromolecules. [52]

All CD measurements presented in the thesis were performed using a Jasco, J815 CD of the model J-815 and serial No. A036961168. This instrument has the ability to characterize secondary structure of macromolecules, and determine changes in structure and conformational stability of DNA due to changes in pH, temperature variation, buffer conditions and addition of stabilizers. The CD spectrometer uses circularly polarized light and measures the differential absorption of the left and right-handed component of the light. It has a usable range between 163-1100 nm.

2.7 References

1. Kaluza, M. C. *Opt. Photonik* **2010**, *5* (2), 56–59.
2. Patil, U. A.; Dhami, L. D. *Indian J Plast Surg*. **2008**, pp 101–113.
3. Milonni. P., Eberly, J., *Laser physics*. Oxford: Wiley-Blackwell, **2010**.
4. Alfano, R. R.; Pradhan, A.; Tang, G. C. *America (NY).* **1989**, *6* (5), 1015–1023.
5. Rohatgi-Mukherjee, K. *Fundamentals of photochemistry;* New Age International: India, 1978.
6. González-ruiz, V.; Olives, A. I.; Martín, M. A.; Ribelles, P.; Ramos, M. T.; Menéndez, J. C.; Analítica, D. Q. *Biomed. Eng. Trends, Reasearch Technol.* **2011**, No. December 2016, 65–90.
7. Hino, S., Introduction to Ultraviolet Photoelectron Spectroscopy. *TANSO*, **2000**, (191), 80-82.
8. Sheehan, D., *Physical biochemistry principles and applications*. Hoboken,
9. N.J: Wiley, 2013.
10. Wojczewski, C.; Stolze, K.; Engels, J. W. *Synlett* **1999**, *1999* (10), 1667–1678.
11. Sauer, M.; Hofkens, J.; Enderlein, J. *Handb. Fluoresc. Spectrosc. Imaging* 2011, 1–29.
12. Lakowicz, J. R.; Gryczynski, I.; Malak, H.; Schrader, M.; Engelhardt, P.; Kano, H.; Hell, S. W. *Biophys. J.* **1997**, *72* (2 Pt 1), 567–578.
13. Patterson, G. H.; Piston, D. W. *Biophys. J.* **2000**, *78* (4), 2159–2162.
14. McLean, A. M.; Socher, E.; Varnavski, O.; Clark, T. B.; Imperiali, B.; Goodson, *T. J. Phys. Chem. B* **2013**, *117* (50), 15935–15942.
15. Bukowski, E., & Bright, *Appl Spectrosc*, **2002**, *56*(12), 1588-1592.
16. Makarov, N. S.; Drobizhev, M.; Rebane, A. *Opt. Express* **2008**, *16* (6), 4029–4047.

17. Collini, E. *SPIE Newsroom* **2012**, 4–6.

18. Berezin, M. Y.; Achilefu, S. *Chem. Rev.* **2010**, *110* (5), 2641–2684.

19. Badea, M.; Brand, L., *Methods Enzymol*. **1979**, 61:378-425.

20. Lakowicz, J. R.; Masters, B. R. *J. Biomed. Opt.* **2008**, *13* (2), 29901.

21. Becker, W.; Bergmann, A.; Biscotti, G. L.; Rück, A. *Proc. SPIE 5340, Commer. Biomed. Appl. Ultrafast Lasers IV, 104* **2004**, *5340*, 104–112.

22. Demas, J., N, *Excited state lifetime measurements*; Academic Press: Newyork, 1983.

23. Shapiro, H. *Practical flow cytometry*. Hoboken, N.J: Wiley-Liss 2003.

24. Wiederrecht, G. P.; Giebink, N. C.; Hranisavljevic, J.; Rosenmann, D.; Martinson, A. B. F.; Schaller, R. D.; Wasielewski, M. R. *Appl. Phys. Lett.* **2012**, *100* (11), 1–5.

25. Devadas, M. S.; Kim, J.; Sinn, E.; Lee, D.; Iii, T. G.; Ramakrishna, G. *J. Phys. Chem. C* **2010**, *114*, 22417–22423.

26. Chang, Y.-M.; Chen, C. K.-M.; Hou, M.-H. *Int. J. Mol. Sci.* **2012**, *13* (3), 3394–3413.

27. Greenfield, N. J. *Nat. Protoc.* **2006**, *1* (6), 2876–2890.

CHAPTER 3

TWO-PHOTON SPECTROSCOPY TO DIFFERENTIATE INTERCALATION AND GROOVE-BINDING INTERACTIONS

3.1 Introduction

The main goal of this thesis is to develop novel spectroscopic tools to monitor Drug-DNA binding interactions with the ability to differentiate between the binding modes, whether it's intercalation or minor groove binding. To accomplish this goal, a proof-of-principle study was carried out with two well-known DNA binding drugs, DAPI (4', 6-Diamidino-2-Phenylindole, Dihydrochloride) and Thiazole Orange (ThO) binding with both Salmon sperm and Calf Thymus DNA. A study of the feasibility of two-photon absorption (2PA) spectroscopy to differentiate the intercalation and minor-groove binding is presented in this Chapter. [1]

In recent years, interactions between small molecules and DNA have attracted increasing interest of many research groups as it is crucial for the design of novel DNA–targeted drugs. Different kinds of techniques have been employed to study these interactions. It is well known that DNA plays a major role in life processes and is quite often the main cellular target for many drugs. [2] The influence on the biological system is the main requirement for DNA-targeting drugs. Thus the interaction of drugs with DNA may be applied in therapeutic approach in which the suppression of DNA replication and gene transcription can be used to destroy tumor cells or infected tissues.[5] There are many drugs are known to interact with DNA and exert their biological activities as anti-cancer, anti-tumor and anti-viral drugs.[3, 4] In addition for the drugs to be active, they should bind to DNA with high binding constants. Thus, it is important to understand the interaction of drugs

with DNA. Also, the study of drug-DNA interactions is quite essential in developing diagnostic tools required to study this interaction that has many applications in biomedical field. [6]

Drugs can interact with DNA predominately through an intercalating or groove binding mechanism. Intercalating molecules have planar aromatic rings incorporated into the structure that bind with DNA by inserting between the DNA nucleobases to form a binding pocket. Lengthening, unwinding, and distortion of the DNA helical axis are most notable upon intercalation, which requires important driving factors, such as π-stacking, dipole−dipole interaction, electrostatic factors, and dispersive interaction with the aromatic nucleobases in DNA. Whereas groove binding is characterized by disturbance in the DNA structure. Groove-binding molecules generally contain unfused-aromatic structures with terminal basic that require conformational flexibility to allow the molecule to fit into the DNA groove. Also it has functional groups that interact with the nucleobases through H-bonding and/or van der Waals interactions with minimal steric hindrance. Groove depth, groove width, electrostatic potential, and floor functionality are structural features found to be critical for groove binding recognition. Understanding the mechanisms of the DNA binding interactions of small molecules can provide valuable information toward the development of therapeutics targeted at DNA.[7]

There are several techniques that have been used to monitor Drug-DNA interactions which include optical absorption, fluorescence spectroscopy, fluorescence resonance energy transfer and circular dichroism (CD). These techniques are quite successful in monitoring the binding interactions, but they cannot differentiate whether it is intercalation or minor groove binding. Absorption and fluorescence measurements show only small differences between intercalation and groove binding. Thus, there is a need to develop novel spectroscopic tools that can monitor and differentiate Drug-DNA interactions. In this thesis we propose to use the power of two-photon

absorption (2PA) spectroscopy to monitor and differentiate Drug-DNA interactions. The hypothesis is that the 2PA cross-sections of the drug is sensitive to the DNA local electric field depending on their orientation. It is well established that DNA is made of aligned electric fields because of the phosphate backbone.[8-10] The molecules that bind to DNA can be sensitive to this electric field and the enhancement of 2PA cross-section for the molecules can be observed based on their dipolar alignment with the electric field vector. It is known from simple geometry that when a molecule is intercalated, its transition dipole is either perpendicular or aligned away from the phosphate backbone while the dipolar orientation is parallel to the phosphate backbone's electric field in minor groove-binding case. This difference in orientation should enable the 2PA cross-sections to differentiate intercalation versus groove-binding interactions. To support this hypothesis, 2PA cross-section measurements were carried out on two well-known drug molecules that can bind to DNA via intercalation and minor groove mechanisms. Two drug molecules that were chosen are DAPI and ThO (Figure 3.1). DAPI is a well-known minor groove-binder. A study of the crystal structure of DAPI with DNA confirmed its binding mode (Figure 3.1A). While, optical measurements and crystal structures have proven that ThO binds to DNA via intercalation. (11, 12)

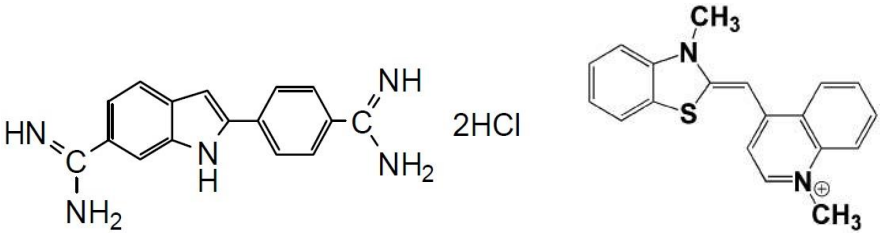

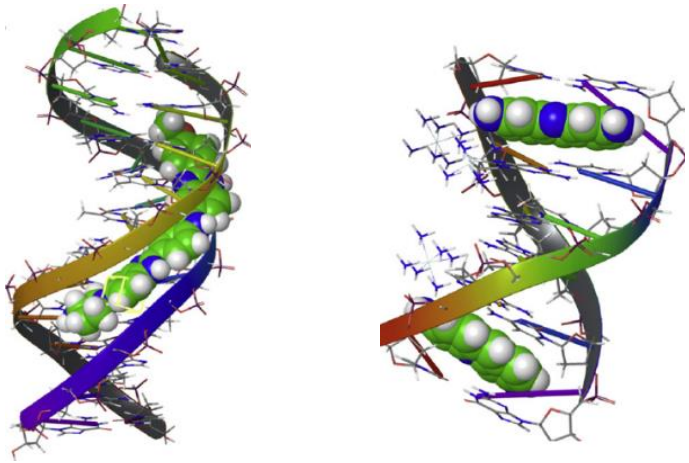

Figure 3.1. (A) DAPI binding with DNA via minor groove, (B) ThO binding with DNA via intercalation [11, 12]

Optical absorption, one-photon fluorescence, two-photon fluorescence, CD and fluorescence lifetime measurements for the drugs interacting with salmon-sperm and Calf Thymus DNA were carried out to confirm the binding of the investigated drugs with DNA. The 2PA cross-sections were determined with increasing DNA concentrations and interesting trends were observed with respect to intercalating and minor groove-binding interactions.

3.2 Materials and Methods

3.2.1 Materials

Salmon-sperm, Calf-thymus DNAs, and DAPI, Thiazole Orange drugs were obtained from Sigma-Aldrich and were used as such. Tris (hydroxymethyl) aminomethane hydrochloride, NaCl were obtained from Sigma-Aldrich and were used as received. Nanopure water from Millipore was used. All measurements were carried out in buffered solutions unless stated otherwise. A buffer stock solution (pH = 7.2) was made using TRIS-HCL (5 mM) and sodium chloride (50 mM) and MilliQ water. The salmon sperm and Calf Thymus DNA were combined with the buffer solution (10 mL) to create a stock solution of DNA. The drugs were dissolved in small amount of

DMSO and diluted to make 10 mL of 1 mM of stock solution. Twelve samples were made from the stock solutions with increasing concentrations of DNA placed in each. Each sample was 1 mL, so buffer was added decreasingly as each sample was made, while keeping drug concentration at 20 μM. This process was repeated for all the investigated drugs molecules.

3.2.2 Optical Methods

The optical absorption measurements were carried out utilizing a Shimadzu UV2101 PC spectrophotometer. One-photon fluorescence measurements were performed on a Hitachi F2500 spectrofluorimeter. Fluorescence quantum yield measurements were determined with C485 in methanol as the standard. The 2PA cross-sections were obtained using the two-photon excited fluorescence technique.[13, 14] In this technique, the output from Tsunami (Spectra-Physics), 720 nm to 900 nm, 100 fs was used to carry out the measurements and the relative 2PA cross-sections were determined from the ratio of one and two-photon fluorescence from the samples. The CD measurements were measured under N_2 over the range of 200-600 nm using a Jasco (J815) CD, model J-815.

3.3 Results and Discussion

The main objective of this thesis, is to prove the principle, that the two-photon fluorescence spectroscopy can be used to monitor Drug-DNA binding and differentiate between the binding mode whether it's intercalation or minor groove-binding. Two well-known drugs (Tho and DAPI) have been used to prove the hypothesis with two different kinds of DNA (Salmon-sperm DNA and Calf-thymus DNA). ThO well-known in the literature as an intercelator drug, whereas DAPI well known as a minor-groove binding drug. The optical absorption and fluorescence steady state

measurements of DAPI and ThO with increasing concentrations of salmon and calf-thymus DNA were carried out first to prove the binding interactions of both drugs with DNA.The concentrations of salmon DNA were determined from the absorption at 260 nm using the following empirical equation: A/ (L*0.02), where *A* is the absorbance and *l* is the path length of cuvette (0.4 cm). Further measurements were carried out to monitor the binding of drug molecules with DNA.

3.3.1 Salmon DNA with DAPI and ThO

3.3.1.1 Optical Absorption and Steady-State Fluorescence Measurements

Optical absorption and steady-state fluorescence measurements were carried out for DAPI and ThO in buffer solution with and without salmon DNA. The optical absorption and steady-state fluorescence spectra of DAPI and ThO with and without 130 μg/mL of salmon DNA shown in figure 3.2 (A, B) and 3.3 (A, B). From figure 3.2A, the absorption maximum of DAPI drug has shifted to longer wavelength (from 342 nm to 358 nm) with increasing DNA concentration and the inset of figure 3.2A shows the absorption of DAPI at 375 nm as a function of DNA concentration. The results show the binding of DAPI with salmon DNA. Similarly, the optical absorption spectra of ThO with and without salmon DNA shown in figure 3.2B. The absorption maximum of ThO has shifted to longer wavelength from 421 nm to 507 nm with increasing DNA concentration and the inset of figure 3.2B shows the absorption of ThO at 500 nm as a function of DNA concentration that shows increase in absorption. These results suggest the binding of ThO with salmon DNA. The shift of absorption spectra to longer wavelength for both drugs show that the drug molecules absorption spectra were influenced by salmon DNA because of the increase in system rigidity due to the binding of the drug to DNA. This arises because of the retardation of

rotation around the single bond between aromatic rings as elucidated in the chemical structure for both drugs (figure 3.1), suggesting the binding of the drugs with DNA.

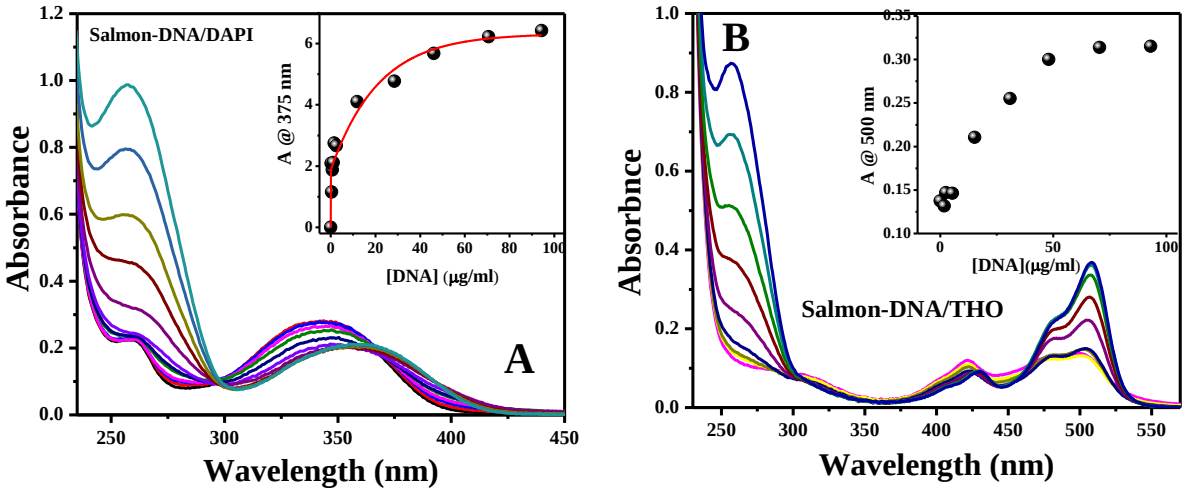

Figure 3.2. (A) Absorption spectra of DAPI with increasing concentration of salmon DNA and the inset shows the absorbance at 375 nm as a function of DNA concentration. (B) Absorption spectra of ThO with increasing concentrations of salmon DNA and the inset shows the absorbance at 500 nm as a function of DNA.

One-photon fluorescence measurements were carried out for DAPI with increasing concentrations of DNA. Figure 3.3A shows the fluorescence spectra of DAPI at different DNA concentrations. The fluorescence measurements were carried out after 360 nm excitation, and monitoring the spectra from 380 nm to 650 nm. The inset of the graph is the normalized intensity of DAPI at 460 nm as a function of DNA concentration and it shows the increase in the intensity with increasing DNA concentration suggesting the binding of DAPI with DNA. The enhancement of DAPI fluorescence with DNA was well documented, and the observed increase in fluorescence is quite similar to what has been reported by other research groups. [15, 16, 17]

Similar fluorescence measurements for ThO were carried out after 420 nm excitation and monitoring the fluorescence spectra from 430 nm to 750 nm. The fluorescence intensity of ThO increased as more DNA was added to the system (Figure 3.3B). Inset represents the normalized intensity of ThO at 535 nm as a function of DNA concentration and it shows the trend of change in fluorescence intensity with increasing DNA concentration. The results obtained for ThO with DNA matched well with what was reported for ThO and DAPI with other DNA systems [18, 19]. Optical absorption and fluorescence measurements have shown that the drug molecules are bound to DNA, and the different changes in absorption and fluorescence has something to do with the way that these drugs bind to DNA.

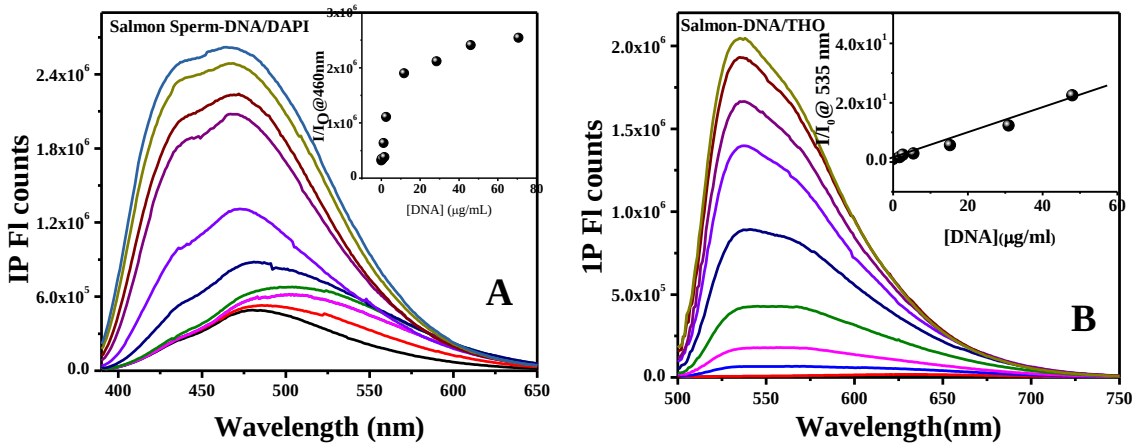

Figure 3.3. (A) One-photon fluorescence spectra of DAPI with increasing concentration of DNA. Inset shows the normalized fluorescence intensity at 460 nm as a function of DNA concentration. (B) Fluorescence spectra of ThO with increasing concentrations of DNA. Inset shows the normalized fluorescence intensity at 535 nm as a function of DNA.

3.3.1.2 Time–Resolved Fluorescence Measurements

Another way to monitor the binding of a drug with DNA is by following the fluorescence lifetime of the binding drug. The drugs that we have used for the investigation, DAPI and ThO are known fluorescent markers and their binding can be monitored by their lifetimes. Fluorescence lifetimes for DAPI and DAPI/salmon DNA are measured by using a laser diode of 373 nm after excitation and monitoring fluorescence at 450 nm. The life time decay for the free drug in buffer solution should be rapid or fast as the rotational diffusion is fast in low viscosity medium (buffer). However, when the drug molecule bind to DNA its rotation is restricted. Figure 3.4A shows the fluorescence decay traces of DAPI in buffer solution and also for DAPI with (130 μg/mL) salmon DNA at 450 nm. The figure shows that the fluorescence decay of DAPI is fast and consistence with more DNA added to the system and majority of the decay is complete within 50 ns. Fluorescence decay of DAPI was fitted with a multi-exponential function given by:

$$F(t) = \sum_{i=1}^{n} a_i \; e^{-t/\tau_i}$$

where a_i and τ_i are pre-exponential factor and lifetime, respectively. The decay trace was deconvoluted with instrument response to obtain the lifetimes and pre-exponential factors.

Average lifetime was calculated from the fitting parameters using the expression given by:

$$< \tau_{avg} > = \frac{\sum_{i=1}^{n} a_i \; \tau_i}{\sum_{i=1}^{n} a_i}$$

The fast decay for DAPI in buffer solution can be attributed to single bond rotation around aromatic rings giving rise to fast non-radiative relaxation. The fluorescence decay of DAPI became considerably longer when it is bound to DNA. Fluorescence decay traces are fitted with exponential functions and corresponding lifetime data is provided in Table 3.1.

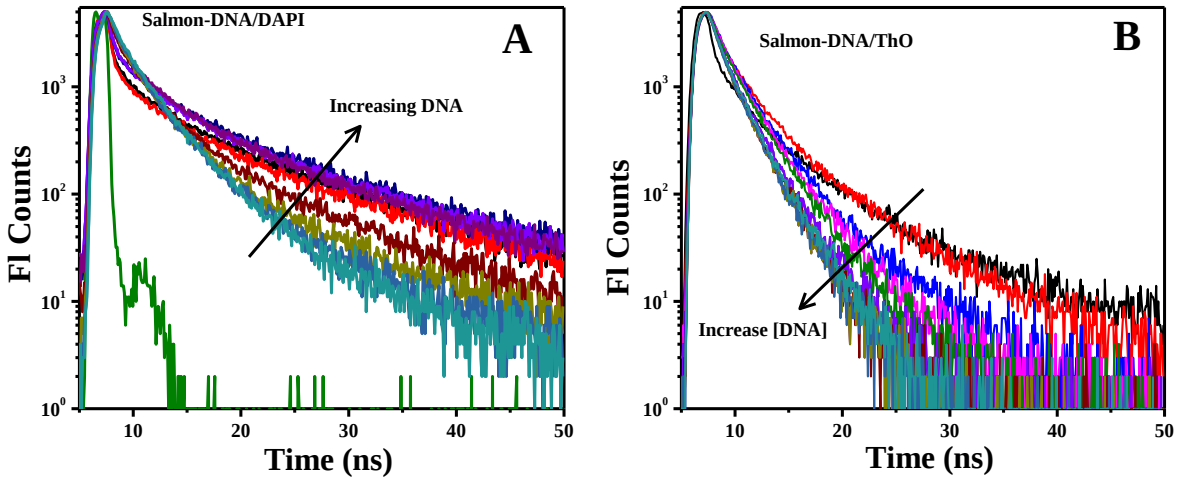

Figure 3.4. (A) Fluorescence decay traces of DAPI and DAPI/salmon DNA monitored at 450 nm after excitation with 373 nm diode laser. (B) Fluorescence decay traces of ThO and ThO/DNA monitored at 530 nm.

Figure 3.4 B shows the fluorescence decay traces of ThO in buffer solution and also with (130 μg/mL) salmon DNA after excitation with a 457 nm laser diode and monitored the fluorescence decay at 530 nm. The figure shows that the fluorescence decay of ThO is fast and consistent with more DNA added to the system (similar to DAPI result) and majority of the decay is completed within 50 ns. Changes in fluorescence decays were observed with increasing DNA concentration. The obtained decay traces are fitted with exponential functions and corresponding lifetime data is provided in Table 3.2. The lifetime trends show that they increase with increase in DNA concentrations for the most part with small deviations.

Table 3.1. Fluorescence Lifetimes for DAPI at Different Concentrations of Salmon-DNA

[DNA] μg/mL	**Life times (ns)**	**Avg life time(ns)**

0	1.66 ± 0.045 (44.0%), 3.80 ± 0.054 (56.0%)	2.86
0.4	1.36 ± 0.040 (36.0%), 3.63 ± 0.037 (64.0%)	2.81
0.7	0.54 ± 0.007 (41.0%), 8.20 ± 0.053 (59.0%)	5.11
0.2	0.49 ± 0.007 (43.0%), 7.90 ± 0.053 (57.0%)	4.76
1.6	0.51 ± 0.007 (45.0%), 8.06 ± 0.057 (55.0%)	4.67
1.2	0.71 ± 0.010 (33.0%), 8.27 ± 0.051 (67.0%)	5.74
2.5	0.78 ± 0.010 (36.0%), 7.9 ± 0.051 (64.0%)	5.40
11.8	1.34 ± 0.017 (41.0%), 8.23 ± 0.065 (59.0%)	5.43
28.4	1.47 ± 0.017 (54.0%), 6.78 ± 0.070 (46.0%)	3.92
46.0	1.59 ± 0.017 (60.0%), 3.07 ± 0.071 (40.0%)	3.37
70.6	1.71 ± 0.023 (61.0%), 5.45 ± 0.073 (39.0%)	3.16
94.3	1.77 ± 0.027 (59.0%), 4.97 ± 0.072 (41.0%)	3.09

Table 3.2. Fluorescence Lifetimes for ThO at Different Concentrations of Salmon-DNA

[DNA]	**Life Time (ns)**	**Avg.Life time(ns)**
0	1.03 ± 0.032 (50.0%), 2.37 ± 0.038 (50.0%)	1.39
1.7	1.10± 0.015 (57.0%), 6.35 ± 0.042 (43.0%)	3.46
2.5	1.84 ± 0.024 (52.0%), 4.65 ± 0.093 (48.0%)	3.92
5.4	1.70 ± 0.019 (58.0%), 5.78 ± 0.070 (42.0%)	2.04
15.2	1.76 ± 0.024 (70.0%), 4.53 ± 0.086 (30.0%)	2.09
30.9	1.62 ± 0.027 (65.0%), 3.78 ± 0.073 (35.0%)	2.54
47.9	1.45 ± 0.031 (58.0%), 3.27 ± 0.059 (42.0%)	2.44
70.4	1.21 ± 0.029 (55.0%), 2.81 ± 0.047 (45.0%)	2.10
93.0	1.10 ± 0.030 (52.0%), 2.51 ± 0.042 (48.0%)	1.87

3.3.1.3 CD Measurements

CD was used to monitor the binding of the drugs (DAPI, ThO) with salmon DNA. DAPI is originally a non-chiral molecule and hence should not give any signal in CD. When DAPI binds to DNA it can become a chiral as it imparts the chirality of the DNA. With these considerations the CD spectra of DAPI with and without salmon DNA were obtained and are shown in Figure 3.5A. DAPI did not show any signal (as expected) without DNA, as it is not chiral. However, a clear signal at 350 nm matching the absorbance of DAPI was observed suggesting that the drug was bound to DNA. Also, the positive signal suggest minor-grove binding interactions. Similarly, ThO shows a CD signal when it is bound to Salmon-DNA (figure 3.5 B) and a clear signal was obtained around 375 nm matching the absorbance spectrum of ThO. However, the signal has a negative features suggesting that the interaction might be different than DAPI interaction.

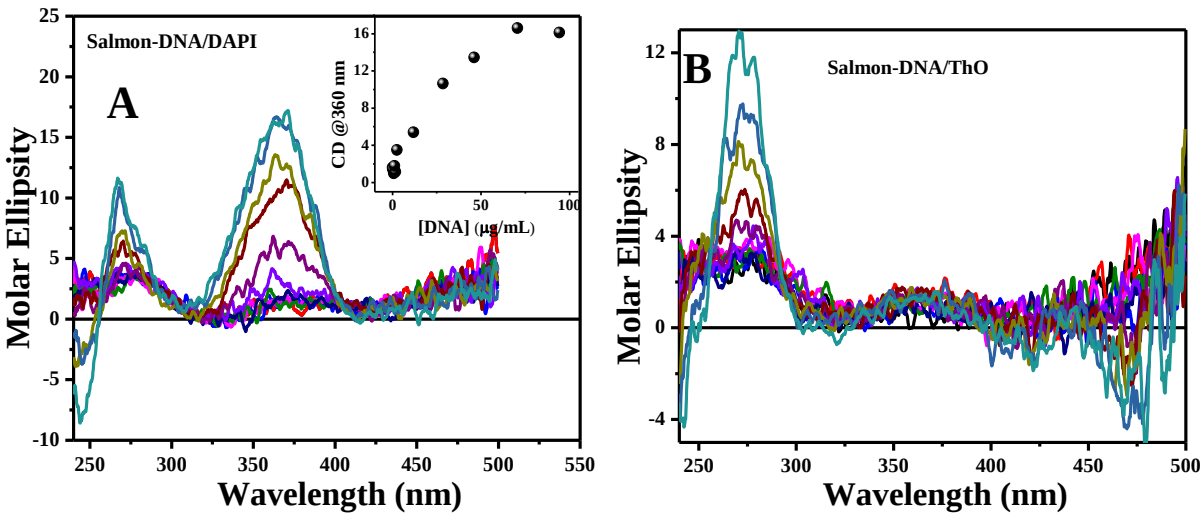

Figure 3.5. (A) Molar ellipsity of DAPI with and without Salmon-DNA. The spectrum shows the changes in ellipsity spectrum of DAPI around 350 nm as more is DNA added to the system. The result suggest the binding of DAPI to Salmon-DNA. (B) Molar ellipsity of ThO with and without Salmon-DNA, Here again, the ellipsity changed observed around 375 nm at different concentration

of DNA that matches the absorption spectrum of ThO and suggest the binding of ThO to Salmon-DNA.

3.3.1.4 Two-Photon Fluorescence Measurements

The results that were obtained from steady-state, CD and time-resolved fluorescence measurements confirm the binding of the investigated drugs molecules with DNA, but the results were different from each other. There were small differences between the interactions of the two drugs with DNA. These differences can be attributed to the way that each drug bound to DNA (the interaction mode). However, these results can not differentiate whether the interaction via intercalation or minor groove binding. Our hypothesis is that, 2PA measurements can differentiate both interactions. To address this hypothesis, two-photon fluorescence measurements were carried out on DAPI and ThO in buffer with increasing concentrations of salmon DNA. Figure 3.6A is the corresponding fluorescence spectra of DAPI with increasing concentrations of DNA, after excitation at 800 nm with the fundamental wavelength of the Ti:Sapphire laser. The inset of Figure 3.6A shows the normalized intensity enhancement at 465 nm as a function of DNA concentration and the increase is similar to one photon result confirming the binding of DAPI with DNA.

Two-photon fluorescence measurements also were carried out for ThO with increasing concentrations of DNA after excitation at 800 nm. Figure 3.6B shows the corresponding fluorescence spectra of ThO at different DNA concentrations. The inset of 3.6B shows the consistant increase in fluorescence intensity enhancement at 535 nm as a function of salmon DNA, which is similar to what was observed with one-photon event. These result confirm the binding of ThO to Salmon-DNA. We can notice from the results of DAPI and ThO that the 2P FL enhancement for DAPI binding to salmon DNA is higher than the 2P FL enhancement for ThO,

which means that the sensitivity of 2P FL for DAPI is higher than its sensitivity for ThO. These results might be due to the difference in the binding mode between the two drugs with Salmon-DNA, which is an indication that two-photon fluorescence is able to differentiate the binding modes of the two drugs with DNA.

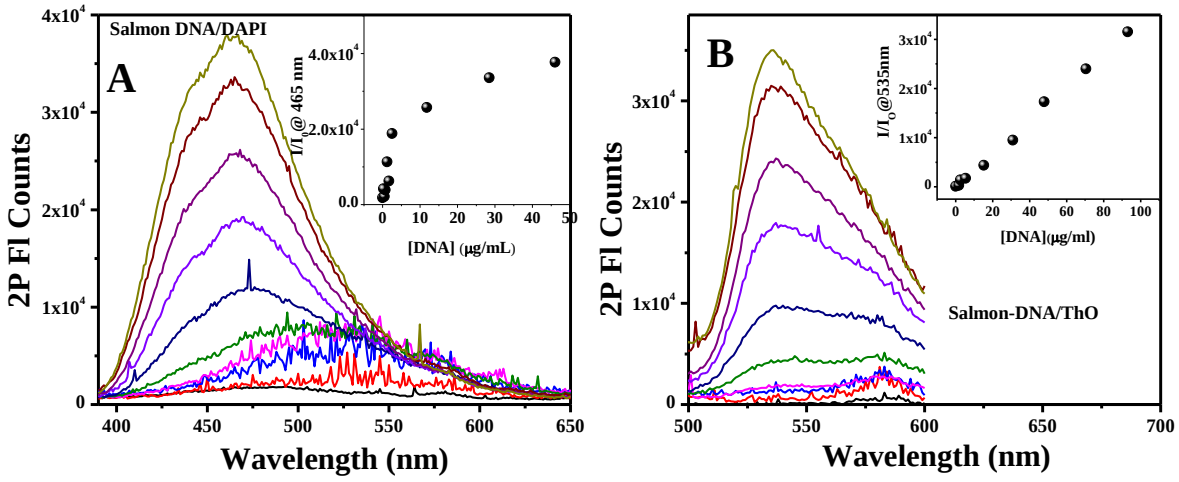

Figure 3.6. (A) Fluorescence spectra of DAPI at different concentrations of DNA after excitation at 800 nm. Inset shows the normalized intensity enhancement at 465 nm as a function of DNA concentration. (B) Fluorescence spectra of ThO at different concentrations of DNA after excitation at 800 nm. Inset shows the intensity change at 535 nm as a function of DNA concentration.

3.3.1.5 Relative Two-Photon Fluorescence Enhancements

For further confirmation of our hypothesis and to check if two-photon fluorescence measurements can be used to differentiate the different binding modes of the drugs with DNA, we carried out relative two-photon fluorescence measurements for the two investigated drugs at 800 nm. Relative two-photon enhancement is a measure of two-photon absorption cross-section which can be determined by:

$$\frac{\delta[\mathrm{DNA}]}{} = \frac{I_{2\mathrm{PE}}[\mathrm{DNA}]}{} \times \frac{I_{1\mathrm{PE}}[0]}{}$$

δ[0] I_{2PE}[0] I_{1PE}[DNA]

where, δ represents the two-photon cross-section; (I_{2PE}) and (I_{1PE}) are fluorescence intensities after two-photon and one-photon excitation, respectively.

Relative two-photon cross-sections for the two drugs were determined by above equation and the two-photon and one-photon enhancements for DAPI and ThO were plotted as a function of DNA concentration as shown in Figure 3.7A and 3.7B, respectively. It was observed from Figure 3.7A that the two-photon enhancement for DAPI with Salmon-DNA was significantly higher than that of one-photon fluorescence and the enhancement about 22-fold. This trend was more pronounced at higher DNA concentrations. However, contrasting trends were observed for ThO with salmon DNA figure 3.7B. It was observed that the fluorescence intensity enhancement was the same for both one-photon and two-photon measurements, and there is no enhancement for two-photon, which indicates that the 2PA is not sensitive toward the binding of ThO drug to dalmon DNA and that might be due to the mode that ThO binds to salmon DNA.

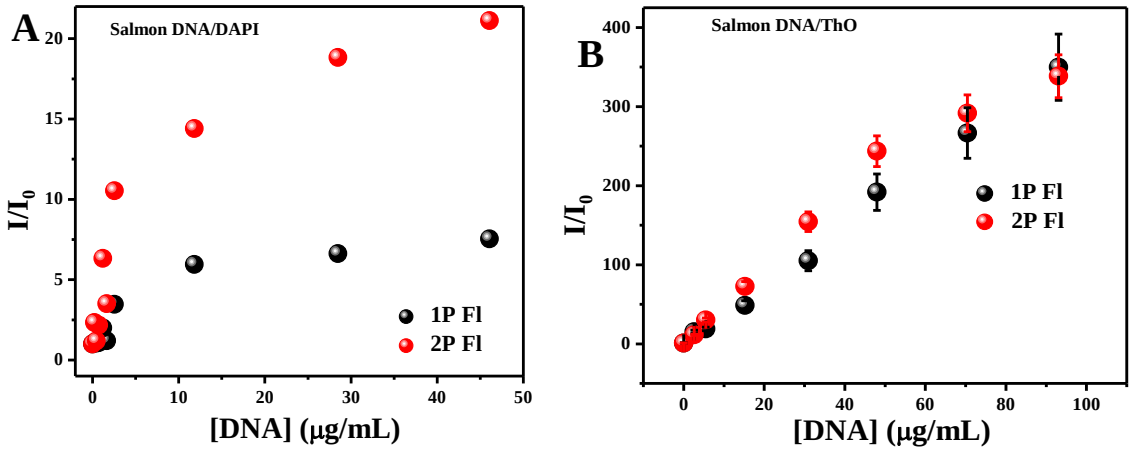

Figure 3.7. Comparison of fluorescence enhancement for (A) DAPI/Salmon DNA and (B) ThO/Salmon-DNA with one and two-photon excitation.

A comparison between the relative two-photon enhancements (which is a measure of two-photon absorption cross-section) for both DAPI and ThO drugs was determined from the ratio of 2-phootn to 1-photon fluorescence. Figures 3.8A and 3.8B show the results of relative 2PA cross-sections determined for DAPI and ThO, respectively. Figure 3.8A shows the interesting trends where the relative-2PA enhancement as a function of DNA concentration is about 3-fold for DAPI bound to salmon DNA while it is unchanged for ThO bound to DNA. The differences can be attributed to the way they are bound to salmon DNA.

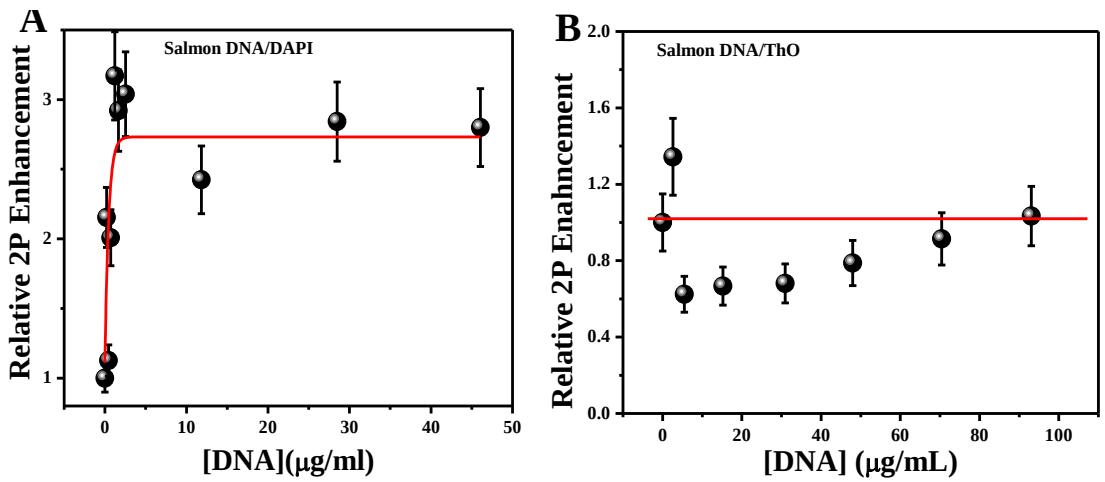

Figure 3.8. Relative 2PA cross-section enhancement for (A) DAPI/Salmon-DNA and (B) ThO/Salmon-DNA.

3.3.1.6 Power Dependence Measurements

In order to prove that the 2PA cross sections obtained for the two drugs DAPI and ThO was arising out of the two-photon excitation event only, power dependence fluorescence measurements were carried out while varying the laser power with a neutral density filter. Figure 3.9A and 3.9B show the power dependence plots for DAPI and ThO, repsectively. The results

show the slope of log (Fl.counts) vs log (power) gave a slope of almost 2.0 for all the systems thereby confirming that the fluorescence is a result of two-photon event.

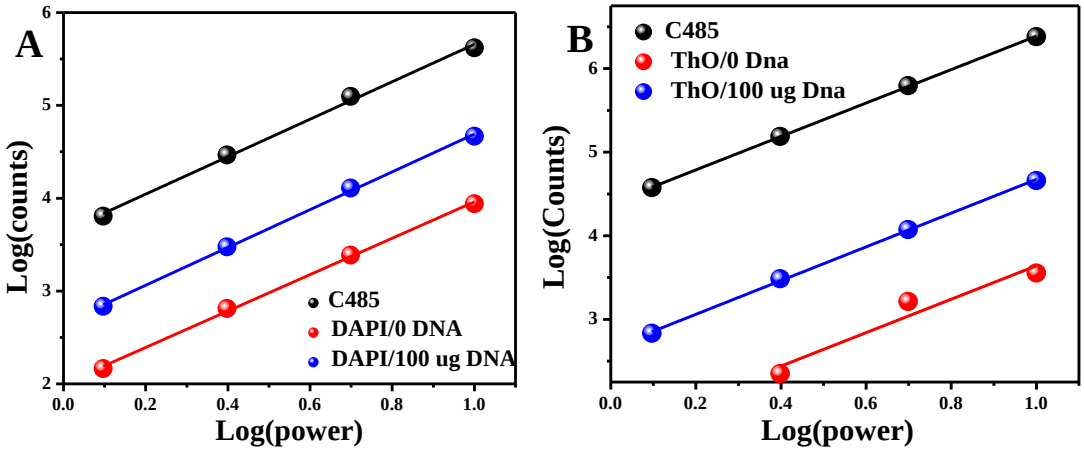

Figure 3.9. (A) Power dependence plot for C485, DAPI/Salmon Sperm DNA system after excitation at 800 nm. (B) Power dependence plot for C485, ThO/ Salmon Sperm DNA system after excitation at 800 nm. All the systems have shown slope 2.0 dependence suggesting that it is a two-photon event.

3.3.2 Calf Thymus-DNA with DAPI and ThO

3.3.2.1 Optical Absorption and Steady-State Measurements

Similar measurements were carried out for DAPI and ThO with and without 130 µg/mL of calf-thymus (CT) DNA. Optical absorption measurements are illustrated in Figure 3.10A and 3.10B for DAPI and ThO, respectively. The absorption maxima of DAPI drug has been shifted from 341 nm to 357 nm with increasing concentration of CT-DNA as shown in figure 3.10 A, and the inset shows the absorbance of DAPI at 380 nm as a function of CT-DNA concentration. These results show the binding of DAPI to CT-DNA. Figure 3.10B shows the absorption spectra of ThO

with increasing concentration of CT-DNA, and the inset shows the absorbance at 500 nm of ThO as a function of CT-DNA concentration. These results also suggest the binding of ThO drug with CT-DNA.

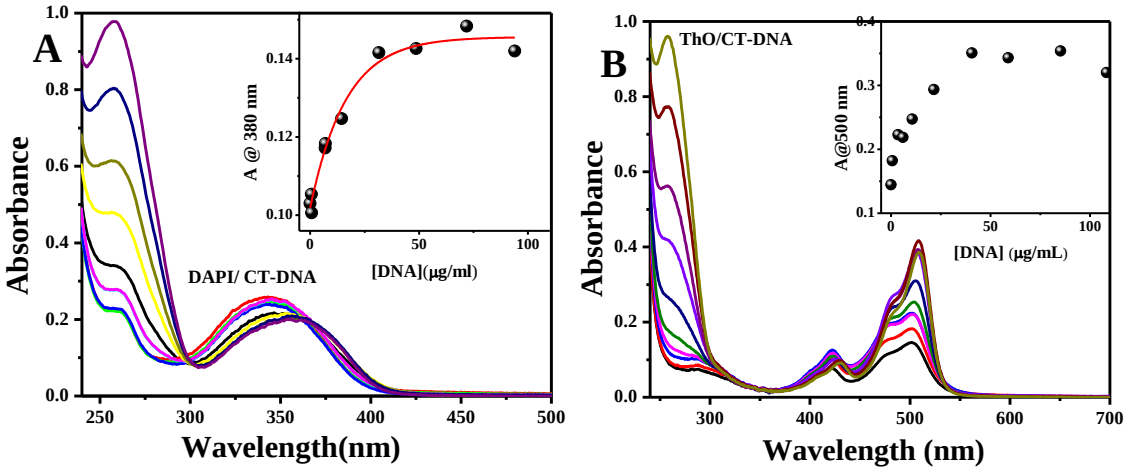

Figure 3.10 (A) Absorption spectra of DAPI with increasing concentration of CT-DNA. (B) Absorption spectra of ThO with increasing concentrations of CT-DNA.

One–photon fluorescence measurements also were carried out for both drugs with CT-DNA. Figure 3.11A represents the fluorescence measurements for DAPI with CT-DNA that were carried out after 360 nm excitation and monitoring the spectra from 380 nm to 650 nm. These results show a small increase at low DNA concentration then become higher at high DNA concentration, which is different from the optical absorption results that show a sharp increase in the absorption spectra at low DNA concentration. This difference might be due to the environment changes around the drug molecule at higher concentration of DNA. The inset of Figure 3.11A shows the normalized intensity of DAPI at 460 nm with increasing concentration of CT-DNA. One can notice the increase of DAPI intensity with increase in DNA concentration suggesting the binding of the drug with DNA. The fluorescence measurements for ThO with CT-DNA were

carried out after 480 nm excitation and monitoring from 500 nm to 700 nm (figure 3.11B). The fluorescence intensity of ThO increases as the DNA concentration increases, and the inset of figure 3.11B represents the intensity of ThO at 530 nm as a function of DNA concentration. Optical absorption and Steady state measurements for ThO/CT-DNA shows that the drug molecule bonded to CT-DNA and the changes in absorption and fluorescence spectra related to the mode that the drug bound to DNA.

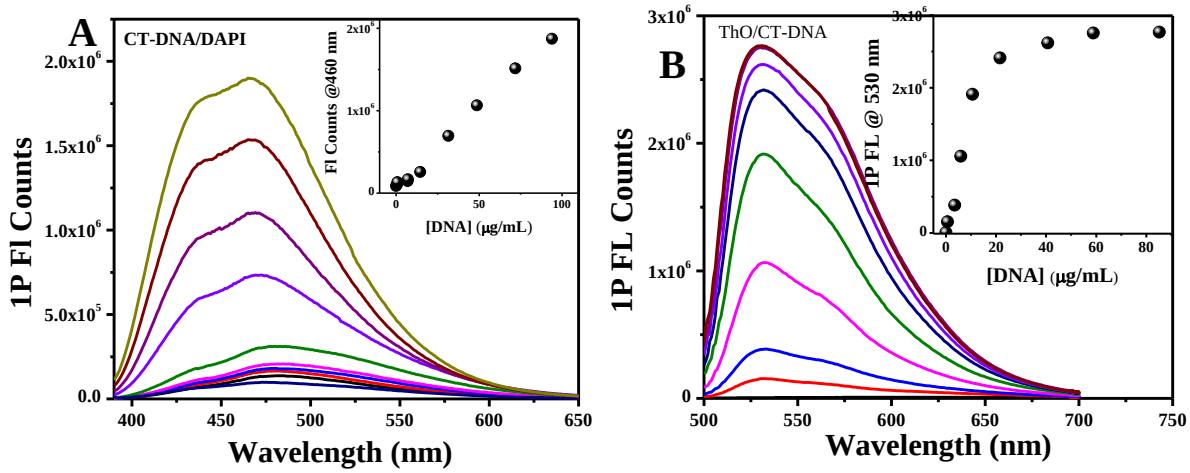

Figure 3.11. (A) One-photon fluorescence spectra of DAPI with increasing concentration of CT-DNA. Inset shows the normalized intensity at 460 nm with increasing DNA concentration (B) Fluorescence spectra of ThO with increasing concentrations ofCT- DNA. Inset shows the fluorescence intensity at 530 nm with increasing DNA concentration.

3.3.2.2- Time-Resolved Fluorescence Measurements

Fluorescence lifetime measurements were also carried out for CT-DNA with DAPI and ThO. DAPI has low fluorescence quantum yield (as the rotation around the single bound can lead to fast non-radiative relaxation) and long fluorescence life time, thus TCSPC measurements were

carried out after excitation with laser diode of 373 nm and monitoring the fluorescence at 450 nm for DAPI in buffer solution and DAPI with 130 □g/mL CT-DNA. Figure 3.12A represents the fluorescence decay traces of DAPI with and without CT-DNA and the majority of the decay finished within 20 ns. The fluorescence decay traces were fitted with exponential functions, and the corresponding life time data is provided in Table 3.3. The fluorescence life time for ThO were obtained after excitation with a laser diode of 457 nm and monitoring the fluorescence at 530 nm (similar to salmon DNA). The majority of the decay traces were finished within 25 ns (figure 3.12B). The fluorescence decay traces were fitted with exponential functions and the corresponding life time data is provided in Table 3.4.

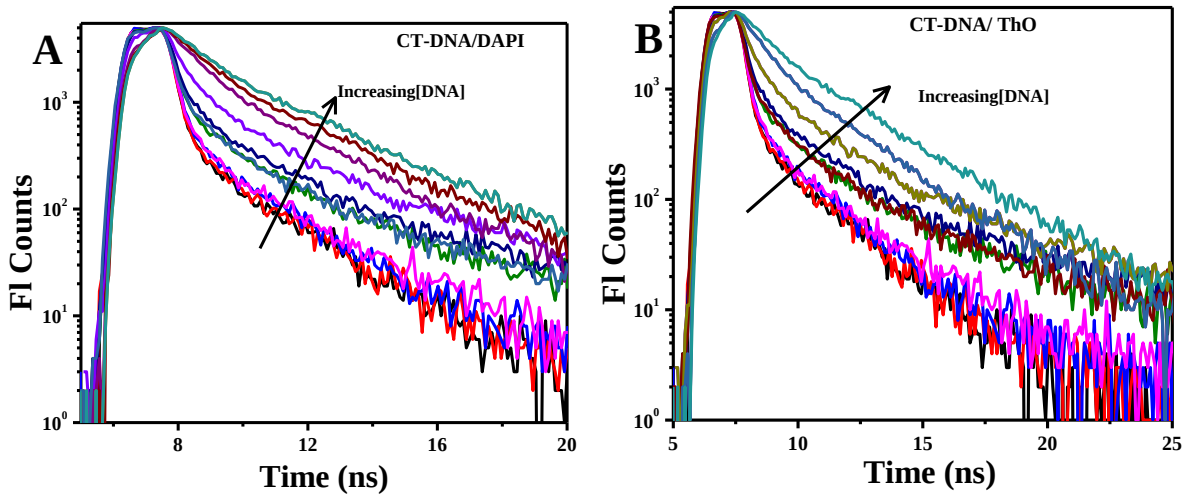

Figure 3.12. **(**A) Fluorescence decay traces of DAPI and DAPI/ CT-DNA monitored at 450 nm after excitation at 373 nm laser diode (B) Fluorescence decay traces of ThO and ThO/ CT-DNA monitored at 530 nm after excitation at 457 nm with laser diode.

Table 3.3. Fluorescence lifetimes for DAPI at different concentrations of CT-DNA.

[DNA] μg/ml	**Life times (ns)**	**Avg life time(ns)**
0	0.30 ± 0.003 (86.0%), 2.33 ± 0.041 (14.0%)	0.57
0.6	0.24 ± 0.004 (86.0%), 2.14 ± 0.037 (14.0%)	0.57
0.7	0.23 ± 0.004 (85.0%), 2.15 ± 0.036 (15.0%)	0.51
6.9	0.26 ± 0.005 (83.0%), 2.24 ± 0.035 (17.0%)	0.52
7.0	0.27 ± 0.005(83.0%), 2.54 ± 0.039 (17.0%)	0.60
14.5	0.35 ± 0.004 (76.0%), 3.42 ± 0.040 (24.0%)	0.66
31.5	0.40 ± 0.004 (73.0%), 3.81 ± 0.042 (27.0%)	0.70
48.6	0.61 ± 0.006 (66.0%), 4.06 ± 0.041 (34.0%)	0.80
71.8	0.90 ± 0.012 (63.0%), 3.49± 0.041 (37.0%)	1.03
93.9	0.91 ± 0.020 (49.0%), 3.00 ± 0.030 (51.0%)	1.40

Table 3.4. Fluorescence lifetimes for ThO at different concentrations of CT-DNA.

[DNA] μg/ml	**Life times (ns)**	**Avg life time(ns)**
0	0.30 ± 0.003 (86.0%), 2.33 ± 0.041 (14.0%)	0.57
0.6	0.24 ± 0.004 (86.0%), 2.14 ± 0.037 (14.0%)	0.57
0.7	0.23 ± 0.004 (85.0%), 2.15 ± 0.036 (15.0%)	0.51
6.9	0.26 ± 0.005 (83.0%), 2.24 ± 0.035 (17.0%)	0.52
7.0	0.27 ± 0.005(83.0%), 2.54 ± 0.039 (17.0%)	0.60
14.5	0.35 ± 0.004 (76.0%), 3.42 ± 0.040 (24.0%)	0.66
31.5	0.40 ± 0.004 (73.0%), 3.81 ± 0.042 (27.0%)	0.70
48.6	0.61 ± 0.006 (66.0%), 4.06 ± 0.041 (34.0%)	0.80
71.8	0.90 ± 0.012 (63.0%), 3.49± 0.041 (37.0%)	1.03
93.9	0.91 ± 0.020 (49.0%), 3.00 ± 0.030 (51.0%)	1.40

3.3.2.3 CD Measurements

CD measurements were carried out to monitor the binding of the DAPI and ThO with CT-DNA. DAPI and ThO are a non-chiral molecules and hence should not give any signal in CD measurements. When both drugs bind to CT-DNA they become chiral as they impart the chirality of the DNA. With these considerations, the CD spectra of DAPI and ThO with and without CT-DNA were obtained and are shown in Figure 3.13A, B. Both drugs did not show any signal at zero DNA. However, a clear signal at 360 nm for DAPI matching the absorbance spectrum was observed suggesting that the drug was bonded to DNA. Also, the positive signal had features of minor-grove binding interactions. Similarly, ThO shows a CD signal when it bonds to CT-DNA (figure 3.13 B) and a clear signal was obtained around 375 nm matching the absorbance spectrum of ThO. However, the signal has a negative feature suggesting that the interaction is different than DAPI interaction.

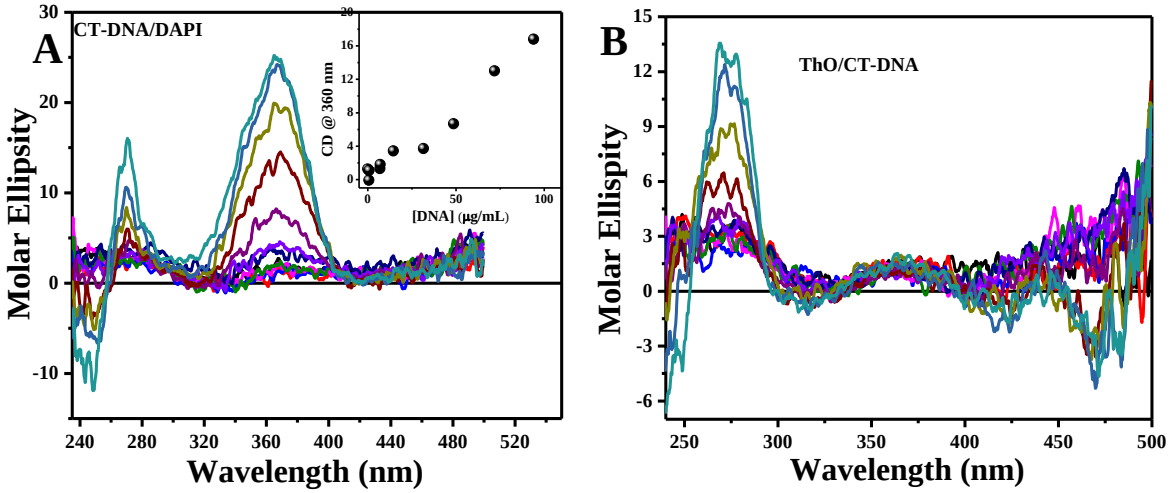

Figure 3.13. (A) Molar ellipsity of DAPI with and without CT-DNA. The changes in ellipsity spectrum of DAPI is around 360 nm as more DNA added to the system. This result suggests the

binding of DAPI to CT-DNA. (B) Molar ellipsity of ThO with and without CT-DNA, Here again, the ellipsity spectrum change observed around 375nm at different concentration of CT-DNA suggests the binding of ThO to CT-DNA.

3.3.2.4 Two-Photon Fluorescence Measurements

All the previous measurements were carried out to prove and show the binding nature of the investigated drugs with CT-DNA, but in order to differentiate between the binding mode of them with CT-DNA, two-photon fluorescence measurements were carried out for DAPI and ThO in buffer with increasing concentrations of CT-DNA. Figure 3.14A shows the fluorescence spectra of DAPI with increasing concentrations of CT-DNA, after excitation at 800 nm. The inset of Figure 3.14A shows the intensity enhancement at 466 nm as a function of CT-DNA concentration and the increase is similar to one photon result confirming the binding of the DAPI with CT-DNA. Figure 3.14B shows the fluorescence spectra for ThO with increasing concentrations of CT-DNA after excitation at 800 nm. The inset of 3.14B is the intensity enhancement at 534 nm and it shows the consistent increase in fluorescence intensity enhancement as a function of CT-DNA, which is similar to what was observed with one-photon excitation. These results confirm the binding of ThO to CT-DNA.

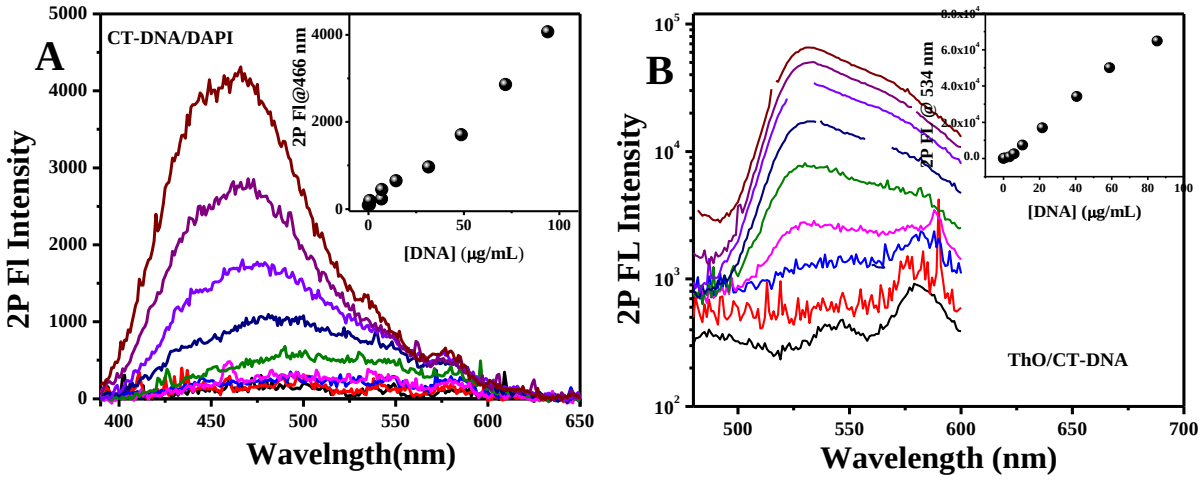

Figure 3.14. (A) Fluorescence spectra of DAPI at different concentrations of CT-DNA after excitation at 800 nm. Inset shows the normalized intensity enhancement at 466 nm as a function of DNA concentration. (B) Fluorescence spectra of ThO at different concentrations of CT-DNA after excitation at 800 nm. Inset shows the normalized intensity change at 534 nm as a function of CT-DNA concentration.

3.3.2.5 Relative Two Photon Fluorescence Enhancement

For further confirmation of our hypothesis, relative two-photon fluorescence measurements were carried out for the two investigated drugs with CT-DNA. Relative two-photon cross-sections were determined by the same equation used above. The two-photon and one-photon intensity for DAPI and ThO were plotted as a function of CT-DNA concentration as shown in Figure 3.15A, B, respectively. It was observed from Figure 3.15A that the two-photon enhancement for DAPI/CT-DNA was significantly higher than its one-photon fluorescence measurements and the enhancement about 50-fold, which indicates that the two photon is more sensitive to DAPI/CT-DNA system than one photon, suggesting the minor-groove binding. The 2PA enhancement was more pronounced for higher DNA concentrations. Whereas, for ThO/CT-

DNA system the fluorescence intensity enhancement for one-photon and two-photon are about the same, and there is no enhancement for two-photon which indicates that the 2PA is not sensitive toward ThO/CT- DNA system and that might be due to the kind of interaction mode between ThO and CT-DNA, suggesting the intercalating binding mode rather than minor groove mode.

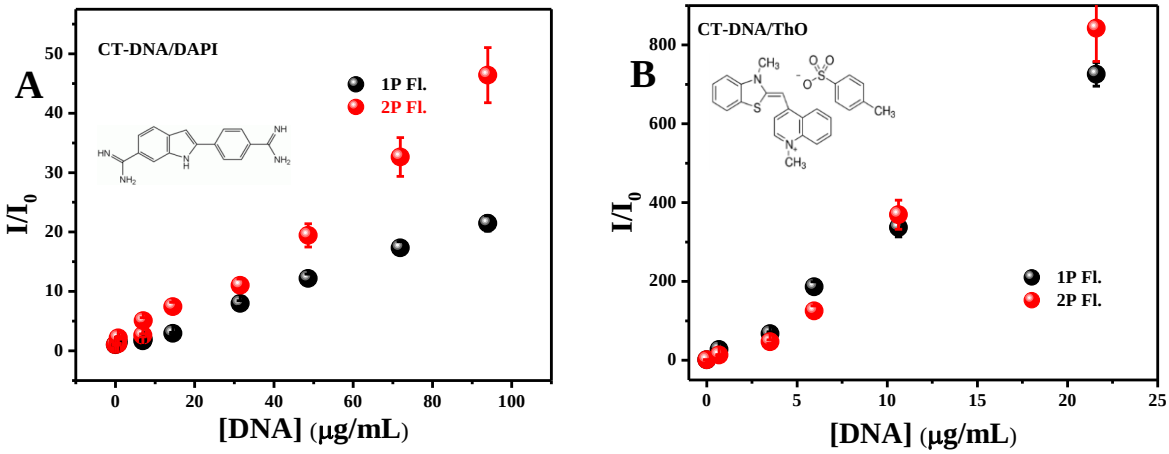

Figure 3.15. Comparison of fluorescence intensity enhancement of (A) DAPI/CT-DNA and (B) ThO/CT- DNA with one and two-photon excitation.

Then we carried out a comparison between the relative two-photon enhancements (which is a measure of two-photon absorption cross-section) for both DAPI and ThO drugs with CT-DNA. Figures 3.16A, B show the result for each one. Figure 3.16A shows the interesting trends where the relative-2PA enhancement as a function of DNA concentration is about 3-fold for DAPI binding to CT-DNA, while it is unchanged for ThO. The differences can be attributed to the way that the two drugs are bonded to CT- DNA.

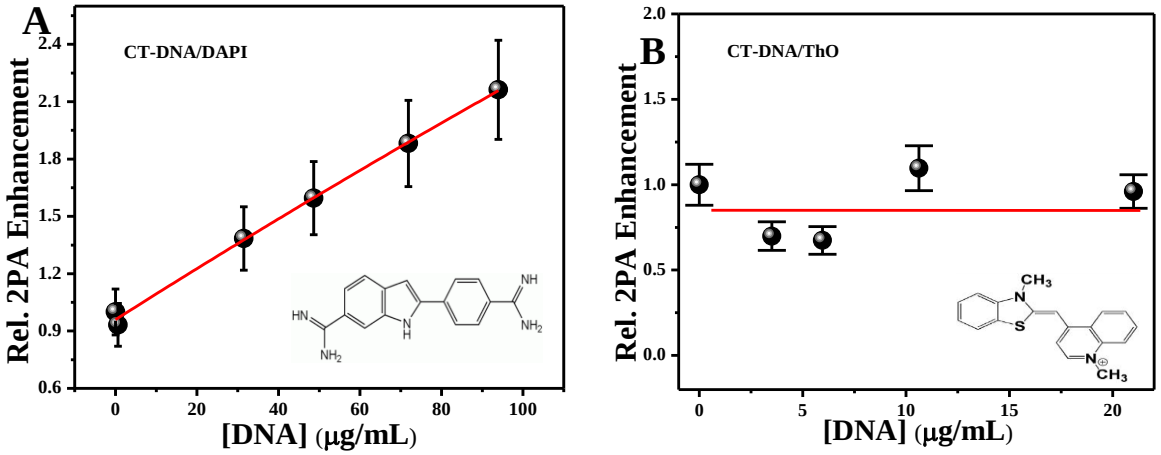

Figure 3.16. Relative 2PA enhancement for (A) DAPI/CT-DNA and (B) ThO/CT-DNA.

Power dependence fluorescence measurements were carried out for CT-DNA in order to prove that the 2PA cross section measurements were arising out of the two-photon excitation event only. These measurements carried out while varying the laser power with a neutral density filter. Figure 3.16A, B are the power dependence plots for DAPI and ThO at different concentration of CT-DNA in addition to the power dependence fluorescence for the standard. The results show a slope of 2.0 for all the systems, confirming that the fluorescence is a result of two-photon event.

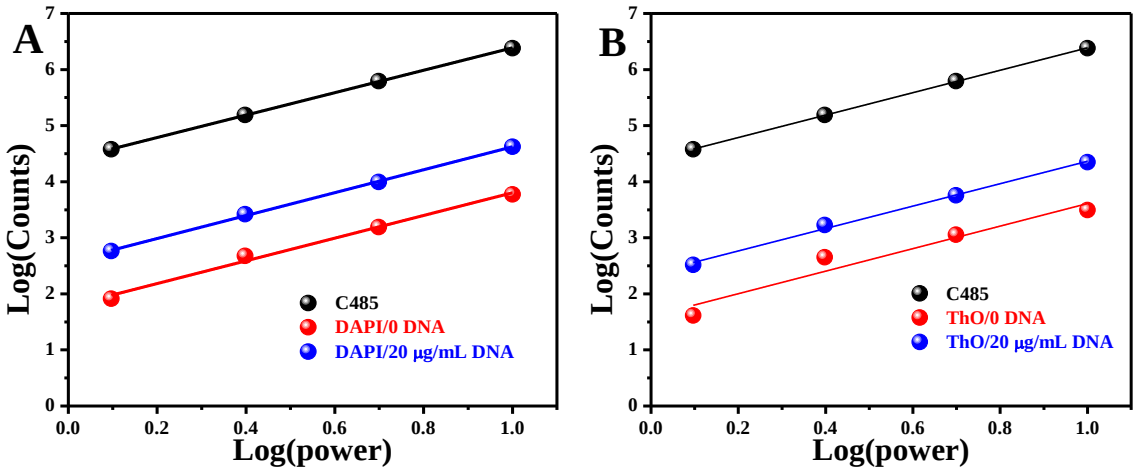

Figure 3.17. Power dependence plots for (A) C-485and DAPI/CT- DNA and (B) ThO/CT-DNA.

3.4 Mechanism of Drug-DNA Binding

The results of relative 2PA enhancement have shows that DAPI has shown increase in 2PA with increase in DNA concentration while ThO did not show any change. The results are interesting and are related to the way the drugs are bound to DNA. Our hypothesis that the 2PA cross-section of drugs are sensitive to the local electric field and specifically in case of DNA, which is considered an electric wire can influence the 2PA cross-sections of the drug. The 2PA can be influenced and altered depending on electric field's direction for the oriented drugs. This can be explained in the flowing sum over state relationship.

$$\delta_{2-state} = \frac{2(2\pi)^4 f_l^4}{15(nhc)^2} (1 + 2\cos^2\theta) \left|\overrightarrow{M_{ge}}\right|^2 \left|\overrightarrow{\Delta\mu_{ge}}\right|^2 g(2v)$$

Where, $\overrightarrow{M_{ge}}$ is the transition dipole moment between the ground state (g) and excited state (e), $\overrightarrow{\Delta\mu_{ge}}$ the difference between the permanent dipole moments in the ground and excited state, and θ is the angle between these two vectors. $g(2v)$, is the normalized line shape function, n is the refractive index, c the speed of light, h is the Planck's constant, and f_l is the local field factor (optical) given by $f_l = (n^2 + 2)/3$. It can be seen that the 2PA cross-section of the chromophore is proportional to the square of the transition dipole moment and the change in permanent dipole moment. The local electric field of DNA can contribute in a change to the total dipole moment of the system by in induced the drug's dipole moment[23, 24]

$$\Delta\mu_{ge} = \Delta\mu^{0}_{ge} + 0.5\Delta\mu^{ind}_{ge} = \Delta\mu^{0}_{ge} + 0.5(\Delta\alpha).E = \Delta\mu^{0}_{ge} + 0.5(\Delta\alpha).E\cos\theta$$

where, $\Delta\mu^{0}_{ge}$ corresponds to the permanent dipole moment change in the zero field situation, $\Delta\alpha = \alpha_e - \alpha_g$ is the change in polarizability between ground and excited states, E is the local electric field, and θ is the angle between the polarizability vector and the electric field. If the θ is zero degree angle (parallel to the electric field), the effect is maximum and one can observe large increases in 2PA cross-sections. Whereas, when the θ is 90 degrees (perpendicular to the electric field), one observes no change in the 2PA cross-section. If the θ is between 90 and 270 degrees, it can lead to a decrease in the 2PA cross-section. As a result, the orientation of the local electric field of DNA's back bone with respect to the orientation of the binding drug molecule is very important in altering the measurements of their 2PA cross-sections.

The DNA's electric field runs along the phosphate-sugar backbone in different directions. When drug molecules bind to duplex DNA, either via intercalation or minor-groove binding, the electric field is possibly affected in different ways (Figure 3.18). The 2PA cross-section can be used as an indicator of whether the DNA is intercalation or minor-groove binding, depending on the mode that the drug molecules bound to DNA.

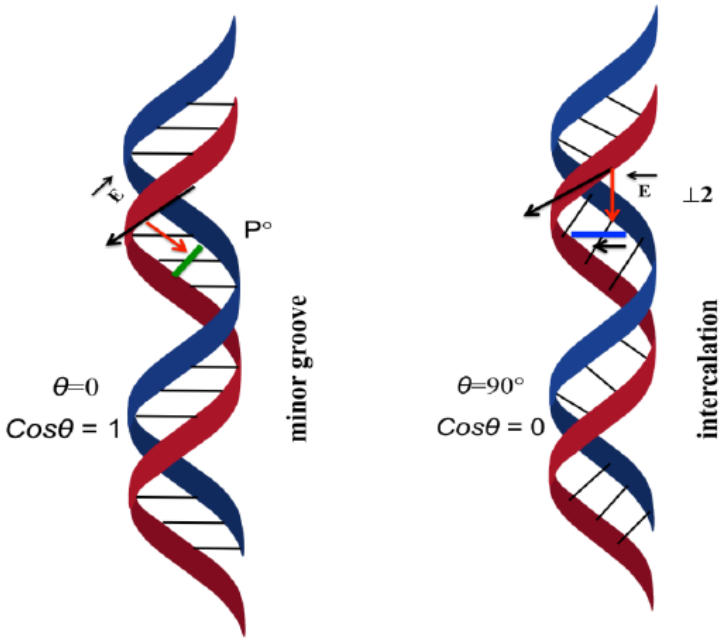

Figure 3.18. Drug molecules binding to duplex DNA and interacting with the electric field induced by the sugar-phosphate backbone.

The two-photon cross-section for our investigated drug DAPI, shows 2-fold enhancement between when bound to DNA, conforming that its interaction with duplex DNA was via the minor-groove binding mode. That is due to the parallel orientation of its dipole with the local electric field of DNA. This parallel interaction induced DNA's electric field and enhanced the 2PA cross-sections. However, the 2PA cross section results for ThO showed a decrease in 2PA measurements as it bound to DNA. The aromatic rings for ThO π-π stacking interaction with the DNA's base pairs. As a result, its dipole was perpendicular to the electric field offered by the DNA backbone, diminishing the effect of the electric field, which causes a decrease or no-change in 2PA cross-sections. The results showed that the 2PA cross-sections of chromophores are good indicators of intercalating binding versus minor-groove binding interactions. Also it can be used to differentiate

between them because the minor groove-binding drugs molecules should show an enhancement of 2PA cross-sections while intercalators should not have much effect on 2PA.

3.5 Conclusions

Combined optical measurements were carried out on two drug molecules, DAPI and ThO bound to salmon-sperm and CT DNA to prove the hypothesis that 2P spectroscopy can differentiate the mode of drug binding to DNA. Optical absorption, steady-state fluorescence and time-resolved fluorescence measurements have shown changes with increase in DNA concentration. CD measurements also confirmed the binding of the drugs with DNA. Relative 2PA cross-sections were determined from the ratio of 2-photon to 1-photon fluorescence for the drugs with both DNA. The results have shown increase in 2PA cross-sections for DAPI while ThO did not show increase with both DNA concentrations. These results were rationalized based on the fact that the DNA backbone's electric field when it is parallel to the drug dipole results in a minor-grove binding mode, while when it is perpendicular or more than 90 degree angle with respect to the drug's dipole, there is a decrease or no change in the 2PA cross-sections and results in intercalating binding mode. From these findings, DAPI is confirmed as a minor-grove binder while ThO is assigned as a intercalator that mach with literature reports. This study suggests that 2PA cross-sections is a new spectroscopic technique that can be used to monitor drug-DNA interactions and differentiate between their binding modes.

3.6 Summary

- This Chapter has focused on proving the hypothesis that relative 2PA cross-sections can differentiate drug-DNA interactions, as they are sensitive to the local electric fields offered by the DNA's backbone.
- To prove the hypothesis, investigations were carried out on two drugs, DAPI and ThO binding to salmon-DNA and CT-DNA.
- Optical absorption, steady-state fluorescence, time-resolved fluorescence and CD measurements confirmed the binding of drugs with DNA.
- Relative 2PA cross-sections were determined from the ratio of 2P fluorescence to 1P fluorescence and the results indicate an enhancement of 2P cross-sections for DAPI with both salmon-DNA and CT-DNA.
- Relative 2PA cross-sections of ThO did not change much with either salmon-DNA or CT-DNA.
- The results can be rationalized the way with which DAPI binds to DNA which is via minor-groove and where the drug's dipole is parallel to the DNA backbone's electric field and thereby enhancing the 2P cross-section.
- ThO binds to DNA via intercalation and its orientation is perpendicular to DNA backbone's electric field and thus no change in 2PA cross-section was observed.
- The results have shown that 2P spectroscopy is a sensitive technique to not only monitor the binding of drugs with DNA but also can differentiate the modes of binding.

3.7 References

1. Makarov, N. S.; Drobizhev, M.; Rebane, A. Two-photon absorption standards in the 550-1600 nm excitation wavelength range. *Optics Express* **2008**, *16*, 4029-4047.
2. Cui, F.; Jin, B. J.; Niu, A. X.; Liu, A. Q. Spectroscopic and Modelling Analysis on the Interaction of 39-Azidodaunorubicin Semicarbazone with ctDNA, **2014**, 234–240.
3. Leonard, D. *Molecular Pathology In Clinical Practice*; Springer: New York, **2007**, p 290.
4. Krogsgaard-Larsen, P. *Textbook Of Drug Design And Discovery*; Taylor & Francis: London, **2002**.
5. Ihmels, H.; Faulhaber, K.; Vedaldi, D.; Dall'Acqua, F.; Viola, G. *Photochem. Photobiol.* **2005**, *81*, 1107–1115.
6. Dey, B.; Rani, V.; Manghani, C.; Gupta, S.; Chakrobarty, M.; Krishnan, S.; Thukral, S. DNA-Protein Interactions: Methods For Detection And Analysis. *Mol Cell Biochem,* **2012**, *365*, 279-299.
7. Phi Doan, Demar R. G. Pitter, Andrea Kocher, James N. Wilson, Theodore Goodson, A New Design Strategy and Diagnostic to Tailor the DNA-Binding Mechanism of Small Organic Molecules and Drugs, *ACS Chemical Biology*, 2016, **11**, 11, 3202
8. Asbury, C.; Engh, G. Trapping Of DNA In Nonuniform Oscillating Electric Fields. *Biophysical Journal,* **1998**, *74*, 1024-1030.
9. Amos, M. *Theoretical And Experimental DNA Computation*; Springer: Berlin, **2006**, p 13.
10. Randall, G.; Doyle, P. DNA Deformation In Electric Fields: DNA Driven Past A Cylindrical Obstruction. *Macromolecules,* **2005**, *38*, 2410-2418.
11. Jansen, K.; Nordbn, B.; Kubista, M. Society **1993**, No. 28, 10527–10530.

12. H.S. Rye, S. Yue, D.E. Wemmer, M.A. Quesada, R.P. Haugland, R.A. Mathies, A.N. Glazer, *Nucl. Acids Res.* 20 (1992) 2803–2812.

13. Xu, C.; Webb, W. W. *J. Opt. Soc. Am. B* **1996**, *13*, 481-491.

14. Makarov, N. S; Dorbizhev, M; Rebance, A. *Opt Exp.* **2008**, *6*, 4029-4047.

15. Hawkins, C. *Nucleic Acids Research*, **2001**, *29*, 936-942.

16. Jansen, K.; Nordbn, B.; Kubista, M. Society **1993**, No. 28, 10527–10530.

17. Kapuściński, J.; Szer, W. *Nucleic Acids Res.* **1979**, *6* (11), 3519–3534.

18. Tan, S.; Yiap, B. *Journal of Biomedicine and Biotechnology*, **2009**, *2009*, 1-10.

19. Hermanson, G. *Bioconjugate techniques*. Amsterdam: Elservier/Academic Press **2013**.

20. Bairu, S.; Ramakrishna, G. *J. Phys. Chem. B* **2013**, *117*, 10484-10491.

21. Dorbizhev, M.; Makarov, N. S.; Tillo. S. E.; Hughes, T. E.; Rebane, A. Two-Photon Absorption Properties of Fluorescent Proteins. *Nature Methods* **2011**, *8*¸ 393-399.

22. Bairu, S.; Ramakrishna, G. Two-photon absorption properties of chromophores in micelles *J. Phys. Chem. B* **2013**, *117*, 10484-10491.

23. K ning, H.; Unden, G.; Fr hlich, J. *Biology Of Microorganisms On Grape, In Must And In Wine*; Springer-Verlag: Berlin, **2009**, pp 441-442.

24. Primrose, S.; Twyman, R. *Principles Of Genome Analysis And Genomics*; John Wiley & Sons: New York, NY, **2009**, p 39.

CHAPTER 4

CHARACTERISATION THE BINDING INTERACTION OF NETROPSIN AND DOXORUBICIN WITH SALMON SPERM-DNA VIA TWO-PHOTON ABSORPTION SPECTROSCOPY

4.1 Introduction

In this Chapter, research is carried out to use 2PA spectroscopy to monitor the binding interactions and modes of binding of drugs that are fluorescent and non-fluorescent with DNA. To achieve this target, investigations were carried out two drugs, Netropsin and Doxorubicin that are known to work as antitumor and antiviral drugs. In Chapter 3, we presented a study that showed the feasibility of the 2PA spectroscopy to distinguish different binding modes of the drugs with DNA.

The studies of drug-DNA interaction are crucial for understanding the mechanism of the drug action. Several drugs work via the drugs binding to DNA. Netropsin, for example and its close relative distamycin are antiviral antitumor antibiotics that, although too toxic for clinical use, have received an extensive study as a model of base-specific ligand with non-intercalative DNA-binding. Chemical protection studies and NMR experiments, indicate that Netropsin does not intercalate between base pairs, but it binds with the minor groove of the intact double helix, using hydrogen bonds between Netropsin amide NH and exposed adenine N-3 and thymine 0-2 on the floor of the minor groove. Binding involves both an electrostatic component from the two cationic ends and hydrogen bonds from the central three amide NH groups.[1,3] Netropsin amide NH extend hydrogen bonds to bridge DNA adenine N-3 and thymine O-2 atoms occurring on adjacent base pairs and opposite helix strands, exactly as with the spine of hydration. The narrowness of the

groove forces the Netropsin molecule to sit symmetrically in the center, with its two pyrrole rings slightly non-coplanar so that each ring is parallel to the walls of its respective region of the groove. Drug binding neither unwinds nor elongates the double helix, but it does force open the minor groove by 0.5-2.0 A, and it bends back the helix axis by 8 degrees across the region of attachment. Netropsin (figure 4.1) and other minor groove binding compounds are of current research interest because of their therapeutic potential against diseases in addition to their use in biocenology applications. Furthermore, DNA minor groove continues to be an important target to improve and develop anti-cancer, anti-viral drugs.[1, 4]

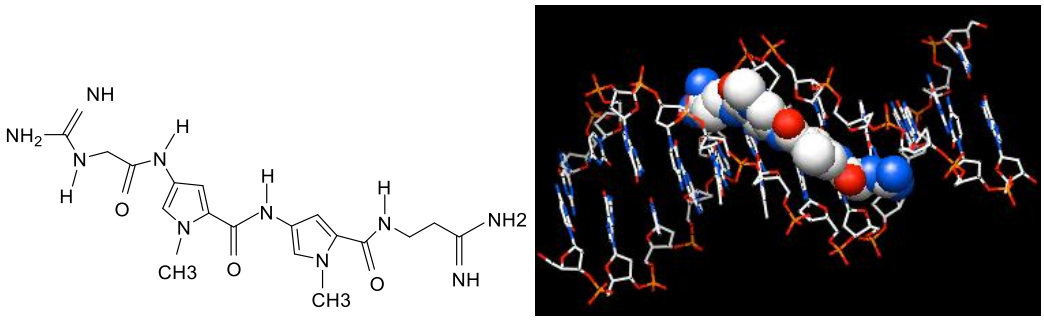

Figure 4.1. The chemical structure of Netropsin drug and the binding interaction mode of the drug with ds-DNA (minor groove binding)

On the other hand, there are other kinds of interactions and complexations that the biological molecules can adopt when they bind to DNA. Intercalation, is one of these binding interactions that can be utilize in therapeutic applications and biological diagnostic. Doxorubicin is considered an example of an intercalation binding drugs. It's one of the most important anti-cancer chemotherapeutic drugs, being widely used for the treatment of solid tumors and acute leukemias (figure 4.2). Millions of cancer patients have been treated with Doxo, or its variants

daunorubicin. The action of doxorubicin drug (which is belong to a class of compounds called anthracyclines), has been intensively investigated during the last several decades, but the mechanisms that have been proposed for cell killing remain irregular and controversial. Doxorubicin and anthracyclines drugs are mostly planar molecules that preferentially intercalate between neighboring DNA base pairs, anchored on one side by one or more sugar moieties that sit in the DNA minor groove. The strand separation that occurs during intercalation, unwinds the double helix and produces DNA supercoils, resulting in increased torsional stress.[5] Doxo acts by inhibiting topoisomerase II (TopoII), resulting in DNA double-strand breaks. The cells then activate the DNA damage response (DDR) signaling to guide recruitment of the repair machinery to these breaks.[6] Complexation between the drugs and a nucleic acid can be effected by different properties which have been considered as an important requirements for the successful modeling of Drug-DNA interaction such as, degrees of freedom, role of base pair sequence, counter ion effects, and role of solvent ligand-receptor binding.[7]

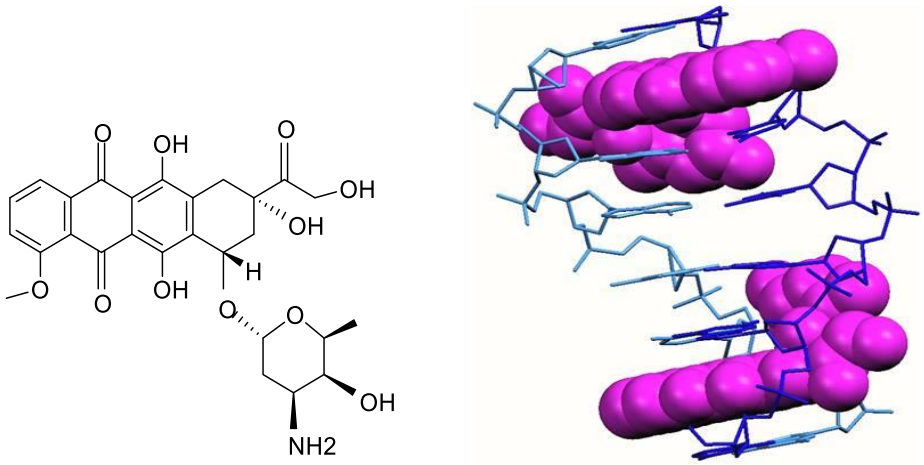

Figure 4.2. The chemical structure of Dxorubicin drug and the binding interaction mode of the drug with ds-DNA (intercalation.)

There are number of techniques focused on monitoring drug-DNA interactions. These include, UV-VIS spectrophotometry, competition dialysis assay, HPLC-MS, capillary electrophoresis-mass spectrometry, NMR spectroscopy, viscometry and vibrational spectroscopy (IR and Raman spectrometries) [8]. These techniques can reveal details about the DNA-drug stoichiometry such as the thermodynamics of complex formation. However, they are not useful in differentiating the binding modes of the drugs with DNA (intercalation versus groove-binding). In Chapter 3, we have shown that 2P spectroscopy can monitor drug-DNA interactions and also differentiate the binding modes. In this work, we have used the same approach to monitor the binding interactions of two well-known anti-cancer, anti-viral drugs, Netropsin and Doxorubicin.[9] Optical absorption, one- photon, 2P fluorescence, time resolved fluorescence and circular dichroism were carried out to monitor the binding interaction of the two drugs with salmon DNA.

4.2 Experimental

4.2.1 Materials

Doxorubicin and Netropsin were obtained from Sigma-Aldrich. Salmon Sperm DNA, Thioflavin T and Hoechst 33258 (structures shown in Figure 4.3) were obtained from Sigma-Aldrich and were used as such. Tris-HCl, NaCl were obtained from Sigma-Aldrich and were used as received. Nanopure water from Millipore inc., was used. All the measurements were carried out in buffered solutions unless stated otherwise. A buffer stock solution (pH = 7.2) was made using tris-HCL (5 mM), NaCl (50 mM) and milli-Q water. The salmon sperm DNA was combined with the buffer solution (10 mL) to create a stock solution of DNA. The drug was combined with DMSO (5 mL) to create the stock solution. Ten samples were made from the stock solutions with

increasing concentrations of DNA placed in each (0, 10, 20, 30, 50, 70, 100, 150, 200, 300 μL) vial. Each sample was 1 mL, so the buffer solution was added decreasingly as each sample was made, while the drug solution (20 μL) was added to each sample uniformly. This process was repeated for both Netropsin and Doxorubicin.

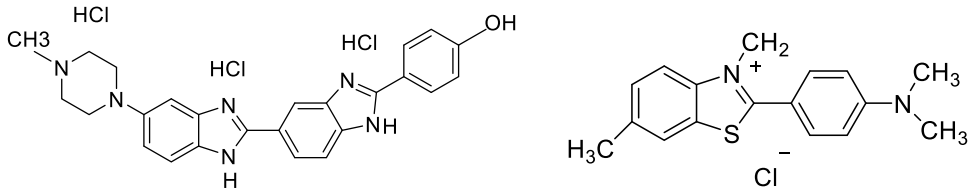

A **B**

Figure 4.3. Chemical structure of Hoechst 33258 (A) and ThT (B).

4.2.2 Optical Methods

The UV/Vis absorption spectrometric measurements were carried out in a Shimadzu UV2101 PC spectrophotometer. One-photon fluorescence measurements were carried out using Hitachi F2500 spectrofluorimeter. The 2PA cross-sections were measured using the two-photon excited fluorescence technique with C485 in methanol as a standard.[11,12] The output from Tsunami (Spectra-Physics), 720 nm to 900 nm, 100 fs was used to carry out the measurements. The relative 2PA cross-sections were determined from the ratio of one and two-photon fluorescence of the samples. The CD spectra were measured under N_2 over the range of 200-600 nm. Time-correlated single photon counting measurements were carried out with diode laser excitation were carried out to monitor nanosecond lifetimes. The measurements were carried out on an Edinburgh F900 spectrofluorimeter; a cooled Hamamatsu-R928P PMT was used as the detector.

4.3 Results and Discussion

4.3.1 Interaction of Netropsin with salmon DNA

4.3.1.1 Optical Absorption and Steady-State Fluorescence Measurements

Optical absorption and fluorescence measurements were carried out for all investigated drug molecules with and without (100 μg/mL) salmon DNA to understand their interaction with DNA. Figure 4.4 shows the optical absorption spectra at different concentrations of salmon DNA (0, 10, 20, 30, 50, 70, 100, 150, 200, and 300 μL). From the figure, it can be observed that the absorbance increased with increasing DNA concentration. The DNA concentration in all samples was calculated from the absorbance at 260 nm by using this relation: [DNA] (μg/mL) = A/ (0.02 * *l)*, where *l* is the path length of the cuvette and A is the absorbance at 260 nm.

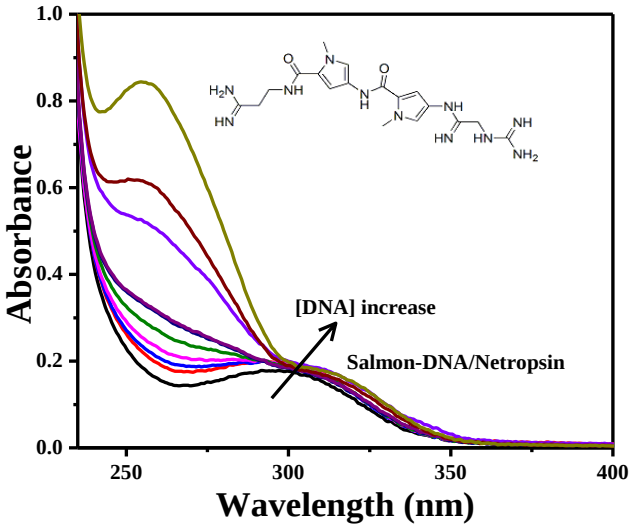

Figure 4.4. Optical absorption spectra of Netropsin as a function of salmon-DNA concentration.

Figure 4.5 presents the steady-state fluorescence measurements for the binding of Netropsin with salmon DNA, and the inset shows the intensity of Netropsin at 432 nm as a function of DNA concentration. The increase in the fluorescence intensity indicates the electronic

interaction of Netropsin drug with DNA, which results from the increase in the rigidity of the drug due to binding mode that leads to enhanced fluorescence intensity.

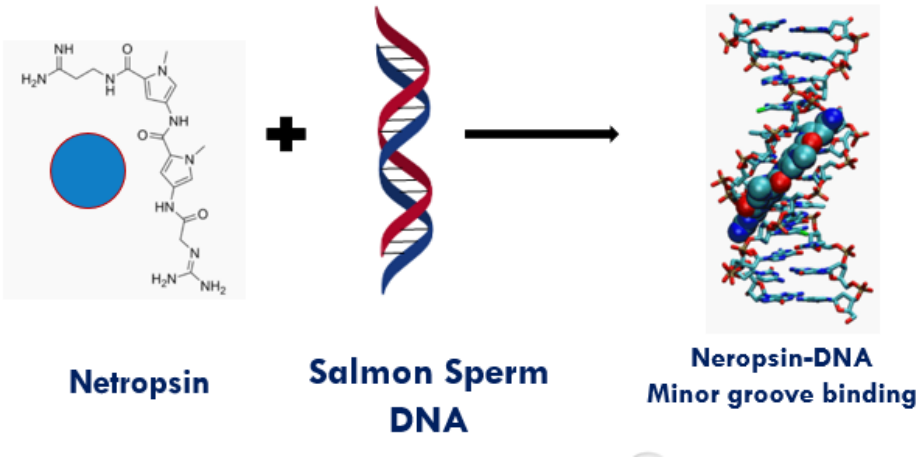

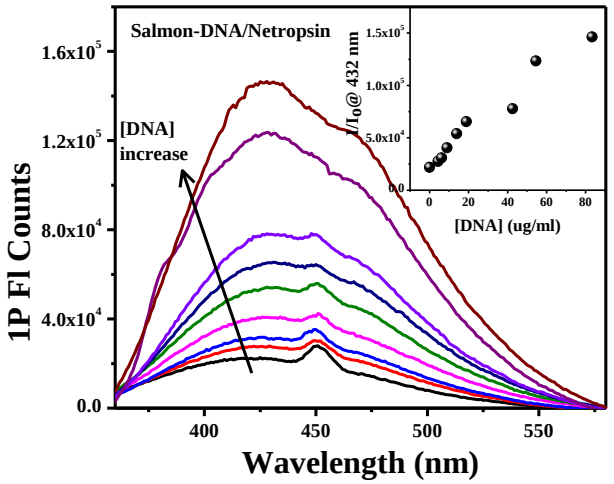

Figure 4.5. (A) The binding interaction of Netropsin with Salmon-DNA. (B) Steady-state fluorescence spectra of Netropsin as a function of salmon DNA concentration. Inset shows the fluorescence intensity at 432 nm as a function of DNA concentration.

4.3.2 Time-Resolved Fluorescence Measurements

Fluorescence lifetime measurements were carried out on Netropsin with and without salmon DNA to probe the binding of the drug with DNA. The measurements were carried out after excitation with 370 nm laser diode and monitoring the emission at 450 nm and corresponding

decay traces are presented in Figure 4.6. The fluorescence decay was fitted with exponential function and the corresponding lifetime data is provided in table 4.1. The lifetime of Netrospin is around 4.5 ns and increased with increasing DNA concentration to reach a lifetime of 5.8 ns. The results suggest the influence of DNA on the excited states of netropsin. It has to be noted that the lifetime increase is marginal when compared to steady-state fluorescence enhancement suggesting that the ultrafast processes are probably involved. Ultrafast relaxation dynamics is expected for Netropsin as the single bond rotation is unhindered in buffer solution because of its low viscosity.

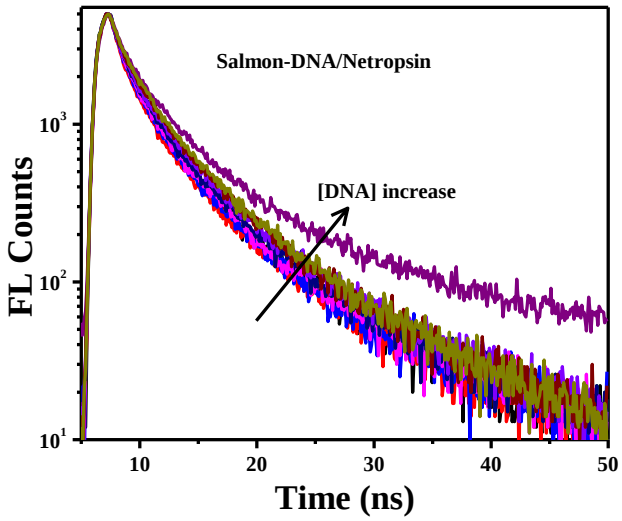

Figure 4.6. Fluorescence decay traces of Netropsin in buffer solution and in Salmon- DNA solution, monitored at 450 nm after excitation with 370 nm laser diode.

Table 4.1 Fluorescence Lifetimes for Netropsin at different concentration of Salmon Sperm DNA

[DNA](µg/ml)	Life time (ns)	Avg. life time(ns)
0	6.55 ± 0.059 (50.0%), 1.47 ± 0.018 (50.0%)	4.65
4.4	6.40 ± 0.062 (50.0%), 1.44 ± 0.017 (50.0%)	4.42
6.1	6.10 ± 0.060 (50.0%), 1.46 ± 0.019 (50.0%)	4.39

8.9	6.21 ± 0.060 (52.0%), 1.48 ± 0.020 (48.0%)	4.48
13.9	1.57 ± 0.021 (48.0%), 6.50 ± 0.063 (52.0%)	4.57
18.9	6.71 ± 0.067 (52.0%), 1.65 ± 0.022 (48.0%)	4.74
42.6	1.62 ± 0.022 (46.0%), 6.72 ± 0.063 (54.0%)	4.76
54.6	7.87 ± 0.095 (55.0%), 1.94 ± 0.028 (45.0%)	5.79

As the wavelength of Netropsin absorption is below 400 nm, we were unable to carry out the two-photon fluorescence measurements. Thus, we have to use a two-photon marker to carry out the binding measurements of Netropsin with DNA. Two well-known markers have been proposed to carry out the measurements, which are Hoechst 33285 and Thioflavin T. Hoechst is a well–known minor-groove binding dye[15, 16] whereas Thioflavine T is a well-known intercalating dye[17, 18].

4.4 Interaction of Netropsin with Salmon-DNA and Hoe as Maker

Firstly, we have attempted to use Hoe/Salmon DNA as a two-photon marker to monitor the binding of the Netropsin with salmon DNA. (Figure 4.7) The samples were prepared with constant concentration of 600 µL of salmon DNA, 20 µL of Hoe and increasing netropsin concentrations (0, 3, 5, 10, 15, 20, 30, 35, 50, 60) µL. Each sample was 1 ml, so buffer was added decreasingly as each sample was made. This process also repeated for the second marker, Thioflavin T.

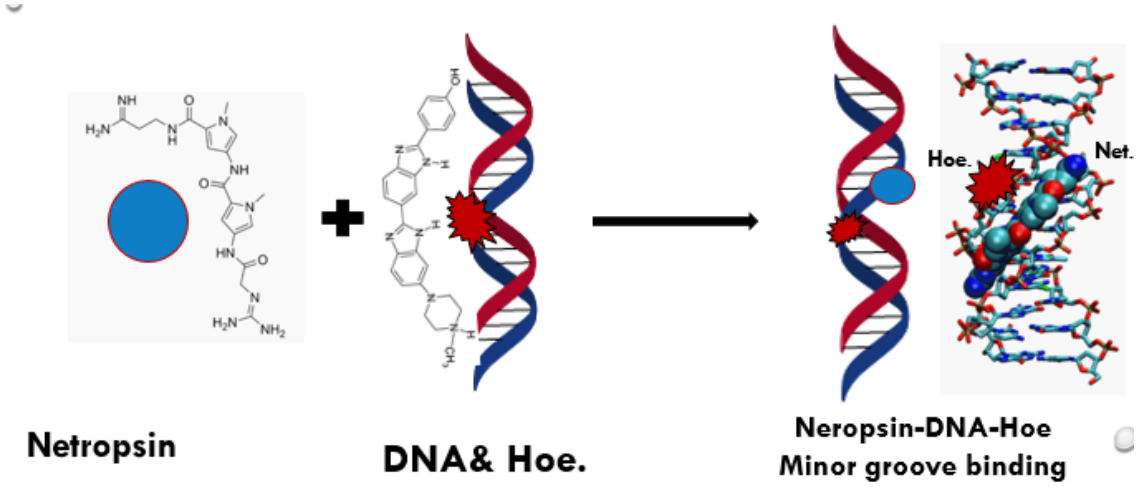

Figure 4.7. Cartoon diagram depicting Netropsin binding Salmon DNA tagged with Hoe.

4.4.1 Optical Absorption and Steady-State Measurements

Optical absorption and fluorescence measurements were carried out for the investigated system (Netropsin/Salmon-DNA/Hoe) with (294 μg/mL) salmon DNA and different Netropsin concentrations. Figure 4.8A shows the optical absorption of the system at different Netropsin concentrations. Hoe, already bound to salmon DNA via minor groove binding mode, has a good fluorescence intensity[19]. Then we introduced Netropsin drug to bind with Salmon-DNA/Hoe system. From the Figure 4.8A, we can notice the increase in optical absorption as more Netropsin is added. The inset shows the absorbance at 312 nm as a function of Netropsin concentration and the increase in absorbance suggest the addition of the drug. Steady-state fluorescence measurements were carried out and shown in Figure 4.8B. The fluorescence intensity of Hoe dye increased with the addition of Netropsin drug, indicating that the drug is interacting with the DNA/Hoe system. The increase in the fluorescence intensity as a result of drug binding action, is confirmed by the intensity progression increases at 468 nm as a function of Netropsin concentration which is shown in the inset of Figure 4.8B. The binding interaction of Netropsin

with a biological system like DNA is well reported in the literature. The resultant complex of this work will offer stabilization for the system by increasing its rigidity and hindering the rotation around the single bond.[20, 21]

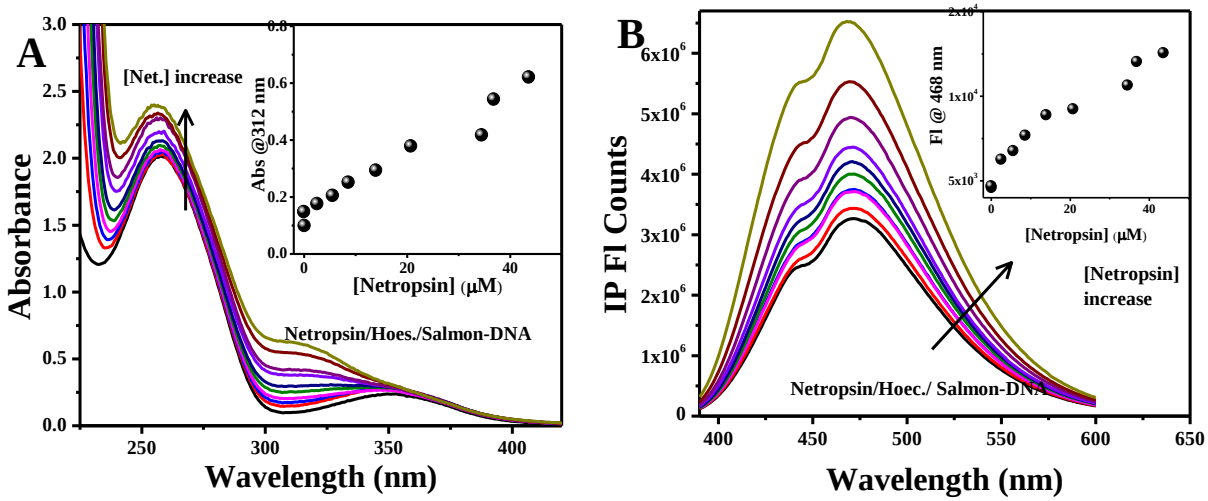

Figure 4.8. (A) Optical absorption spectra of Netropsin/Salmon Sperm-DNA /Hoe, (B) Steady-state fluorescence spectra of Salmon -DNA/Hoe as a function of Netropsin.

4.4.2- Two-photon Fluorescence Measurements

Similar to one-photon fluorescence, two-photon fluorescence measurements were also carried out for Hoe/Salmon-DNA as a function of Netropsin concentration after excitation at 800 nm. Shown in Figure 4.9 are the corresponding fluorescence spectra of the system and we can notice the increase in the two-photon fluorescence intensity as the Netropsin concentration increases. This result is similar to what was obtained in the one-photon fluorescence measurements. The normalized fluorescence intensity at 473 nm is shown in the inset of Figure

4.9 and a increasing trend was observed with increase in the drug concentration. The results confirmed that Netropsin is bound to Salmon-DNA marked with Hoe-dye.

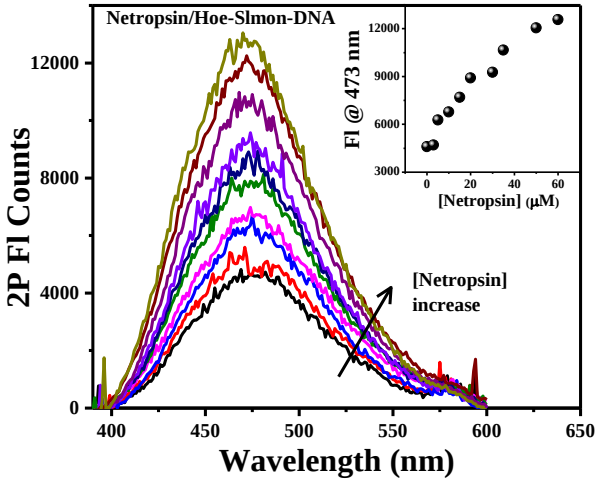

Figure 4.9. Two-photon fluorescence spectra of Netropsin/Hoe/Salmon-DNA as a function of Netropsin concentration after excitation at 800 nm. Inset shows the fluorescence intensity at 473 nm as a function of netropsin concentration.

4.4.3 Relative 2PA Cross-Section Measurements

Figure 4.10A shows the normalized fluorescence intensities of salmon-DNA/Hoe with increasing concentrations of netropsin with one-photon and two-photon excitation. The results show that the 2P intensity increase is higher than 1P photon intensity increase. Relative two-photon absorption cross-sections were determined using the relation:

$$\frac{\delta[\mathrm{DNA}]}{\delta[0]} = \frac{I_{2\mathrm{PE}}[\mathrm{DNA}]}{I_{2\mathrm{PE}}[0]} \times \frac{I_{1\mathrm{PE}}[0]}{I_{1\mathrm{PE}}[\mathrm{DNA}]}$$

where, δ represents the two-photon cross-section; (I_{2PE}) and (I_{1PE}) are fluorescence intensities after two-photon and one-photon excitation, respectively. The corresponding plot of relative 2PA cross-

sections for salmon-DNA/Hoe as a function of Netropsin concentration is provided in Figure 4.10B. It can be observed from Figure 4.10B, that the relative 2PA cross-section of Hoe has increased with increase in netropsin concentration suggesting that the minor-groove binding dye can be a good marker to study the binding of Netropsin with DNA.

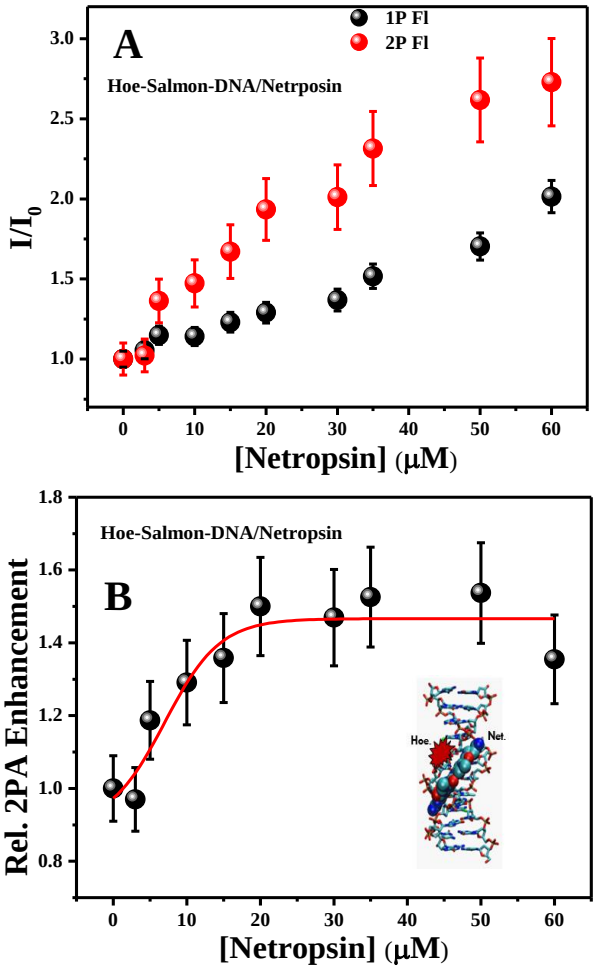

Figure 4.10. (A) Comparison of one-photon and two-photon fluorescence intensities of Salmon-DNA/Hoe as a function of Netropsin concentration. (B) Relative 2PA cross-sections for as a function of Netropsin concentration.

4.4.4 CD Measurements

To further probe the binding of Netropsin with DNA tagged with Hoe, CD measurements were performed. Figure 4.11 shows the CD spectra of Netropsin binding to the Salmon-DNA/Hoe. At zero Netropsin concentration the solution shows small CD signal as it is lacking in chirality. However, when Netropsin was added to the system and bound with DNA, a noticeable signal enhancement occured, indicating the binding of Netropsin with the system, and the positive feature of the signal suggesting the minor-groove interaction of Netropsin with the Salmon-DNA/Hoe.[23]

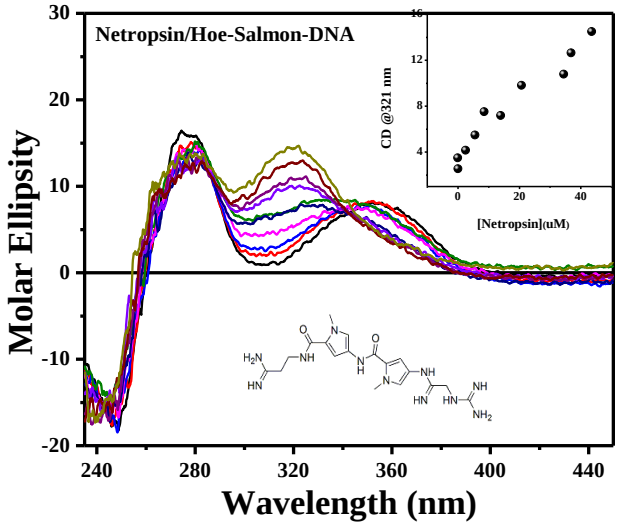

Figure 4.11. CD spectrum of (Hoe/Salmon-DNA) as a function of Netropsin concentration, and the inset showed the increase in CD signal as more Netropsin added to the system suggesting the binding of the drug with Salmon-DNA marked with Hoechst dye.

4.5 Interaction of Netropsin with Salmon-DNA/ThT

In the previous section, the monitoring of Netropsin binding with minor-groove binding marker (Hoe) was studied. In this section the monitoring of Netropsin binding with the intercalator marker, ThT is presented. (Figire 4.12) ThT shows an enhancement for its fluoresence intensity as it binds to micro-molecules like amyloid fibrils, RNA and DNA.[24, 25]

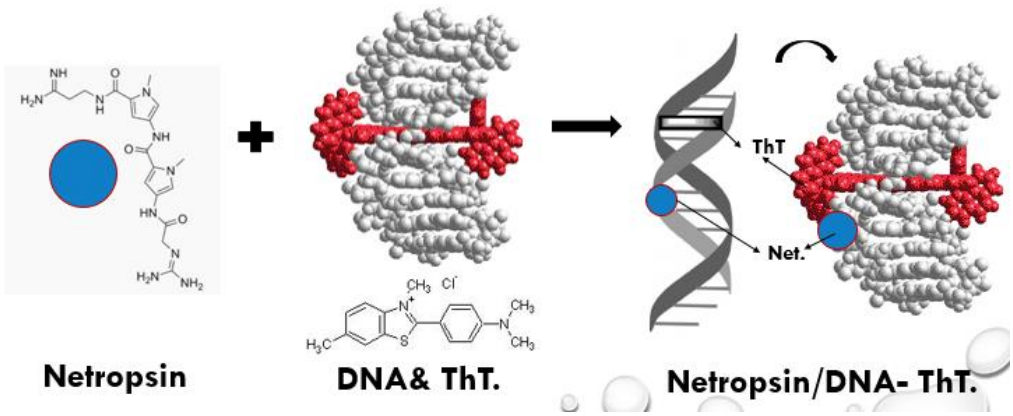

Figure 4.12. Cartoon diagram depicting the binding of Netropsin with Salmon-DNA/ThT.

4.5.1 Optical Absorption Measurements

Optical absorption measurements were carried out to monitor the binding of Netropsin with Salmon-DNA/ThT (243 μg/mL). Figure 4.13 shows the optical absorption of the investigated system at different concentrations of Netropsin drug. The inset of figure 4.13 shows the absorption enhancement at 316 nm as a function of Netropsin concentration, and the trend increased as the concentration of Netropsin increased. This result suggests the binding of Netropsin with salmon-DNA/ThT.

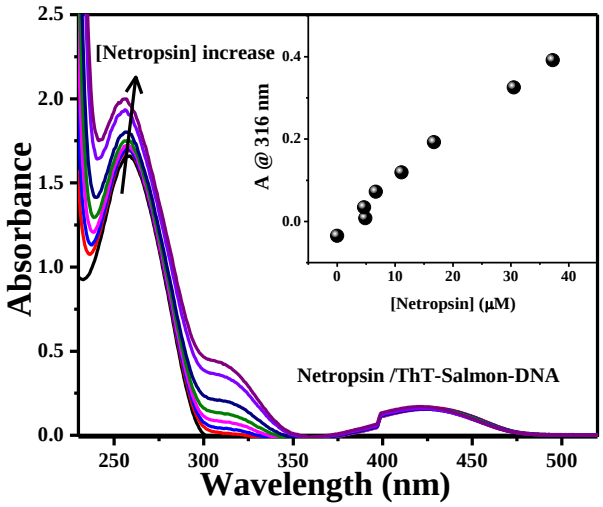

Figure 4.13. Optical absorption spectra of Netropsin/Salmon-DNA/ThT at different Netropsin concentration.

4.5.2 One-Photon Fluorescence Measurements

Figure 4.14 shows the steady-state fluorescence spectra of salmon-DNA/ThT at different concentrations of Netropsin drug after excitation at 420 nm. We can notice from the plot that the fluorescence intensity of ThT increase slightly as more Netropsin drug is added to the system. The fluorescence intensity of ThT enhanced when it binds to ds-DNA because of the rigidity it provides. Then the binding of Netropsin will increase the rigidity of the system, and restrict the torsional rotation around the single C–C bond in ThT molecule between the benzothiazole and dimethylaminobenzene moieties and thereby further increase the fluorescence intensity of ThT.[26, 27] The increase in the fluorescence intensity was plotted as a function of Netropsin concentration in the inset of figurer 4.14 and an enhancement of about 2-fold was observed. These result indicating that the netropsin interacting with the Salmon-DNA/ThT by enhancing the fluorescence intensity.

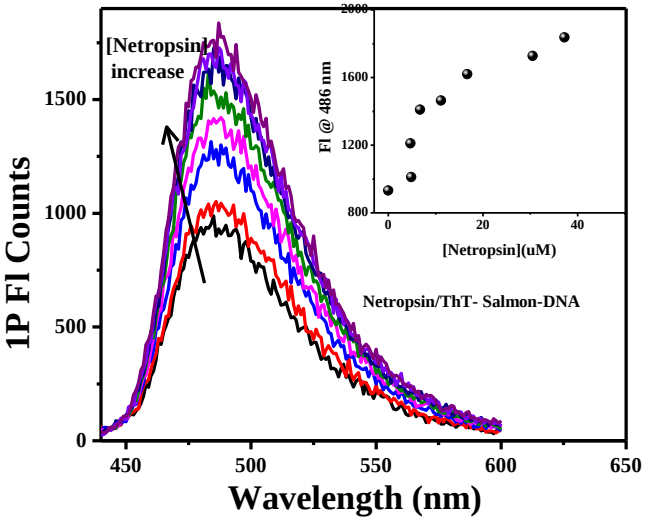

Figure 4.14. Steady-state fluorescence spectra of Salmon-DNA/ThT as a function of Netropsin concentration. The inset shows the fluorescence intensity at 486 nm that exhibit about 2-fold enhancement.

4.5.3 Two–Photon Fluorescence Measurements

Similar to one-photo fluorescence, 2P fluorescence measurements were carried out to monitor the binding of Netropsin with salmon-DNA/ThT after excitation at 800 nm. Figure 4.15 shows the increase in the fluorescence intensity with the increase in Netropsin concentration. The inset of figure 415 shows the normalized intensity enhancement at 483 nm as a function of Netropsin concentration whith enhanced progression suggesting the binding of the drug with Salmon-DNA/ThT system.

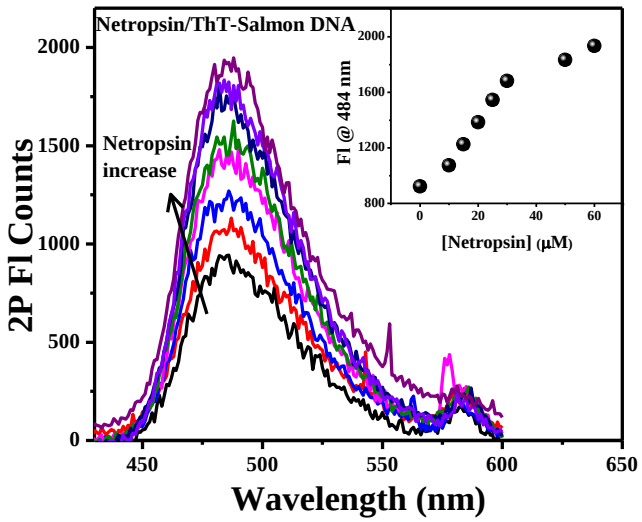

Figure 4.15. Two–photon fluorescence spectra of Salmon-DNA/ThT after excitation at 800 nm at different Netropsin concentration, the inset shows the intensity at 484 nm.

4.5.4 Relative-Two Photon Fluorescence measurements

To observe the impact of intercalated dye (ThT) as a marker to read the binding interaction of Netropsin drug with Salmon-DNA, relative two photon cross-sections were determined as explained above. Figure 4.16A shows the comparison of normalized fluorescence intensities of

salmon-DNA/ThT system at different netropsin concentrations after one-photon and 2-photon excitation. The results show enhancement in both cases and it is similar. Then, relative 2PA enhancement was determined from the ratio of 2-photon fluorescence to 1-photon fluorescence and Figure 4.16B shows the relative cross-section for Netropsin binding Salmon-DNA/ThT system. The relative 2P cross-section remained unchanged with netropsin concentration suggesting that the intercalator dye is not a good indicator for the binding of drug with DNA. This is expected as intercalator dyes cannot sense the local electric fields of DNA and cannot be used to monitor the binding of the drugs with 2P spectroscopy.

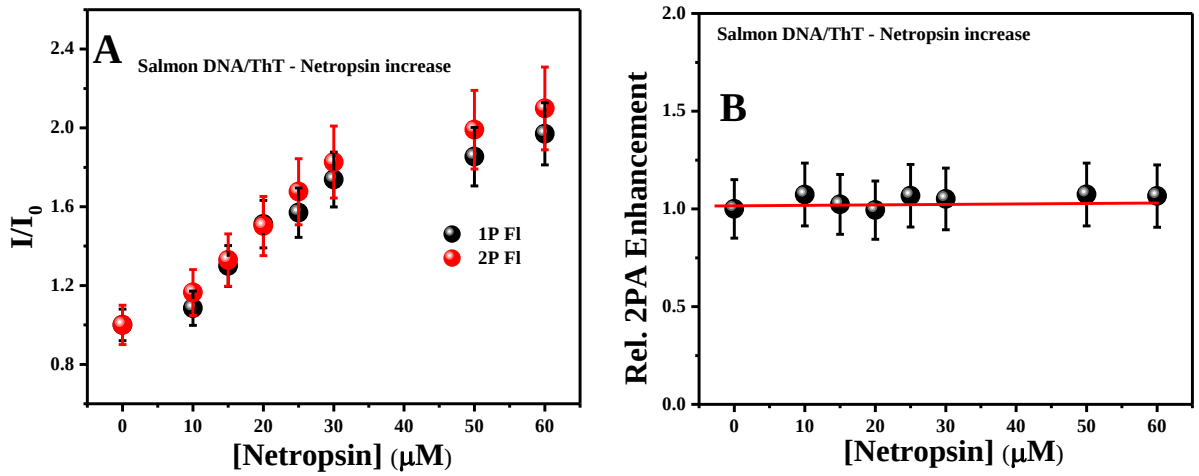

Figure 4.16. (A) Comparison between the one-photon and two-photon fluorescence intensity for Netropsin binding Salmon Sperm-DNA/ThT. (B) Relative 2PA cross-section plot for Netropsin binding Salmon-DNA/ThT at different concentration of Netropsin drug.

4.6 Doxorubicin Binding Interaction with Salmon-DNA

The anthracycline anti-tumor drugs doxorubicin (DXR) and daunomycin (DNM) are powerful anticancer drugs employed in chemotherapy. The fluorescence characteristics of DXR, DNM and other anthracycline drugs are often used to assess the interaction of the drug with DNA

and other macromolecules, in addition to monitoring the localization of the drug within lipid bilayers and liposomal delivery systems.[28] DXR causes DNA double-strand breaks in a rapidly dividing cell and kills the mutant cells[30]. This is considered to be the reason behind using it as anti-tumor drug.[29] Thus, because of the biological importance of Doxorubicin as a cure for tumor diseases, we have characterized the binding interaction of DXR drug with DNA using combined optical spectroscopic techniques. These measurements are part of our efforts to prove that our proposed technique 2PA-spectroscopy can be used to differentiate the binding interaction modes of different drugs with DNA. All the measurements were carried out in a buffer solution unless stated otherwise. Ten samples were prepared with increasing concentrations of DNA placed in each (0, 20, 50, 70, 100, 200,350, 500, 700, 900 μL). Each sample was 1 mL, so buffer was added decreasingly as each sample was made, while the drug (20 μL) was added to each uniformly.

4.6.1 Optical Measurements

Optical absorption measurements were carried out to monitor the binding interaction of DXR with 332 μg/mL Salmon-DNA and figure 4.17 shows the absorption spectra of the drug at different concentrations of DNA. From the plot we can notice that the absorption spectra increased as the concentration of DNA increased.

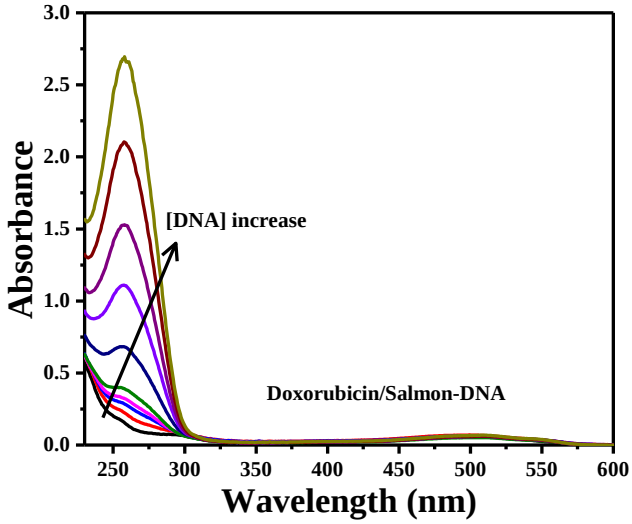

Figure 4.17. Optical absorption spectra as a function of DNA concentration for DXR drug.

4.6.2 One-Photon Fluorescence Measurements

Figure 4.18 shows the fluorescence spectra of DXR at different concentrations of DNA obtained after excitation at 480 nm and monitoring the spectra from 500 nm to 750 nm. From the plot we can notice that the fluorescence intensity drastically increased as the DNA concentration increased with the slight shift to shorter wavelength. The inset of figure 4.18 shows the normalized fluorescence intensity with progression increase at 580 nm as a function of DNA concentration indicating the binding of the drug with DNA.

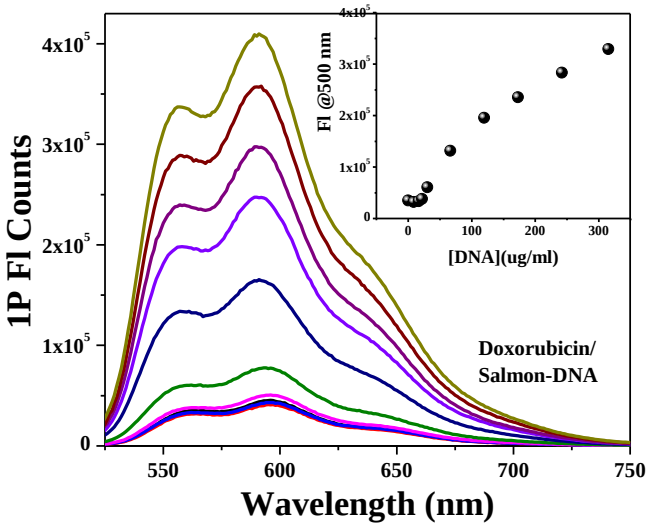

Figure 4.18. Steady-state fluorescence spectra of DXR as a function of DNA concentration. The Inset shows the fluorescence intensity at 580 nm as a function of DNA concentration

4.6.3 Two-Photon Fluorescence Measurements

Similar to one-photon, two-photon fluorescence measurements were carried out to monitor the binding of DXR with DNA. Figure 4.19 shows the fluorescence intensity of the drug at different concentration of DNA after excitation at 800 nm. The inset shows the fluorescence intensity at 582 nm that observed for Doxorubicin at highest DNA concentration. It has to be noted that the fluorescence spectra presented here was cut after 620 nm as it suffered from the scattering of the laser above these wavelengths. The intensity increased is similar to one-photon excitation result suggesting the binding of DXR with DNA.

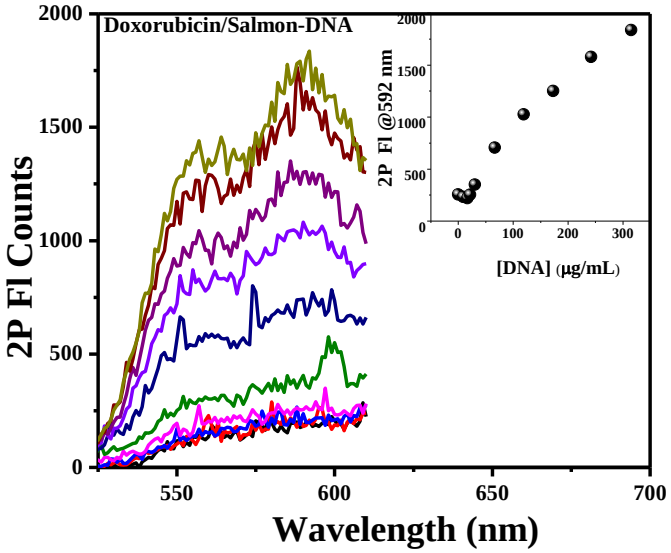

Figure 4.19. Two-Photon fluorescence spectra of DXR at different DNA concentrations after excitation at 800 nm. The inset shows the fluorescence intensity at 582 nm as a function of DNA concentration

4.6.4 Relative 2P Enhancement

A comparison of normalized one-photon and 2-photon fluorescence intensities is presented in Figure 4.20A for DXR at different concentrations of DNA. Interesting trend was observed where the 1P intensity was higher than 2P intensity. Relative 2PA cross-section were estimated from the ratio of two-photon to one-photon fluorescence intensities and Figure 4.20B shows the obtained relative 2P enhancement. From the figure, we can notice that there is no appreciable increase, there was a decrease in relative 2PA cross-section. This situation can be attributed to the way that DXR drug molecule binds to DNA, which is intercalation binding mode. The decrease in 2P cross-section suggest an anti-parallel interaction with the DNA backbone and it has to be some form of intercalation wherein it alters the DNA structure so much so that its orientation becomes anti-parallel to the DNA. [31]

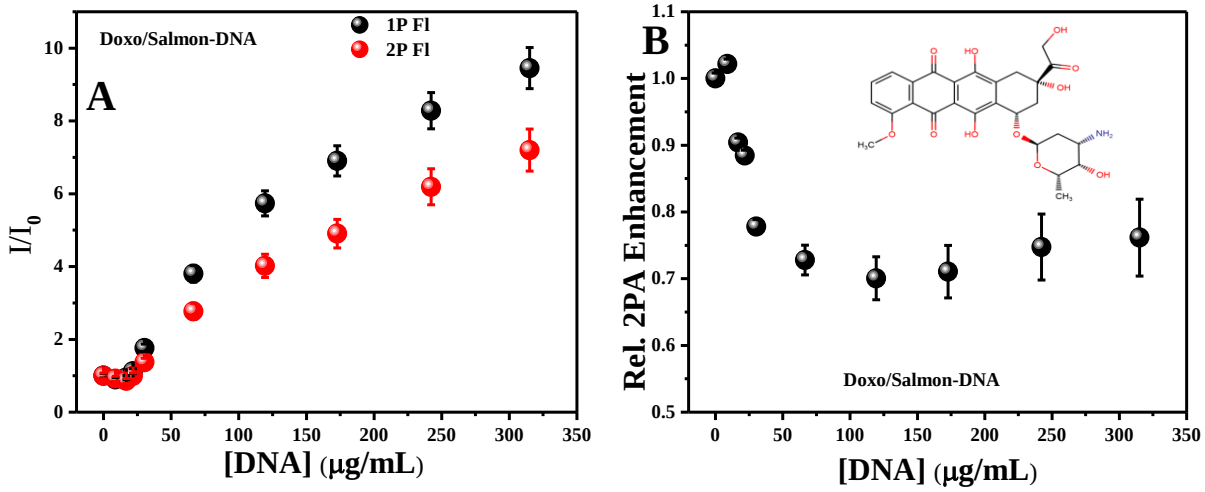

Figure 4.20. (A) Comparison of one-photon and two-photon fluorescence intensity as a function of DNA concentration. (B) Relative 2PA cross-section of DXR with Salmon-DNA.

4.7 Conclusions

This Chapter of the thesis outlines the use of 2P spectroscopy to monitor the drug-binding as well as mode of binding to DNA. The binding of netropsin and DXR with salmon-DNA was studied with combined optical spectroscopic techniques. First of all, absorption, steady-satte

and time-resolved fluorescence measurements of netropsin with DNA suggested the binding of the drug with DNA. As the absorption of netropsin is not suitable to monitor with 2P excitation, markers were used to monitor the binding of netropsin with DNA. Two kinds of markers were used, intercalator (ThT) and minor-groove (Hoe). All optical measurements along with CD and 2-photon fluorescence measurements were carried out with these markers at different concentrations of netropsin. The results have shown relative 2-photon enhancement with the minor-groove marker while no change was observed with intercalator marker. The results show that minor-groove marker is a good system to monitor the binding of drugs with DNA and intercalator by virtue of not being sensitive to the electric field of DNA backbone is not a sensitive technique. Secondly, direct one-photon and 2-photon fluorescence monitoring of DXR drug with DNA was studied. The results of 2P enhancement suggested a decrease in 2P cross-section when DXR was bound to DNA indicating an anti-parallel alignment with DNA backbone. This can be explained by the fact that the DXR intercalation binding alters the structure of DNA so much so that the dipole of the drug becomes anti-parallel to the DNA's electric field. Overall, the results presented here suggested that 2P spectroscopy can be sensitively used to monitor the binding of the drugs with DNA and it can shed light on the interaction of binding.

4.8 Summary

- This Chapter of the thesis has focused on the use of 2P spectroscopy to monitor the drug binding with DNA as well as the orientation of the drug binding.
- To accomplish this target, measurements were carried out on two different drug molecules, Netropsin and Doxorubicin. These drugs are chosen as they are known to bind to biological systems and have good biological significance.
- The results with netropsin suggested that it cannot be studied by 2P spectroscopy as its absorption is below 400 nm.
- 2P markers (intercalator and minor-groove binder) were used to monitor the binding of netropsin with DNA. The result shave shown that minor-groove marker is a sensitive 2P marker to monitor the binding of netropsin with DNA while intercalator marker is not sensitive.

- The binding of DXR with DNA was monitored with 2P spectroscopy. Interesting decrease in 2P cross-section was observed with increase in DNA concentration was observed that can be explained by the intercalation binding of the drug with DNA that alters the structure of DNA so much that its dipole becomes anti-parallel to DNA backbone's electric field.

4.9 References

1.Kopka, M. L.; Yoon, C.; Goodsell, D.; Pjura, P.; Dickerson, R. E. *Proc. Natl. Acad. Sci. U. S. A.* **1985**, *82* (5), 1376–1380.

2. Baruah, H.; Rector, C. L.; Monnier, S. M.; Bierbach, U. **2002**, *64*, 191–200.

3. Zasedatelev, A. S.; Gursky, G. V. *Mol. Biol. Rep.* **1974**, *1*, 337–342.

4. Lewis, E. A.; Munde, M.; Wang, S.; Rettig, M.; Le, V.; Machha, V.; Wilson, W. D. **2011**, *39* (22), 9649–9658.

5. Yang F, Teves SS, Kemp CJ, Henikoff S. *Biochimica et biophysica acta***. 2014**, 1845(1), 84-89.

6. Pang, B.; Qiao, X.; Janssen, L.; Velds, A.; Groothuis, T.; Kerkhoven, R.; Nieuwland, M.; Ovaa, H.; Rottenberg, S.; van Tellingen, O.; Janssen, J.; Huijgens, P.; Zwart, W.; Neefjes, J. *Nat. Commun.* **2013**, *4* (May), 1908.

7. Yang, F.; Kemp, C. J.; Henikoff, S. *Curr. Biol.* **2013**, *23* (9), 782–787.

8. González-ruiz, V.; Olives, A. I.; Martín, M. A.; Ribelles, P.; Ramos, M. T.; Menéndez, J. C.; Analítica, D. Q. Biomed. Eng. Trends, Research Technol. 2011, No. December 2016, 65–90.

9. Nelson, D., Cox, M. &Lehninger, A. *Lehninger principles of biochemistry*. New York: W.H. Freeman **2013**.

10. Reginato, E., Wolf, P., & Hamblin, M. R. *World Journal of Immunology*, **(2014**). *4*(1), 1–11.

11. Xu, C.; Webb, W. W. Measurement of Two-Photon Excitation Cross Sections of Molecular Fluorophores with Data from 690 to 1050 nm. *J. Opt. Soc. Am. B* **1996**, *13*, 481-491.

12. Makarov, N. S; Dorbizhev, M; Rebance, A. Two-Photon Absorption Standards in the 550-1600 nm Excitation Wavelength Range. *Opt Exp.* **2008**, *6*, 4029-4047.

13. Pal, S. K.; Zhao, L.; Zewail, A. H. *PANS***. 2003**, *100* (14),8113-8118.

14. Patel, N.; Berglund, H.; Nilsson, L.; Rigler, R.; McLaughlin, L. W.; Graslund, A. *Eur. J. Biochem.* **1992**, *203* (3), 361–366.

15. Buurma, N. J.; Haq, I. *J. Mol. Biol.* **2008**, *381* (3), 607–621.

16. Latt, S. A.; Wohlleb, J. C. *Chromosoma* **1975**, *52* (4), 297–316.

17. Biancardi, a; Biver, T.; Burgalassi, a; Mattonai, M.; Secco, F.; Venturini, M. *Phys. Chem. Chem. Phys.* **2014**, *16* (37), 20061–20072.

18. Liu, L.; Shao, Y.; Peng, J.; Liu, H.; Zhang, L. *Mol. Biosyst.* **2013**, *9* (10), 2512–2519.

19. Lalande, M. E.; Ling, V.; Miller, R. G. *Proc. Natl. Acad. Sci. U. S. A.* **1981**, *78* (1), 363–367.

20. Wartell, R. M.; Jacquelynn, E.; Wells, D. *The Journal of Bio. Chem.* **1974**, 249 (21), 6719-6731.

21. Zasedatelev, A. S.; Gursky, G. V. *Mol. Biol. Rep.* **1974**, *1*, 337–342.

22. Doan, P. H.; Pitter, D. R. G.; Kocher, A.; Wilson, J. N.; Goodson, T. *J. Am. Chem. Soc.* **2015**, *137* (29), 9198–9201.

23. Zasedatelev, A. S.; Gursky, G. V. *Mol. Biol. Rep.* **1974**, *1*, 337–342.

24. Khurana, R.; Coleman, C.; Ionescu-Zanetti, C.; Carter, S. A.; Krishna, V.; Grover, R. K.; Roy, R.; Singh, S. *J. Struct. Biol.* **2005**, *151* (3), 229–238.

25. Xu, S.; Li, Q.; Xiang, J.; Yang, Q.; Sun, H.; Guan, A.; Wang, L.; Liu, Y.; Yu, L.; Shi, Y.; Chen, H.; Tang, Y. *Sci. Rep.* **2016**, *6* (April), 24793.

26. Sulatskaya, A. I.; Maskevich, A. A.; Kuznetsova, I. M.; Uversky, V. N.; Turoverov, K. K. *PLoS One* **2010**, *5* (10), 1–7.

27. Liu, L.; Shao, Y.; Peng, J.; Liu, H.; Zhang, L. *Mol. Biosyst.* **2013**, *9* (10), 2512–2519.

28. Karukstis, K. K.; Thompson, E. H. Z.; Whiles, J. A.; Rosenfeld, R. J. *Biophys. Chem.* **1998**, *73* (3), 249–263.

29. Yang, F.; Kemp, C. J.; Henikoff, S. *Curr. Biol.* **2013**, *23* (9), 782–787.

30. Pang, B.; Qiao, X.; Janssen, L.; Velds, A.; Groothuis, T.; Kerkhoven, R.; Nieuwland, M.; Ovaa, H.; Rottenberg, S.; van Tellingen, O.; Janssen, J.; Huijgens, P.; Zwart, W.; Neefjes, J. *Nat. Commun.* **2013**, *4* (May), 1908.

31. Motlagh, N. S. H.; Parvin, P.; Ghasemi, F.; Atyabi, F. *Biomed. Opt. Express* **2016**, *7* (6), 2400.